Western University
Scholarship@Western

Digitized Theses
Digitized Special Collections

2011

# THE ROLE OF THE TRANSCRIPTION FACTOR PU.l IN REGULATION OF SELF-RENEWAL IN ACUTE MYELOID LEUKEMIA

Marek R. Gruca

Follow this and additional works at: https://ir.lib.uwo.ca/digitizedtheses

Recommended Citation
Gruca, Marek R., "THE ROLE OF THE TRANSCRIPTION FACTOR PU.l IN REGULATION OF SELF-RENEWAL IN ACUTE MYELOID LEUKEMIA" (2011). *Digitized Theses*. 3607.
https://ir.lib.uwo.ca/digitizedtheses/3607

This Thesis is brought to you for free and open access by the Digitized Special Collections at Scholarship@Western. It has been accepted for inclusion in Digitized Theses by an authorized administrator of Scholarship@Western. For more information, please contact wlswadmin@uwo.ca.

# THE ROLE OF THE TRANSCRIPTION FACTOR PU.1 IN REGULATION OF SELF-RENEWAL IN ACUTE MYELOID LEUKEMIA

(Spine title: The Role of PU.1 in Regulation of Self-Renewal in AML)

Thesis Format: Monograph

By:

**Marek R. Gruca**

Graduate Program in Microbiology & Immunology

A thesis submitted in partial fulfillment
of the requirements for the degree of
Master of Science

The School of Graduate and Postdoctoral Studies
The University of Western Ontario
London, Ontario, Canada

**© Marek R. Gruca 2011**

THE UNIVERSITY OF WESTERN ONTARIO
SCHOOL OF GRADUATE AND POSTDOCTORAL STUDIES

## CERTIFICATE OF EXAMINATION

Supervisor

______________________________
Dr. Rodney DeKoter

Supervisory Committee

______________________________
Dr. S.M. Mansour Haeryfar

______________________________
Dr. David Hess

Examiners

______________________________
Dr. Kelly Summers

______________________________
Dr. Lakshman Gunaratnam

______________________________
Dr. Tom Drysdale

The thesis by

**Marek R. Gruca**

entitled:

**The Role of the Transcription Factor PU.1 in Regulation of Self-Renewal in Acute Myeloid Leukemia**

is accepted in partial fulfilment of the
requirements for the degree of

Master of Science

Date: ______________________________

______________________________
Chair of the Thesis Examination Board

# ABSTRACT

Acute Myeloid Leukemia (AML) is associated with reduced levels or activity of the transcription factor PU.1 in mice and humans. However, little is known about how reduced levels of this essential regulator of hematopoiesis causes AML. We hypothesize that reduced levels of PU.1 cause AML by promoting self-renewal of myeloid progenitors through cell-cycle deregulation. Using mice homozygous for an allele of PU.1 (encoded by *Sfpi1)* which expresses PU.1 at ~20% of normal levels (*Sfpi1*$^{BN/BN}$), we show that these mice are runted and display an abnormal skeletal phenotype. This is due to an absence of TRAP$^{+}$ osteoclasts and a failure to upregulate p57$^{kip2}$ in chrondrocytes. In addition to the skeletal phenotype, a large expansion of immature myeloid cells occurs in the spleen of newborn *Sfpi1*$^{BN/BN}$ mice suggesting unregulated cell cycle *in vivo.* *Sfpi1*$^{BN/BN}$ myeloid precursors had indefinite colony formation ability when grown in differentiating media, which suggests self-renewal. Next, restoration of PU.1 using a retroviral vector opposed self-renewal and promoted differentiation *in vitro* seen by an increase in CD11b and a decrease in c-Kit levels. We have identified *E2f1* as a target gene of PU.1, which regulates cell cycle progression. This model system will allow us to further understand the mechanisms behind hematopoiesis and leukemia. Manipulation of PU.1 levels might be used as a treatment to promote myeloid differentiation and cell cycle arrest.

**Keywords:** Acute Myeloid Leukemia, AML, Purine Rich Box 1, PU.1, hematopoiesis, transcriptional regulation, cell cycle regulation, and immunology.

*To my parents,*

*For their continual support, encouragement and love throughout all my endeavors*

# ACKNOWLEDGEMENTS

I would like to acknowledge all those who have helped me complete this degree. First and foremost I would like to thank Dr. Rodney DeKoter for all his guidance, support, scientific input, and excellent training throughout my degree. He welcomed me into his lab as his first graduate student at the University of Western Ontario and was able to help me throughout this experience. I would also like to thanks the members of my advisory committee: Dr. Mansour Haeryfar, and Dr. David Hess for all of their excellent suggestions, effective constructive criticism, and remembering the date and times of all my meetings.

I would like to thank my family, my parents Roman and Helena and my brother Patrick, for their constant love and support and encouragement.

I would also like to thank all the present and past members of the DeKoter lab: Stephen Li, Rahul Sharma, Sonam Khoosal, Kevin Le, Marc Geadah, Ali Abbas, Kristen Sokalski, Shereen Turkistany, Virginia Pimmett, Sherry Xu, Joel Van Steenbergen, Jan Piskorz, Katie Hotke. Thank you for making my time researching very enjoyable and providing help when needed. I would also the members of the Dr. Beier's lab for providing assistance with the bone dissection work. I would also like to thank all of my friends in the department for all of the fun memories.

Finally, I would like to thank my girlfriend Becky for her constant smile, love and positivity. Without the help of all these individuals, this body of work would not have been possible. Thank you.

# TABLE OF CONTENTS

**Certificate of Examination** ........ II

**Abstract** ........ III

**Acknowledgments** ........ V

**Table of Contents** ........ VI

**List of Figures** ........ VIII

**List of Tables** ........ X

**List of Abbreviations** ........ XI

**Chapter 1: Introduction** ........ 1
- 1.1 Acute Myeloid Leukemia ........ 1
- 1.2 Hematopoiesis ........ 4
- 1.3 Transcriptional Regulation of Myeloid Cell Development ........ 11
- 1.4 Purine-Rich Box 1 ........ 11
- 1.5 The expression and regulation of PU.1 in myeloid development ........ 17
- 1.6 The role of PU.1 during myeloid development ........ 21
- 1.7 Transcriptional targets of PU.1 ........ 22
- 1.8 The Role of PU.1 in skeletal development ........ 23
- 1.9 Cell Cycle Regulation ........ 24
- 1.10 PU.1 and Acute Myeloid Leukemia ........ 25
- 1.11 Hypothesis ........ 27

**Chapter 2: Materials and Methods** ........ 28
- 2.1 Mouse Strains ........ 28
- 2.2 Cell Culture ........ 28
- 2.3 Retroviral Production ........ 31
- 2.4 Lineage Depletion and Retroviral Infection ........ 32
- 2.5 Immunoblotting ........ 32
- 2.6 Flow Cytometry ........ 33
- 2.7 Real-Time quantitative PCR(RT-qPCR) ........ 33
- 2.8 Immunofluorescence staining ........ 34
- 2.9 Colony Forming Assays ........ 34
- 2.10 Skeletal Staining with Alzarin Red and Alcain Blue ........ 37
- 2.11 TRAP staining and Immunohistochemistry ........ 37
- 2.12 Statistical Analysis ........ 39

**Chapter 3: Results** .......... **40**
3.1 Reduction of PU.1 levels result in increased myeloproliferation *in vivo* .......... 40
3.2 Reduced PU.1 levels results in increased serial colony formation ability in differentiating cytokine conditions .......... 50
3.3 Knockdown of PU.1 by miRNA results in increased colony formation in differentiating cytokine conditions .......... 53
3.4 Restoring PU.1 expression in *Sfpi1*$^{BN/BN}$ cells results in differentiation and reduced proliferation .......... 56
3.5 PU.1 controls the cell cycle by reducing E2F1 expression levels .......... 66
3.6 *Sfpi1*$^{BN/BN}$ mice develop an osteopetrotic phenotype .......... 71

**Chapter 4: Discussion** .......... **79**
4.1 Overview .......... 79
4.2 Cells with reduced PU.1 expression have increased self-renewal and acquire hallmarks of cancer. .......... 80
4.3 The mechanism by which PU.1 alters the cell cycle .......... 84
4.4 The osteopetrotic phenotype of *Sfpi1*$^{BN/BN}$ mice .......... 88
4.5 Future Directions .......... 92
4.6 Summary and Conclusions .......... 94

**Bibliography** .......... **95**

**Appendix** .......... **105**

**Curriculum Vitae** .......... **106**

# LIST OF FIGURES

**Figure 1.1 Temporal and spatial locations of hematopoiesis ........................................6**

**Figure 1.2 Classical and alternative models of hematopoiesis ......................................9**

**Figure 1.3 Protein-protein interactions involving PU.1 ...............................................18**

**Figure 2.1 Schematic of colony forming assay ...........................................................35**

**Figure 3.1 *Sfpi1*$^{BN/BN}$ mice are runted and present with a pale spleen ..........................41**

**Figure 3.2 *Sfpi1*$^{BN/BN}$ mouse spleens contain a population of immature myeloid cells ......................................................................................................................43**

**Figure 3.3 *Sfpi1*$^{BN/BN}$ mice display increased proliferation in their spleens ................46**

**Figure 3.4 *Sfpi1*$^{BN/BN}$ mice display altered cell cycle compared to *Sfpi1*$^{+/+}$ mice ........48**

**Figure 3.5 *Sfpi1*$^{BN/BN}$ mice fetal liver cells expressing reduced levels of PU.1 can be cultured indefinitely in GMCSF or IL3/IL6/SCF ...........................................51**

**Figure 3.6 Fetal liver cells expressing normal levels of PU.1 retrovirally infected with the PU.1 silencing shRNA LMP-PU.1-1 display increased self renewal compared to uninfected controls. ....................................................................54**

**Figure 3.7 Production of MigR1 and MigPU.1 retroviruses ........................................57**

**Figure 3.8 Self-renewal is reduced in Sfpi1$^{BN/BN}$ cells retrovirally infected with PU.1 ..........................................................................................................60**

**Figure 3.9 MigPU.1 infected *Sfpi1*$^{BN/BN}$ cells appear to change in morphology ..........62**

**Figure 3.10 *Sfpi1*$^{BN/BN}$ cells infected with MigPU.1 increase in size, intracellular complexity and upregulate CD11b expression ................................................64**

**Figure 3.11 Determining cell cycle regulators under the control of PU.1 using *Sfpi1*$^{BN/BN}$ and *Sfpi1*$^{+/+}$ mice ........................................................................67**

**Figure 3.12 Identification of cell cycle regulators by comparing transcript levels in MigR1 and MigPU.1 infected *Sfpi1*$^{BN/BN}$ cells ....................................................69**

**Figure 3.13 Alzarin red and alcain blue staining of *Sfpi1*$^{BN/BN}$ and *Sfpi1*$^{+/+}$ mouse skulls. ....................................................................................................72**

**Figure 3.14 p57 immunohistochemical (IHC) staining of the growth plate ...............75**

**Figure 3.15 Tartrate Resistant Acid Phosphatase (TRAP) staining of the growth plate in tibia and femur ...........................................................................................77**

**Figure 4.1 ...........................................................................................................89**

# LIST OF TABLES

**Table 1.1 FAB Classification of AML and associated genetic abnormalities..............2**

**Table 1.2 Transcription factors involved in the development of cells in the myeloid lineage....................................................................................................12**

**Table 2.1 PCR and RT-qPCR primer sequences........................................................29**

# LIST OF ABBREVIATIONS

**AGM:** Aorta-gonad mesonephros

**AML:** Acute myeloid leukemia

**BM:** Bone marrow

**CDKs:** Cyclin dependant kinases

**CFA:** Colony forming assay

**CFAC:** Cobblestone area-forming assay

**CKIs:** Cyclin dependant kinase inhibitors

**CLP:** Common lymphoid progenitor

**CMP:** Common myeloid progenitor

**DAB:** 3,3'-diaminobenzidine tetrahydrochloride

**DMEM:** Dulbecco's Modified Eagle Medium

**DNA:** Deoxyribonucleic acid

**D.P.C.:** Days post coitum

**E:** Glutamic Acid

**E14.5:** Embryonic day 14.5

**ECM:** Extracellular matrix

**ETS:** E26 transformation specific

**FAB:** French-American-British classification system

**G-CSF:** Granulocyte colony stimulating factor

**GCSFR:** Granulocyte colony stimulating factor receptor

**GFP:** Green fluorescent protein

**GM-CSF:** Granulocyte-macrophage colony stimulating factor

**GMCSFR:** Granulocyte-macrophage colony stimulating factor receptor

**GMP:** Granulocyte/monocyte progenitor

**HEPES:** 4-(2-hydroxyethyl)-1-piperazineethanesulfonic acid

**HRP:** Horseradish peroxidase

**HSC:** Hematopoietic stem cell

**IHC:** Immunohistochemistry

**IMDM:** Iscove's Modified Dulbecco's Media

**IRF:** Interferon response factor

**kDa:** Kilodalton

**LMPP:** Lymphoid-primed multipotent progenitor

**M-CSF:** Macrophage colony stimulating factor

**MCSFR:** Macrophage colony stimulating factor receptor

**MEP:** Megakaryocyte/erythroid progenitor

**MPP:** Multipotent progenitor

**mRNA:** messenger RNA

**miRNA:** micro RNA

**NK Cells:** Natural killer cells

**P:** Proline

**PBS:** Phosphate-buffered saline

**PCR:** Polymerase chain reaction

**PEI:** Polyethelenimine

**PI:** Propidium iodide

**Plat-E:** Platinum-E

**PU.1:** Purine Rich Box-1

**qPCR:** Quantitative PCR

**Rb:** Retinoblastoma protein

**RNA:** Ribonucleic acid

**S:** Serine

**SFFV:** Spleen focus forming virus

***Spi-1:*** SFFV proviral integration site-1

**T:** Threonine

**TNF:** Tumor necrosis factor

**TRAP:** Tartrate-resistant acid phosphatase

**TSS:** Transcription start site

**URE:** Upstream regulatory element

# CHAPTER 1: INTRODUCTION

## 1.1 Acute Myeloid Leukemia

Acute myeloid leukemia (AML) is a relatively rare but devastating form of leukemia characterized by a maturation block in the myeloid lineage of hematopoiesis. According to the National Cancer Institute, there were over 12,000 new diagnoses of AML in the U.S.A., and over 8,000 deaths in 2010 alone (1). AML is diagnosed when the marrow contains more than 30% blasts that are of myeloid lineage (2). From 2004-2008, the median age at diagnosis for AML was 67 years old (1). These numbers show that AML is the most common acute leukemia affecting adults, however all age groups can develop AML (3). The most common causes of death in AML patients stem from bone marrow failure due to insufficient hematopoiesis (2, 4). The most recent five year relative survival rate for AML is 24.2%, however there is variability depending on the age and subtype of AML at diagnosis (1, 2, 4). The subtype of AML is based on the French-American-British (FAB) classification system. This system divides AML into nine distinct subtypes of AML based on the myeloid lineage involved and the degree of differentiation (4). Subtypes are based on morphological appearance, histological staining results and translocations or genes involved (Table 1.1). Once an individual is diagnosed with AML, the goal of the first phase of treatment is to produce complete remission of the disease, which is defined as marrow which contains less than 5% blasts, a neutrophil count higher than 1000, and a platelet count over 100,000 (4, 5). The goal of the second phase of treatment is to extend the length of remission, since once a patient has been in remission more than 3 years, the likelihood of relapse declines to less than 10% (6).

Since transcription factors play a central role in normal hematopoiesis, it

**Table 1.1 FAB Classification of AML and associated genetic abnormalities**

Table 1.1 adapted from Lowenberg *et al.* 1999(4)

| **FAB Subtype** | **Common Name (% of cases)** | **Results of Staining** | | | **Associated translocations and rearrangements (% of cases)** | **Genes Involved** |
|---|---|---|---|---|---|---|
| | | **Myeloperoxidase** | **Sudan Black** | **Non-specific esterases** | | |
| M0 | Acute myeloid leukemia with minimal differentiation (3%) | Negative | Negative | Negative | Inv (3q26) and t(3;3) (1%) | *EVI1, PU.1, RUNX1* |
| M1 | Acute myeloblastic leukemia without maturation (15-20%) | Positive | Positive | Negative | | *c/EBPa* |
| M2 | Acute myeloblastic leukemia with maturation (25-30%) | Positive | Positive | Negative | t(8;21) (40%) ,t(6;9) (1%) | *AML1-ETO, DEK-CAN, c/EBPa* |
| M3 | Acute promyelocytic leukemia (5-10%) | Positive | Positive | Negative | t(15;17) (98%), t(11;17) (1%), t(5;17) (1%) | *PML-RARa, PLZF-RARa, NPM RARa, PU.1* |
| M4 | Acute myelomonocytic leukemia (20%) | Positive | Positive | Positive | 11q23 (20%), inv(3q26) and t(3;3) (3%), t(6;9) (1%) | *MLL, DEK-CAN, EVI1, PU.1, c/EBPa* |
| M4Eo | Acute myelomonocytic leukemia with abnormal eosinophils (5-10%) | Positive | Positive | Positive | inv (16), t(16;16) (80%) | *CBFβ-MYH11, PU.1, c/EBPa* |
| M5 | Acute monocytic leukemia (2-9%) | Negative | Negative | Positive | 11q23 (20%), t(8;16) (2%) | *MLL-MOZ-CBP, PU.1* |
| M6 | Erythroleukemia (3-5%) | Positive | Positive | Negative | | PU.1 |
| M7 | Acute megakaryocytic leukemia (3-12%) | Negative | Negative | Positive | T(1;22) (5%) | GATA1 |

should come as no surprise that transcription factors are frequently mutated or dysregulated in many forms of AML (Table 1). The majority of AML subtypes display chromosomal rearrangements or mutations of transcription factors that are normally involved in hematopoiesis. Many cases of AML are associated with chromosomal rearrangements of transcription factors, such as the t (8; 21) translocation that results in the oncogenic RUNX1-ETO fusion protein. This fusion protein is found in up to 15% of AML cases and results in the RUNX1 DNA binding domain being fused to the ETO repressor which results in repression of the transcription factors PU.1, c/EBPα and RUNX1 (7, 8). Interestingly other fusion proteins such as the FLT3-ITD protein and the PML-RARα protein also result in the downregulation of PU.1 (9, 10). Point mutations in transcription factors can result in cases of AML. Table 1 shows that many transcription factors are mutated in cases of AML and can be regarded as prognostic markers. Since AML is characterized by a developmental block in hematopoiesis, knowledge of normal hematopoiesis and its transcriptional regulation is critical.

## 1.2 Hematopoiesis

Hematopoiesis is the development of all blood cell lineages from a hematopoietic stem cell (HSC). It is possible to identify HSCs by flow cytometry based on expression of the following cell surface markers: c-Kit$^{+}$, Thy-1.1$^{lo}$, Sca-1$^{+}$, Lineage$^{-}$, Mac-1$^{lo}$ (11-13). A hematopoietic stem cell is defined by two main properties, namely self-renewal and multipotency. Self-renewal is defined as the ability to undergo many cellular divisions while remaining undifferentiated. This includes the ability of dividing asymmetrically, which allows one daughter cell to maintain the HSC population while allowing the second daughter cell to differentiate. Multipotency is the ability to differentiate into cell types of multiple different lineages. The HSC has the ability to generate progenitors which may differentiate into all lineages of cells in the blood in a hierarchical fashion (14). The terminally differentiated cell types that a HSC may produce include erythrocytes (red blood cells), megakaryocytes, macrophages, neutrophils, eosinophils, basophils, mast cells, natural killer (NK) cells and B- and T-lymphocytes. These can all be distinguished based on the expression of unique cell surface markers, gene expression or morphology.

In mammals, hematopoietic cells develop from the mesodermic layer of the embryo which becomes commited or specialized towards a hematopoietic fate (14, 15). While there are certain differences between humans and mice, mouse models provide us with valuable information on the development and function of the hematopoietic system (16, 17). Hematopoiesis occurs in two waves at the following locations: the yolk sac, the aorta-gonad mesonephros (AGM) region, the fetal liver, and finally the bone marrow (18) (Figure 1.1). The first wave, also known as primitive or embryonic hematopoiesis, occurs in the blood islands of the yolk sac and AGM region at approximately 7.5 days post coitum (d.p.c.)(19, 20) The yolk sac is the location of the production of erythrocytes containing fetal hemoglobin, which allows for tissue oxygenation during development (18). The AGM region produces many hematopoietic precursors (21). At approximately 9.5 d.p.c., primitive hematopoiesis is replaced by the second wave of hematopoiesis termed definitive hematopoiesis. This occurs in the fetal liver with maximal hematopoietic activity occurring 14.5 d.p.c. (12) Following 15 d.p.c., the amount of hematopoiesis begins to decrease in the fetal liver which is thought to be a

**Figure 1.1 Temporal and spatial locations of hematopoiesis.** Hematopoiesis first begins at the yolk sac at approximately 7 days post coitum (d.p.c.), followed by the aorta, gonad, mesonephros (AGM) region. Fetal circulation begins at approximately 9 d.p.c., at at which point hematopoiesis also begins to take place in the fetal liver where it is maintained until it relocates to the bone marrow at approximately 20 d.p.c where it will occur for the rest of the animal's life (22).

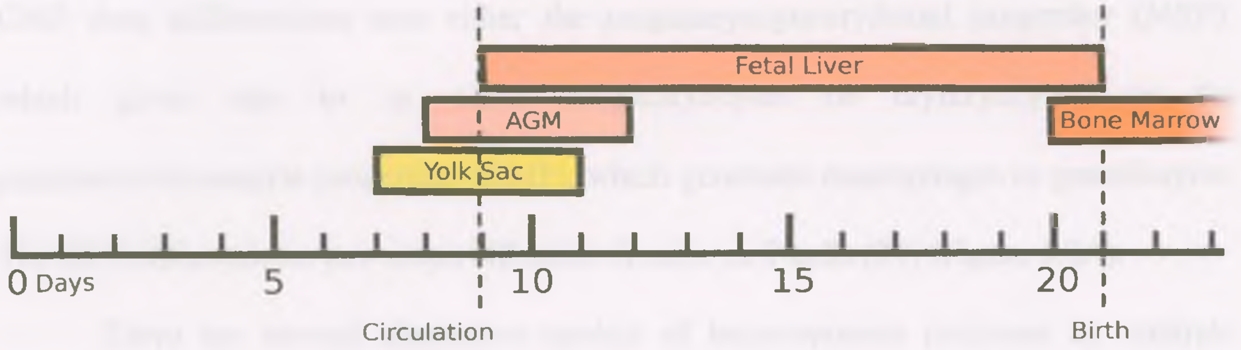
Fetal Liver
AGM
Bone Marrow
Yolk Sac
0 Days
5
10
15
20
Circulation
Birth

consequence of mobilization of HSC to the bone marrow (BM), spleen and accessory lymphoid organs where it will remain for the remainder of life (22).

The pathways by which hematopoiesis occurs are currently the subject of debate (23). The "classical" model of hematopoiesis states that lineages undergo hierarchical binary divisions to drive development. In this scheme, the HSC first differentiates into the common myeloid progenitor (CMP) or common lymphoid progenitor (CLP). The CMP then differentiates into either the megakaryocyte/erythroid progenitor (MEP), which gives rise to in either megakaryocytes or erythryocytes, or the granulocyte/monocyte progenitor (GMP), which generates macrophages or granulocytes. The CLP differentiates into either NK-cells, B cells, or T cells (24) (Figure 1.2A).

There are several alternative models of hematopoiesis proposed by multiple groups such as the stochastic model, the sequential restriction model, myeloid-based models, as well as models based on studies of transcription factors (25). One such revised model was originally proposed by Adolfsson *et al* (26) (Figure 1.2B). In this model, the HSC first differentiates into a multipotent progenitor (MPP). The MPP then differentiates into either a megakaryocyte-erythroid progenitor (MEP), which leads to megakaryocytes or erythroid cells, or a lymphoid-primed multipotent progenitor (LMPP). The LMPP then differentiates into either the granulocyte-macrophage progenitor (GMP), which leads to granulocytes or macrophages, or to the common lymphoid progenitor (CLP), which leads to NK cells, B cells, and T cells (27).

Hematopoiesis is a complex and finely tuned process that is tightly controlled both temporally and spatially. It is controlled by the extracellular environment as well as intracellularly by combinations of transcription factors (28). Without proper control, this

## Figure 1.2 Classical and Stochastic Models of Hematopoiesis

**(A) Classical model of hematopoiesis.** This figure shows the classical model of hematopoiesis. **(B) Stochastic model of hematopoiesis.** This figure shows an alternative model of hematopoiesis as adapted from Adolfsson *et al* (26). Hematopoietic stem cell, HSC; Multipotent Progenitor, MPP; Lymphoid Primed Multipotent Progenitor, LMPP; Common Lymphoid Progenitor, CLP; Common Myeloid Progenitor, CMP; Granulocyte Macrophage Progenitor, GMP; Megakaryocyte Erythrocyte Progenitor, MEP. PU.1 expression gradient is shown in by colour. The top portion of the being darkest indicating highest expression of PU.1 in these cells, while the bottom portion of the panel is the lightest indicating the lowest expression of PU.1.

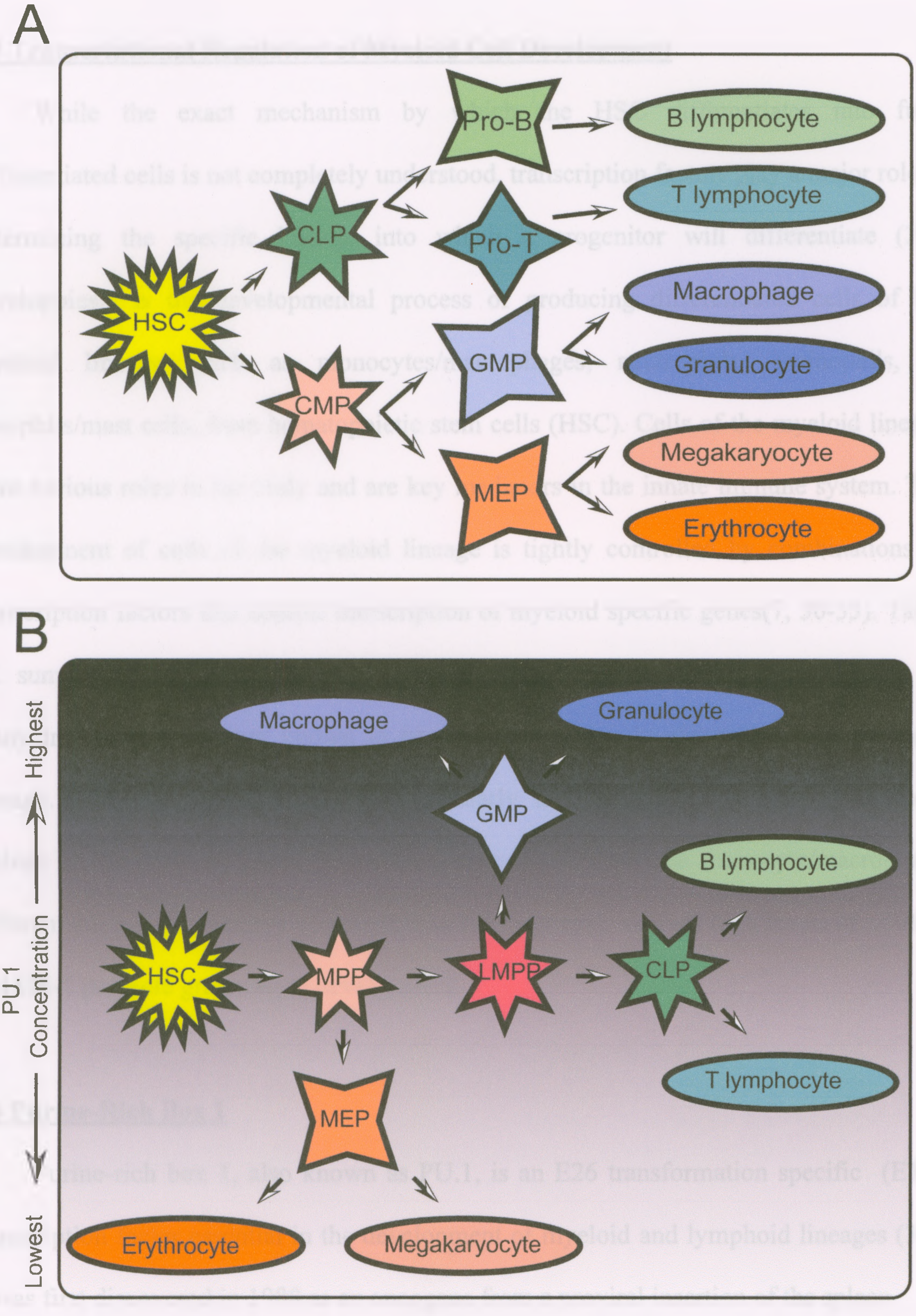
A
Pro-B
B lymphocyte
CLP
Pro-T
T lymphocyte
HSC
Macrophage
GMP
Granulocyte
CMP
MEP
Megakaryocyte
Erythrocyte
B
Highest
PU.1 Concentration
Lowest
Macrophage
Granulocyte
GMP
B lymphocyte
HSC
MPP
LMPP
CLP
MEP
T lymphocyte
Erythrocyte
Megakaryocyte

process may result in different diseases such as AML.

## 1.3 Transcriptional Regulation of Myeloid Cell Development

While the exact mechanism by which the HSC differentiates into fully differentiated cells is not completely understood, transcription factors play a major role in determining the specific lineage into which a progenitor will differentiate (29). Myelopoiesis is the developmental process of producing differentiated cells of the myeloid lineage, such as monocytes/macrophages, neutrophils, eosinophils, or basophils/mast cells, from hematopoietic stem cells (HSC). Cells of the myeloid lineage have various roles in the body and are key mediators in the innate immune system. The development of cells of the myeloid lineage is tightly controlled by combinations of transcription factors that control transcription of myeloid specific genes(7, 30-33). Table 1.2 summarizes the structural family, expression pattern and knockout phenotype of many transcription factors known to be involved in the development of the myeloid lineage. Some transcription factors particularly important for myeloid development include PU.1, c/EBPα, and Gfi-1. High levels of PU.1 enforce monocyte/macrophage differentiation at the expense of granulocyte development, whereas high levels of c/EBPα and Gfi-1 promote granulocyte development.

## 1.4 Purine-Rich Box 1

Purine-rich box 1, also known as PU.1, is an E26 transformation specific (ETS) transcription factor essential in the development of myeloid and lymphoid lineages (34). It was first discovered in 1988 as an oncogene from a proviral insertion of the spleen

**Table 1.2 Transcription factors involved in the development of cells in the myeloid lineage**

| **Name** | **Structural Family** | **Expression Pattern** | **Knockout Phenotype** |
|---|---|---|---|
| PU.1 | ETS family transcription factor, helix loop helix protein. | B-lymphoid, early T-lymphoid, granulocytic and monocytic cells | *Sfpi1*$^{-/-}$ mice lack B cells, monocytes and have reduced neutrophils. (35) |
| Spi-B | ETS family transcription factor, helix loop helix protein. | B and T cells, pDCs | *Spib*$^{-/-}$ result in defective T and B cell responses. Knockout mice have non-functional B cells.<br>Spi-B is able to rescue macrophage and granulocyte development in PU.1$^{-/-}$. (36-38) |
| Spi-C | ETS family transcription factor, helix loop helix protein. | B cells and macrophages | *Spic* $^{-/-}$ results in fewer red pulp macrophages. (39) |
| c/EBPα | CCAAT enhancer binding protein (C/EBP) family basic leucine zipper class (bZIP) of transcription factors | HSC, CMP and GMP, liver and adipose tissue | *Cebpa*$^{-/-}$ mice lack neutrophils and eosinophils and monocytes and increased numbers of myeloid blasts in blood and fetal liver. Loss of the G-CSF receptor. (40) |
| c/EBPβ | CCAAT enhancer binding protein (C/EBP) family basic leucine zipper class (bZIP) of transcription factors | Up regulated during myeloid differentiation | *Cebpb*$^{-/-}$ results in reduced myeloid development. (41) |
| c/EBPε | CCAAT enhancer binding protein (C/EBP) family basic leucine zipper class (bZIP) of transcription factors | Granulocytes and lymphoid cells. | *Cebpe*$^{-/-}$ mice fail to generate functional neutrophils and eosinophils. (42) |
| Gfi1 | Nuclear zinc finger transcriptional repressor containing N-terminal SNAG domain | Lymphoid and granulocytic cells but not in the monocyte lineage | *Gfi1*$^{-/-}$ display defects in neutrophil maturation subsequent to the promyelocyte stage. (43, 44) |
| Gfi1b | Nuclear zinc finger transcriptional repressor containing N-terminal SNAG domain | Highly expressed in erythroid and megakaryocytic precursors, T cells | *Gfi1b*$^{-/-}$ mice are embryonic lethal due to lack of erythropoiesis. (44) |

| | | | |
|---|---|---|---|
| MafB | Member of Maf family of proteins, a subgroup of AP-1-type bZip transcription factors | Myeloid lineage of cells, upregulated in differentiating monocytes and macrophages | *MafB*$^{-/-}$ results in formation of immature myeloid cells, but cannot differentiate into F4/80 expressing macrophages.<br>*MafB(D/N)* inhibits both mye- loid colony formation and the differentiation of myeloblasts into macrophages. |
| c-Jun | Component of AP-1 family of transcription factors. Contains basic leucine zipper | Expression increases during monocytic maturation | *Jun*$^{-/-}$ is embryonic lethal (E13.0). Results in increased levels of apoptotic cells. (45) |
| Egr-1 | EGR family of C2H2 - type zinc-finger proteins | Myeloid and lymphoid cells | *Egr1*$^{-/-}$ develops normally, have increased levels of dividing HSC. *Egr1* (D/N) results in defective monocyte maturation. *Egr1* stimulates monocyte differentiation in myeloid cell lines and murine marrow progenitors at the expense of granulopoiesis. (46, 47) |
| Egr-2 | EGR family of C2H2 - type zinc-finger proteins | Myeloid and lymphoid cells | Functions redundantly with *Egr2* to promote monocyte differentiation. (46) |
| KLF2 | Krüppel-like family of transcription factors. Contains C2H2 zinc fingers | T cells, B cells, erythrocytes and macrophages. | *Klf2*$^{-/-}$ is embryonic lethal, due to defective erythropoeisis. |
| KLF4 | Krüppel-like family of transcription factors. | Myeloid lineage, and macrophages | *Klf4*$^{-/-}$ is lethal. KLF4loxP models demonstrate a reduction in mature monocytes and an increase in granulocyte formation. (48) |
| PLZF | Krüppel-like family of transcription factors | LT-HSC, erythroid, monocyte, and granulocyte progenitors. Not in differentiated cells. | *Zbtb16*$^{-/-}$ knockdown results in increased number of granulocytes. Important in development of megakaryocytes and NKT cells lineages. |

| | | | |
|---|---|---|---|
| Evi1 | SET/PR domain family of transcription factors | Expression is limited to HSC and progenitors. Evi1 is essential for the maintenance of HSCs, dispensable for blood cell lineage commitment. | *Mecom*$^{-/-}$ is embryonic lethal. (Blocks granulocytic differentiation in myeloid cells). (49) |
| Mef2c | Myocyte enhancer factor 2 (Mef2) family of MADS-box transcription factors | B cells, myeloid cells | *Mef2c*$^{-/-}$ absense from hematopoetic progenitors results in deficiency in lymphoid development and enhanced myeloid development. (50) |
| RARα | NHR / NR1 Thyroid hormone-like | Myeloid lineage cells | *Rara*(D/N) results arrests granulopoiesis at the promyelocyte stage. (51) |
| HoxA10 | Homeobox gene family | Immature myeloid cells | *Hoxa10*$^{-/-}$ show an increase in increase in peripheral blood neutrophils and monocytes. |
| Runx1 | Runt-related transcription factor (RUNX) family. Also called core binding factor-α (CBFα) | All hematopoetic lineages | *Runx1*$^{-/-}$ results in lack of hematopoesis. Conditional knockouts result in impared megakaryocyte maturation. Defective T and B cell development and myeloid proliferation. (52) |
| c-Myc | Myc family of transcription factors. Basic helix-loop-helix (HLH) leucine zipper protein | All proliferating cells. Repressed in terminally differentiated cells. | *Myc*$^{-/-}$ mice embryonic lethal between E9.5 and 10. Conditional knockout leads to increased HSC, and reduced differentiation. (53) |
| c-Myb | MYB family of transcription factor | c-Myb expression is largely restricted to progenitor cells and downregulated in differentiating cells. | *Myb*$^{-/-}$ mice embryonic lethal by E15.5; fetal liver contains drastically reduced numbers of hematopoietic progenitors, and lack of erythroid and myeloid cells. (54) |

| | | | |
|---|---|---|---|
| c-Myb (cont.) | | Overexpression inhibits erythroid and myeloid lineages. Can be expressed in activated T and B cells. | |
| IRF4 | Interferon regulatory factor family of transcription factors | T and B cells. Upregulated during myeloid differentiation | *Irf4* $^{-/-}$ results in B and T cells maturation deficiencies. |
| IRF8 | Interferon regulatory factor family of transcription factors | IRF8 expression occurs in macrophages, dendritic cells, B cells and stimulated T cells | *Irf8*$^{-/-}$ results in abnormal neutrophil maturation, block in eosinophil development and defective macrophage function. |
| TFEC | Microphthalmia-TFE (MiT) subfamily of basic helix-loop-helix (bHLH) transcription factors | Myeloid lineage cells | *Tcfec*$^{-/-}$ has no phenotype despite being cell specific. May be redundant with other family members. |
| MITF | Microphthalmia-TFE (MiT) subfamily of basic helix-loop-helix (bHLH) transcription factors | Osteoclasts and mast cells | *Mitf*$^{-/-}$ results in severe reductions in osteoclasts, mast cells and NK cells. (55) |
| Id1 | Helix–loop–helix (HLH) family of transcription factors | Myeloid progenitors and mature macrophages, decreased during neutrophil differentiation. | *Id1*$^{-/-}$have increased monocytes and granulocytes. Lymphocytes and platelet numbers are decreased. |
| Id2 | Helix–loop–helix (HLH) family of transcription factors | Differentiating DCs | *Id2*$^{-/-}$ results in loss of mature T cells, reduction in DC levels. |

focus forming virus (SFFV), which resulted in erythroleukemia. The gene is named SFFV proviral integration site-1 (*Spi-1*) in humans and *Sfpi1* in mice (56). PU.1 is a 42 kilodalton (kDa) protein encoded by the gene *Sfpi1* whose primary isoform is composed of 272 amino acids (57). The human homologue is quite similar showing 85% amino acid homology with mouse PU.1 (58, 59).

PU.1 contains three major functional domains: a C-terminal DNA binding domain, a PEST domain and an N-terminal transactivation domain (60). As with all ETS family transcription factors, PU.1 contains a highly conserved helix-turn-helix DNA binding domain which is located within the C-terminal 100 amino acids (61). It binds to a 10 base pair segment of double stranded DNA, which requires the consensus core sequence “GGAA” or “AGAA”. In addition to DNA binding, the ETS domain is able to interact with a number of accessory proteins such as c-Jun, c/EBPα, and GATA-1, among others (62-64) (Figure 1.3). The N-terminal transactivation domain consists of three acidic amino acid rich regions and one gluatamine rich region. This region also allows for direct interaction with other proteins such as TFIID, TBP, among others (Figure 1.3). Finally, the PEST domain is located between the transactivation domain and the ETS domain. This domain gets its name as an acronym, which stands for Proline (P), Glutamic Acid (E), Serine (S), and Threonine (T). This domain is typically involved in protein stability/degradation (65) but is also involved in protein-protein interactions with IRF-4 and IRF-8 (66, 67)(Figure 1.3).

## 1.5 The expression and regulation of PU.1 in myeloid development.

The expression of PU.1 is limited to the hematopoietic system. PU.1 is an

**Figure 1.3 Protein-protein interactions involving PU.1**

The transcription factor PU.1 shown in red contains 3 domains: An N-terminal transactivation domain, a PEST domain, and a C-terminal ETS domain. The named proteins have been shown to directly interact with PU.1 within the corresponding domain.

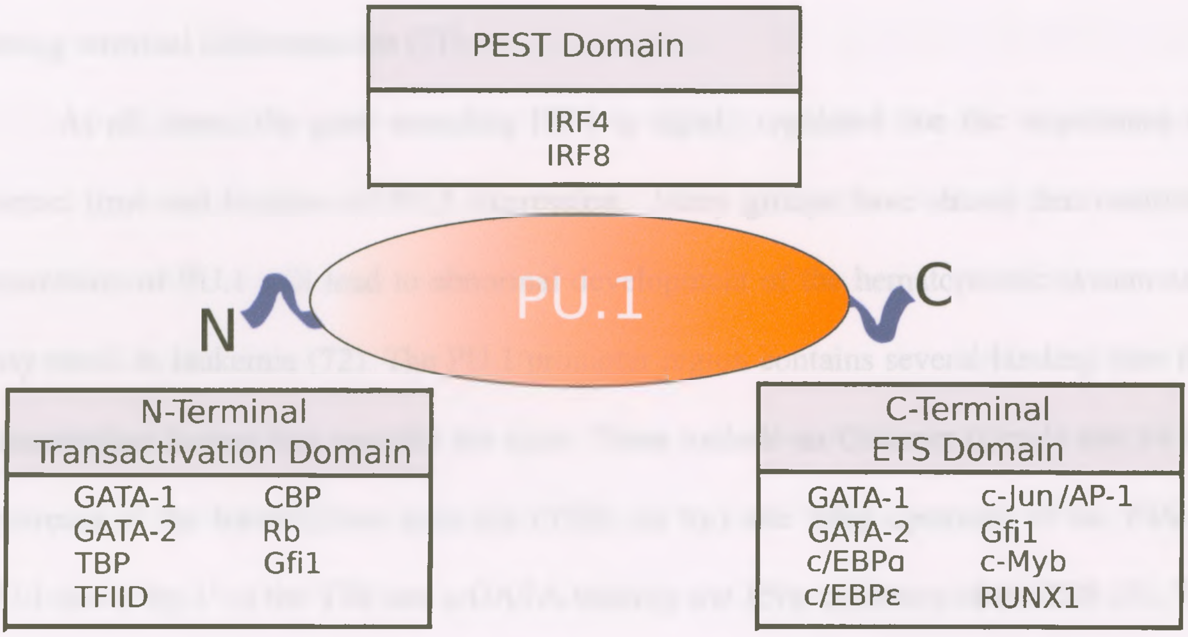
PEST Domain
IRF4
IRF8
PU.1
N
C
N-Terminal Transactivation Domain
GATA-1
GATA-2
TBP
TFIID
CBP
Rb
Gfi1
C-Terminal ETS Domain
GATA-1
GATA-2
c/EBPα
c/EBPε
c-Jun/AP-1
Gfi1
c-Myb
RUNX1

essential transcription factor in hematopoiesis, particularly in myeloid development. PU.1 is expressed at low levels in HSCs, and in the early progenitor cells CMPs and CLPs (68, 69). Expression levels of PU.1 increase dramatically during terminal myeloid development; they are decreased during terminal B cell development and shut off during terminal erythrocyte/megakaryocyte development (68-70). PU.1 also gets shut off during T cell differentiation, however there are certain subsets of T cells that re-express PU.1 during terminal differentiation (71).

At all times, the gene encoding PU.1 is tightly regulated due the importance of correct time and location of PU.1 expression. Many groups have shown that incorrect expression of PU.1 will lead to abnormal development of the hematopoietic system and may result in leukemia (72). The PU.1 promoter region contains several binding sites for transcription factors that regulate the gene. These include an Octamer (Oct-1) site 54 bp upstream of the transcription start site (TSS), an Sp1 site 39bp upstream of the TSS, a PU.1 site 20bp 3' of the TSS and a GATA binding site 15bp upstream of the TSS (56, 73, 74). All of these transcription factors are expressed in HSC, and may initiate differentiation. It has also been discovered that there is an upstream regulatory element (URE), which is 14kb upstream of the TSS (75). Deletion of the URE downregulated the expression of PU.1 to approximately 20% of wild-type levels in myeloid cells (76). PU.1 may be able to direct its own expression through the URE as well as the binding site within the PU.1 promoter. RUNX1, also known as AML1, is another important regulator of PU.1. It has been shown to regulate PU.1 in a lineage specific positive and negative manner in the promoter and URE regulatory regions (77). In addition to these transcription factors, PU.1 is targeted and upregulated by the Notch1 signaling pathway(78).

## 1.6 The role of PU.1 during myeloid development

PU.1 is essential for the development of cells in the myeloid lineage. This has been shown through many mouse models where PU.1 has either been knocked-out, knocked-in, over expressed or restored. There have been two labs that have created an *Sfpi1*$^{-/-}$ mouse. The first group, lead by Dr. Harinder Singh, generated the *Sfpi1*$^{-/-}$mouse by knocking out the ETS DNA domain and replacing it with a neomycin resistance gene (79). The second group, lead by Dr. Richard Maki, generated their *Sfpi1*$^{-/-}$mouse by knocking in a neomycin resistance gene into the ETS domain (34). The *Sfpi1*$^{-/-}$ mouse generated by the Singh group was embryonic lethal by 18.5 d.p.c and contained no detectable myelopoiesis, whereas the *Sfpi1*$^{-/-}$ mice generated by the Maki group survived for 2 days after birth, at which point they die due to septicemia. However, it was possible to keep these mice alive for up to 2 weeks using antibiotics. With this treatment, there were a small number of neutrophils generated. It is interesting that in the heterozygous *Sfpi1*$^{+/-}$mice that express PU.1 at 50% of normal levels, the phenotype is relatively normal. These mice have myeloid cells that are functionally normal. These two studies agree that in the absence of PU.1 there are severe defects in myelopoiesis.

While the PU.1 mutants show a portion of the story, other mouse models have shown that PU.1 functions in a dose dependant manner in the myeloid lineage. A group led by Dr. Daniel Tenen generated a mouse model with a deletion in the upstream regulatory enhancer (URE), which is 14kb upstream of the transcription start site (76, 80). When this region was deleted, the mice had reduced expression of PU.1 to 20% of wild-type levels in most tissues with the exception of T cells where it was upregulated. This resulted in impaired myeloid differentiation and acute myeloid leukemia, suggesting an increase in proliferation, as well as a block in B cell development.

Our lab developed an alternate mouse model where PU.1 is reduced in all cell types to 20% of wild-type levels (27, 81). This was performed by insertion of a ß-lactamase gene and neomycin resistance cassette into the first exon of PU.1, which resulted in this allele of *Sfpi1* being named "BN". *Sfpi1*$^{BN}$ alleles of PU.1 are transcribed and translated at a 3rd start codon instead of its normal start site, which results in PU.1 being truncated by 31 amino acids at the N-terminus. Due to altered transcriptional regulation, it also results in the protein being expressed at 20% of wild-type levels. The protein itself is fully functional. Mice that are homozygous for this allele (*Sfpi1*$^{BN/BN}$) display a severe phenotype. While they are viable, they do not survive past weaning (21 days after birth). They are runted, osteopetrotic, and display a macrophage and B cell deficiency (27). Based on these mouse models, it appears that PU.1 expression below 20% of wild-type levels result in severe myelopoiesis defects. This suggests PU.1 functions in a dose-dependent manner, and levels at or below 20% are insufficient to promote normal myeloid or B cell development.

## 1.7 Transcriptional targets of PU.1

PU.1 has been shown to have binding sites in many myeloid promoters (33). PU.1 has been shown to regulate genes encoding granulocyte colony stimulating factor receptor (GCSFR) (82), macrophage colony stimulating factor receptor (MCSFR) (83), and the granulocyte-macrophage colony stimulating factor receptor (GMCSFR) (84).

These genes encode receptors for growth factors, which are essential for the proliferation and differentiation of cells of the myeloid lineage. In addition to regulating growth factors receptors, PU.1 activates genes required for a myeloid phenotype. This includes the adhesion molecule CD11b (85), which is a marker of a differentiated macrophage. PU.1 also activates CD18 (86) which together with CD11b forms the complex Mac-1. PU.1 also activates FcγRI (87) and FcγRIIIA (88), which are receptors for the constant region of immunoglobulin G (IgG), as well as scavenger receptors type I and II, which are involved in the innate immune system responses (89). Furthermore, recent studies have shown that PU.1 is directly involved in the regulation of a large portion of genes involved in inflammation including interleukin-1 beta (IL-1ß), secretory IL-1 antagonist, IL-18, IL12p40 subunit and tumor necrosis factor (TNF)(90). Based on the function of the type of the genes that are targeted by PU.1, it is understandable that loss or downregulation of PU.1 will result in the lack of differentiated or functional differentiated myeloid cells.

## 1.8 The Role of PU.1 in skeletal development

There are two forms of skeletal development. The first is intramembranous bone formation, during which mesenchymal cells condense and directly differentiate into osteoblasts to deposit bone matrix (91). This form of skeletal development occurs in the flat bones such as seen in the skull. While this is a straightforward process, it is seen as the exception in bone development. The second form of skeletal development is endochondral bone formation which begins when mesenchymal cells form condensations, which become chondrocytes (92). Chondrocytes are cells that reside in the growth plate and contribute to the longitudinal growth of bones (93). The innermost chondrocytes enlarge by proliferating to first form the pre-hypertrophic zone and the hypertrophic chondrocytes, which begin to express the cell cycle inhibitor p57. P57 arrests hypertrophic cells in the G1 phase of the cell cycle and is a marker of hypertrophic chondrocytes in the growth plate (94). Hypertropic chondrocyte secrete an extracellular matrix (ECM) that is rich in collagen, which promotes vascularization. Once this is complete, chondrocytes undergo apoptotic death. The ECM is invaded by osteoblasts and osteoclasts, which results in bone formation and remodeling. The ECM that is left behind provides a scaffold that the osteoblasts and osteoclasts may remodel and lay down new bone matrix.

Osteoclasts are derived from cells of hematopoietic origin and are from the myeloid lineage (95-97). The main function of the osteoclast is bone resorption, which is necessary during bone growth, tooth eruption, and fracture healing. Osteopetrosis is a bone disease that is characterized by lack of osteoclast function and results in increased bone mass and a loss of the bone marrow cavity. Osteoclasts are identified by their expression of tartrate-resistant acid phosphatase (TRAP)(98, 99). Osteoclast activity is enhanced by several factors such as IL-1 (100), M-CSF (100-102), TGF-α (103) , TNFα/ß (103), IL-6 (104), and IL-11 (105). PU.1 is essential for the development of osteoclasts since it controls the expression of these factors such as IL-1 and M-CSF.

## **1.9 Cell Cycle Regulation**

The cell cycle is the process by which DNA is replicated and segregated into two separate daughter cells. The process is divided into four stages: the $G_1$ phase, where the cell grows in size and prepares for DNA synthesis; the S phase, where the cell undergoes DNA replication; the $G_2$ phase, where the cell prepares for mitosis and the M phase where cell undergoes mitosis (106). Cells may also enter into $G_0$ phase before $G_1$, which is when cells become quiescent and stop proliferating. Two families of proteins control the cell cycle: the cyclin dependant kinases (CDKs) and cyclins. CDKs are serine/threonine kinases which are activated during particular points in the cell cycle and phosphorylate downstream proteins which leads to cell cycle progression (107). The amount of CDKs remains stable during the cell cycle, but their state of activation fluctuates depending on the particular CDK and the stage of the cell. Cyclins regulate CDK function by physically interacting with CDKs and activating them (107). Cyclin levels constantly fluctuate during the cell cycle. CDKs can be inhibited by cyclin dependant kinase inhibitors (CKIs) that can bind CDKs alone or in their CDK/cyclin complexes. There are 2 main families of CKIs: the INK4 family and the Cip/Kip family (108). Both of these families of inhibitors tend to inhibit the G1-S phase checkpoint of the cell cycle. One major target that the CDK/cyclin complexes target is retinoblastoma protein (Rb) and E2F1 (109). Once the CDK/cyclin complex phosphorylates Rb, it dissociates from E2F1 and allows E2F1 to activate target genes important in the G1- S phase checkpoint. E2F1 has been studied extensively in its role in the cell cycle. It has been shown that ectopic expression of E2F1 alone can drive G1 arrested cells into S phase allowing for cell cycle progression (110-112). Furthermore, dominant-negative forms of E2F1 arrest cells during the G1 phase of the cell cycle (113). In summary, the cell cycle is a tightly coordinated process regulated in both a positive and negative manner, and dysregulation may lead to oncogeneisis.

## 1.10 PU.1 and Acute Myeloid Leukemia

PU.1 is an essential transcription factor in the development of the hematopoietic system, particularly in the myeloid lineage. Therefore it is important to study the effects that deregulation of PU.1 can cause in leukemia since PU.1 has been shown to be involved in human cases of AML. One study showed that PU.1 was mutated in 7% of patients with AML (114). In mouse models, down-regulating PU.1 was sufficient to cause AML in the absence other mutations (76). Dr. Tenen's mouse model of reduced PU.1 develop AML at an average age of 3 months, and die by 9 months from an aggressive form of AML. The *Sfpi1*$^{BN}$ mouse model with reduced PU.1 also appears to have a dramatic expansion of immature myeloid cells after birth. These mice have an expansion of immature myeloid cells and do not survive past weaning, however it is unknown whether the cause of death is leukemia or due to the osteopetrosis they also develop. These results show the importance of PU.1 in the development of AML and the need to further understand the mechanism by which PU.1 causes the differentiation block that leads to AML.

## 1.11 Hypothesis and Objectives

Acute Myeloid Leukemia is a type of cancer in which myeloid progenitors have retained their ability to self-renew and are unable to differentiate. Many subtypes of AML are characterized by mutations in genes encoding transcription factors that regulate differentiation, and PU.1 has been implicated in the development of AML in both humans and in mouse models. Furthermore, PU.1 regulates many genes involved in myeloid development. If PU.1 regulated a gene involved in differentiation through the control of the cell cycle, dysregulation may lead to increased proliferation, lack of differentiation and development of AML. **Therefore, I hypothesize that reduced levels of PU.1 cause AML by promoting self-renewal of myeloid progenitors through deregulation of the cell cycle, which results in increased proliferation and a block in terminal differentiation; where I define self-renewal as an increase in cell division in the absence of differentiation.**

To test this hypothesis, the following objectives were performed:

1. The first objective is to characterize the *Sfpi1*$^{BN/BN}$ mouse phenotype to determine if there is increased proliferation and unregulated cell cycle in the myeloid lineage.
2. The second objective is to determine whether a reduction in PU.1 leads to increased self-renewal.
3. The third objective is to determine the mechanism by which PU.1 is controlling proliferation.

# CHAPTER 2: MATERIALS AND METHODS

## 2.1 Mouse Strains

Mice were housed in the University of Western Ontario Health Sciences animal facility (London, Ontario, Canada). Animal husbandry and breeding was done in compliance with animal protocols approved by the University of Western Ontario University Council on Animal Care. C57BL/6 mice were purchased as required from Charles River Laboratories (Pointe-Claire, Quebec, Canada). *Sfpi1*$^{+/BN}$ mice were previously generated and maintained as an *Sfpi1*$^{+/BN}$ colony(81). *Sfpi1*$^{+/BN}$ were genotyped by PCR using primers found in table 2.1. *Sfpi1*$^{+/BN}$ mice were mated to obtain *Sfpi1*$^{BN/BN}$ neonates. Embryonic day 14.5 (E14.5) fetuses were generated by performing timed matings of *Sfpi1*$^{+/BN}$ mice. At E14.5, pregnant mothers were euthanized and fetuses were collected by dissection and phenotyped by expression of CD11b in the fetal liver. CD11b expression levels are highest in *Sfpi1*$^{+/+}$ mice, intermediate in *Sfpi1*$^{+/BN}$ mice and low in *Sfpi1*$^{BN/BN}$ mice. These results were later confirmed by PCR genotyping.

## 2.2 Cell Culture

All complete media contained 10% fetal bovine serum, 100 U/mL penicillin/streptomycin, 2 mM L-glutamine, 5 x10$^{-5}$ M 2-mercaptoethanol, and 0.5 mM HEPES (HyClone, Logan, UT, USA). Platinum-E (Plat-E) retroviral packaging cells were grown in Dulbecco's Modified Eagle Medium (DMEM) media. NIH3T3 cells were grown in DMEM media. *Sfpi*$^{BN/BN}$ cells were grown in Iscove's Modified Dulbecco's Media (IMDM) medium containing 2 μg/mL GM-CSF. All complete media contained 10% fetal bovine serum, 100 U/ mL penicillin/streptomycin, 2 mM L-glutamine, 5 x10$^{-5}$

U.W.O. LIBRARY

## Table 2.1 PCR and RT-qPCR primer sequences

| **Primer Name** | **Sequence** |
|---|---|
| *Sfpi1 Primer 1* | 5' CGGCCAGAGACTTCCTGTAG-3' |
| *Sfpi1 Primer 2* | 5'-AAGTTGGCCGCAGTGTTATC-3' |
| *Sfpi1 Primer 3* | 5'-GCTCTTCGTCCAGATCATCC-3' |
| *Sfpi1 Primer 4* | 5'-ATGGTCACACATCCCAAAGC-3' |
| *ckit Right* | 5'-TGTCGCCAGCTTCAACTATT-3' |
| *ckit left* | 5'-GATCTGCTCTGCGTCCTG-3' |
| *p15 left (2)* | 5'-ATCCCAACGCCCTGAAC-3' |
| *p15 right (2)* | 5'-TCGTGCACAGGTCTGGTAAG-3' |
| *ki67 left* | 5'-GTCCACCTGGTCACCATCAA-3' |
| *ki67 right* | 5'-TTGACACTACAGGCAGCTGGATAC-3' |
| *p15 right (1)* | 5'-CAGTTGGGTTCTGCTCCGT-3' |
| *p15 left (1)* | 5'-AGATCCCAACGCCCTGAAC-3' |
| *p16 left* | 5'-GCAGAAGAGCTGCTACGTGA-3' |
| *p16 right* | 5'-CGTGAACATGTTGTTGAGGC-3' |
| *p27 right* | 5'-TCTGTTGGCCCTTTTGTTTT-3' |
| *p27 left* | 5'-GGGTCTCAGGCAAACTCTGA-3' |
| *p21 right* | 5'-AGAGACAACGGCACACTTTG-3' |
| *p21 left* | 5'-CGGTGTCAGAGTCTAGGGGA-3' |
| *cdkn1c right* | 5'-GTTTGGAGAGGGACACCCTG-3' |
| *cdkn1c left* | 5'-CTGAAGGACCAGCCTCTCTC-3' |
| *Rb1 right* | 5'-CCATGATTCGATGCTCACAT-3' |
| *Rb1 left* | 5'-ACAGATTTGTCCTTCCCGTG-3' |
| *e2f1 right* | 5'-CAGCGAGGTACTGATGGTCA-3' |
| *e2f1 left* | 5'-CGATTCTGACGTGCTGCTC-3' |
| *e2f2 right* | 5'-GAAGAGGGTGTGACAGCTCC-3' |
| *e2f2 left* | 5'-GGGATCGCAGAGACCATAGA-3' |
| *e2f7 right* | 5'-TAATGGGGTTTCTGTCTGGG-3' |
| *e2f7 left* | 5'-TGAAGATGCAGAGAACGCAC-3' |
| *Cdk6 right* | 5'-CTTGGTTTCTCTGTCCGTCC-3' |
| *Cdk6 left* | 5'-AGTGCAGACCAGTAGGAGG-3' |
| *Tyms right* | 5'-CTGGTCTACTCCTTGTCCCG-3' |
| *Tyms left* | 5'-TTTCTGGACAGCTTGGGATT-3' |
| *PolA1 right* | 5'-GCCACTCCAGGACAAGAACT-3' |
| *PolA1 left* | 5'-CATTTTTGATGCGGACTGTG-3' |
| *cMyc right* | 5'-TGAGCCCCTAGTGCTGCAT-3' |
| *cMyc left* | 5'-AGCCCGACTCCGACCTCTT-3' |
| *c/EBPa right* | 5'-AGCCAAGAAGTCGGTGGACAAGAA-3' |
| *c/EBPa left* | 5'-GCGGTCATTGTCACTGGTCAACTC-3' |
| *skp2 right* | 5'-GAGGTGGACAGTGAGAACATC-3' |
| *skp2 left* | 5'-AGGAAAAGATCCCAAGGAGC-3' |
| *miR-223 left* | 5'-CCGTGTATTTGACAAGCTGAGT-3' |
| *miR-223 right* | 5'-TGGGGTATTTGACAAACTGACA-3' |

M 2-mercaptoethanol, and 0.5 mM HEPES (HyClone, Logan, UT, USA)

## 2.3 Retroviral Production

Previous members of our lab constructed the MigR1, MigPU.1 and LMP-PU.1-1 retroviruses. MigR1 stands for Murine (MSCV) IRES GFP EcoR1. MigPU.1 is a retroviral vector with a 3x-FLAG tagged PU.1 cDNA cloned into the multiple cloning site and is constitutively expressed. LMP-PU.1-1 is a retroviral vector containing a miRNA against PU.1 that is able to knockdown PU.1 expression. Platinum-E (Plat-E) retroviral packaging cells(115) were used to generate retroviral supernatants using polyethelenimine (PEI) transfection. Twenty four hours before transfection, Plat-E cells were plated at a concentration of $5x10^6$ cells in a 10cm dish. One mL of serum-free DMEM, 10 μg of plasmid DNA, 2.5 μg of packaging DNA were mixed. Samples were vortexed and 21 μg of PEI was added and incubated for 15 minutes at room temperature without disturbance. One ml of the DNA/PEI mixture was added to the cells with 1mL of complete DMEM. Transfected cells were incubated overnight. Media was then replaced with 2ml complete DMEM. Virus containing supernatants were collected at 48 hours post transfection. Virus titers were measured by flow cytometry by infection of NIH-3T3 cell. NIH-3T3 cells were plated at 200,000 cells per well in 6 well plate and incubated overnight. Next, serial dilutions of retroviral supernatent were given to NIH-3T3 cells and polybrene was added to an 8 μg/ml final concentration. Cells were then incubated for 4 hours after which media was replaced with fresh DMEM. Cells were then incubated for 48 hours after which they were analyzed for green fluorescent protein (GFP) expression by flow cytometry. Titers were calculated by percentage of infected cells multiplied by

400000 cells, under the assumption of 1 doubling before infection, and multiplied by dilution factor of retroviral supernatant.

## 2.4 Lineage Depletion and Retroviral Infection

Lineage depletions were performed using a MACs Lineage Cell Depletion Kit. Cells were incubated in 200 ml MACS buffer containing the following anti-Lin antibodies: biotin α-CD4 (H129.19), α-CD5 (53-7.3), α-CD8a (53-6.7), α-CD3e (145-2C11), α-Gr-1 (RBC-8C5), α-Ter119 (Ter119), α-B220 (RA3-6B2). Following incubation 10 ml streptavidin-microbeads (Miltenyi Biotec, Auburn, CA) were added and passed through a VarioMacs column. Lineage negative cells were then centrifuged for 6 minutes at 1500 rpm and pellet was used for infection. For retroviral infection, lineage depleted fetal liver progenitors or GM-CSF *Sfpi*$^{BN/BN}$ cells were infected by resuspension in cell- free retroviral supernatants and centrifuged at 2000g for 3 hours in the presence of polybrene to 8-μg/ml final concentration. Following centrifugation, hematopoietic progenitors were washed and stimulated for 2 days in complete IMDM containing 100 ng/mL murine stem cell factor, 10 ng/mL mIL-3, and 10 ng/mL mIL-6 and incubated at 37°C (Peprotech, Rocky Hill, NJ, USA). Infection frequencies were detected by flow cytometric analysis for GFP.

## 2.5 Immunoblotting

Proteins from whole cell lysates were resolved by SDS–PAGE and electrotransferred to a nitrocellulose membrane (Pierce). Immunoblotting was performed with rabbit anti-PU.1 polyclonal antibody (Santa Cruz Biotechnology, Santa Cruz, CA, USA), HRP-conjugated anti-FLAG antibody (Sigma, St. Louis, MO, USA), goat polyclonal anti-ß-actin (Santa Cruz Biotechnology, Santa Cruz, CA, USA), HRP-conjugated anti-rabbit secondary antibody (Pierce, Rockford, IL, USA) and HRP-conjugated anti-goat secondary antibody. Immunoreactive proteins were visualized with SuperSignal West Pico reagent (Thermo-Fisher Scientific, Waltham, MA, USA)

## 2.6 Flow Cytometry

Flow-cytometric analysis was performed on single-cell suspensions of cells washed in phosphate-buffered saline (PBS) containing 0.05 M EDTA and 0.5% BSA. Cells were analyzed on a FACSCalibur (BD, Franklin Lakes, NJ, USA). Propidium iodide uptake and side light scatter gating for cell size were used to exclude dead cells from analysis. Cell cycle analysis was performed using propidium iodide staining as previously described(116). Antibodies used were biotin-conjugated monoclonal antibody M1/70 (CD11b), RB6-8C5 (Ly-6C, Gr-1), 2B8 (CD117, c-Kit), streptavidin-allophycocyanin conjugate, streptavidin-phycoerythrin conjugate, streptavidin-Fluorescein isothiocyanate conjugate (BD Pharmingen, Franklin Lakes, NJ, USA). A minimum of 20,000 cells were collected for analysis. Analysis was performed using FlowJo version 9.3.2 (Ashland, OR) or ModFit LT (Topsham, ME).

## 2.7 Real-Time quantitative PCR (RT-qPCR)

RNA was isolated from cells using RNA Bee RNA Isolation Agent (Tel-Test, Friendswood, Texas) and reverse-transcribed into cDNA using the iScript DNA synthesis kit (Bio-Rad, Hercules, CA). Quantitative PCR (qPCR) was performed using the iQ

SYBR Green Supermix kit (Bio-Rad) and a Rotor-Gene 6000 instrument (Corbett Life Sciences, Valencia, CA). Relative mRNA transcript levels were normalized to GAPDH as a reference gene and compared between samples using the comparative threshold cycle method (117). Results are presented as the mean and SD of triplicate experiments. Primer sequences are listed in Supplemental Table 2.1.

## 2.8 Immunofluorescence staining

Spleens were embedded in Tissue-Tek OCT compound (Sakura-Finetec, Torrance, CA) and frozen in liquid nitrogen. Spleen sections cut at 5 µm were fixed in 4% paraformaldehyde and blocked with 5% BSA. After blocking, the sections were incubated with primary anti-mouse Ki67-Alexafluor 488 antibody (B56; BD Biosciences, San Diego, CA) and biotin-conjugated monoclonal antibody M1/70 (CD11b) with a streptavidin-phycoerythrin conjugate. Sections were mounted in Vestashield mounting medium (Vector Labs, Burlingame, CA) and photographed with a Nikon (Melville, NY) Eclipse 80i microscope attached to an X-cite 120 fluorescence illumination unit.

## 2.9 Colony Forming Assays

Spleens were removed from neonatal *Sfpi1*$^{BN/BN}$, *Sfpi1*$^{+/BN}$ or *Sfpi1*$^{+/+}$ mice and homogenized. Following homogenization, cells were phenotyped by determining CD11b levels by flow cytometric analysis. 50000 cells were then placed in 3.5cm tissue culture dishes with MethoCult (M3234) methylcellulose medium (Stem Cell Technologies, Vancouver, BC, Canada) containing recombinant murine granulocyte macrophage colony-stimulating factor (GM-CSF; 1 ng/mL), IL-3 (5 ng/mL) IL-6 (10 ng/mL), SCF

**Figure 2.1 Schematic of colony forming assay.**

Timed matings are performed to collected E14.5 fetal livers from *Sfpi1*$^{+/+}$, *Sfpi1*$^{+/BN}$ and *Sfpi1*$^{BN/BN}$ mice. Fetal liver cells are then phenotyped then placed in methylcellulose media, which contains differentiating cytokines (GMCSF or IL3/IL6/SCF). These are then incubated for 1 week without disturbance. After incubation, colonies are counted under a microscope after which cells are collected, washed and replated in methocult for a following week. Assay continues until colony formation stops, or at a predetermined timepoint.

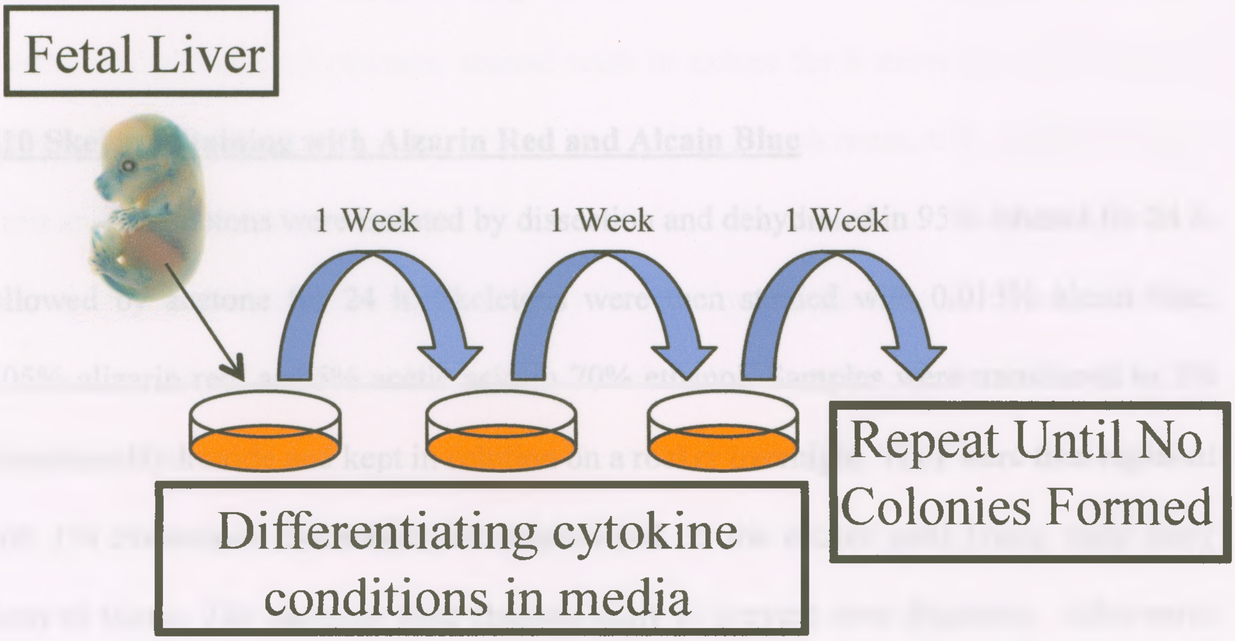
Fetal Liver
1 Week
1 Week
1 Week
Repeat Until No Colonies Formed
Differentiating cytokine conditions in media

(100 ng/mL) (Peprotech) (Figure 2.1). Cells were then incubated for 1 week at 37°C without disturbance. Colonies were counted using a Zeiss Axio observer inverted fluorescent microscope (Zeiss, Göttingen, Germany), where a colony consists of a minimum of 50 cells. Cells were collected, washed 3 times in PBS and replated in methylcellulose as described above. Assays were repeated for as long as colonies were formed or were ended after a 10-week period.

## 2.10 Skeletal Staining with Alzarin Red and Alcain Blue

Skeletons were isolated by dissection and dehydrated in 95% ethanol for 24 h, followed by acetone for 24 h. Skeletons were then stained with 0.015% alcian blue, 0.05% alizarin red, and 5% acetic acid in 70% ethanol. Samples were transferred to 2% Potassium Hydroxide and kept in solution on a rocker overnight. They were then replaced with 1% Potassium Hydroxide, and maintained on the rocker until bones were fairly clean of tissue. The samples were checked daily to prevent over digestion. Afterwards bones were carefully debrided under a dissecting microscope using fine forceps. Afterwards samples were stored in a 1:1 solution of 70% ethanol: glycerol.

## 2.11 TRAP staining and Immunohistochemistry

Limbs were dissected away from torso using tweezers and placed in PSA (modified PBS) on ice. Bones were fixed overnight in 4% paraformaldehyde at room temperature with rocking. Older mice required decalcification of long bones prior to transferring into 70% ethanol. P21 mice required 5-7 days to decalcify adequately. Bones were decalcified in 5% EDTA solution pH7.0 in PBS. Solution was changed every 2-3 days until the bones were decalcified. Decalcified bones were transferred into 70% ethanol at 4°C and stored until sectioning. All sectioning was performed by the molecular pathology core facility (Robart's Research Institute, London, ON, Canada). Samples were paraffin embedded and sectioned at a 5-μm thickness and placed on a glass coverslip.

For TRAP stain, a Leukocyte Acid Phosphatase kit was used (Sigma-Aldrich, Oakville, ON). Paraffin embedded samples were rehydrated by the following protocol: 1. Washed in xylene for 5 minutes, second wash in xylene for 8 minutes, then washed in 100% ethanol, 95% ethanol, 70% ethanol for 2 minutes each wash, then washed twice in water for 5 minutes, then washed twice in PBS for 5 minutes. After rehydration samples were washed in Triton x-100 (0.1% in $H_20$) for 15 minutes, then washed twice in PBS for 5 minutes. Samples were then stained with TRAP stain mixture following the manufacturer's instructions overnight at 4°C. After the staining, cells were washed twice with PBS for 5 minutes, then rinsed with $H_20$ and mounted with vectashield mounting solution (Vector Laboratories, Burlingame, CA, USA).

For p57 immunohistochemistry (IHC), samples were first embedded in paraffin and rehydrated as described above, followed by washing in PBS, blocking in 3% $H_2O_2$ in methanol for 15 minutes and then washed in $H_2O$ for 5 minutes. Antigen retrieval was performed by placing samples in Triton x-100 (0.1% in $H_20$) for 13 minutes and then washing in $H_2O$ for 5 minutes. Slides were blocked with goat serum using a 1:20 dilution in PBS, 100 μL per slide. A 1:200 dilution of primary p57 antibody in blocking buffer (Santa Cruz #Sc-8282) was incubated on the slide overnight at 4°C, 100 μL per slide. After incubation samples were washed 4 times with PBS. Samples were then incubated for 1 hour at room temperature with a 1:200 dilution of secondary horseradish peroxidase

(HRP) goat anti-rabbit antibody. After incubation samples were washed in $H_2O$ for 5 minutes and then stained with 3,3'-diaminobenzidine tetrahydrochloride (DAB) which reacts with HRP to stain areas detected by the primary antibody. After staining, cells were washed in $H_2O$ for 2 minutes are counterstained with methyl green for five minutes and mounted in aqueous mounting media(Dako).

## 2.12 Statistical Analysis

Statistical significance was determined by unpaired or paired Student's t-test or ANOVA using GraphPad Prism v.6. Differences were considered significant with a P-value <0.05.

# CHAPTER 3: RESULTS

## 3.1 Reduction of PU.1 levels result in increased myeloproliferation *in vivo*

Our lab developed a mouse model where an allele for PU.1 named *Sfpi1*$^{BN}$ has reduced expression of PU.1 in all cell types to 20% of wild-type levels (81). *Sfpi1*$^{BN/BN}$ mice are born but do not survive past weaning. Neonatal *Sfpi1*$^{BN/BN}$ mice were previously reported to be runted, osteopetrotic, but with increased spleen size. *Sfpi1*$^{BN/BN}$ mice were obtained by mating *Sfpi1*$^{+/BN}$ breeding pairs. It was confirmed that *Sfpi1*$^{BN/BN}$ mice were runted, and osteopetrotic compared to *Sfpi1*$^{+/+}$ and *Sfpi1*$^{+/BN}$ littermate controls (Figure 3.1A, osteopetrotic data shown in upcoming section). Western blot of whole spleen lysate using anti-PU.1 antibodies confirmed that PU.1 was reduced in *Sfpi1*$^{BN/BN}$ mice compared to littermate controls (Figure 3.1B). Furthermore, the spleens of *Sfpi1*$^{BN/BN}$ mice were pale compared to littermate controls, which suggests an altered cellular composition (Figure 3.1C).

To determine whether the composition of cells was altered in the spleen, flow cytometric analysis was performed for CD11b, Gr-1 and c-Kit. CD11b and Gr-1 were both chosen since they are markers of the myeloid lineage expressed on the cell surface. c-Kit was also chosen because it is expressed on immature myeloid progenitors (118). Flow cytometric analysis of *Sfpi1*$^{BN/BN}$ spleens determined that there was a significant increase in the frequency of immature myeloid lineage cells compared to littermate controls, as seen through an increase in the percentage of CD11b$^{+}$, c-Kit$^{+}$ cells or Gr-1$^{+}$, c-Kit$^{+}$ cells (Fig.3.2 A, B). These results suggested that myeloid proliferation is altered in the spleens of these mice.

To confirm that proliferation was occurring, RT-qPCR was performed to measure

**Figure 3.1 *Sfpi1*$^{BN/BN}$ mice are runted and present with a pale spleen.**

**(A) 21 day old *Sfpi1*$^{BN/BN}$ mice were runted compared to their littermates.** An image of *Sfpi1*$^{BN/BN}$ and *Sfpi1*$^{+/+}$ littermates side by side showing the runted phenotype of the *Sfpi1*$^{BN/BN}$ mice. **(B) Spleens from *Sfpi1*$^{BN/BN}$ mice are pale compared to *Sfpi1*$^{+/+}$ littermates.** In the upper panel, the arrow points towards spleen of an *Sfpi1*$^{+/+}$ mouse. In the lower panel, the arrow points towards spleen of an *Sfpi1*$^{BN/BN}$ mouse. Representative images of results from 3 separate experiments. **(C) Construction of the *Sfpi1*$^{BN}$ hypomorphic allele.** The *Sfpi1*$^{BN}$ hypomorphic allele was constructed by inserting ß-Lactamase and an inverted PGK-neomycin resistance cassette in to the first exon of PU.1. Image not to scale.

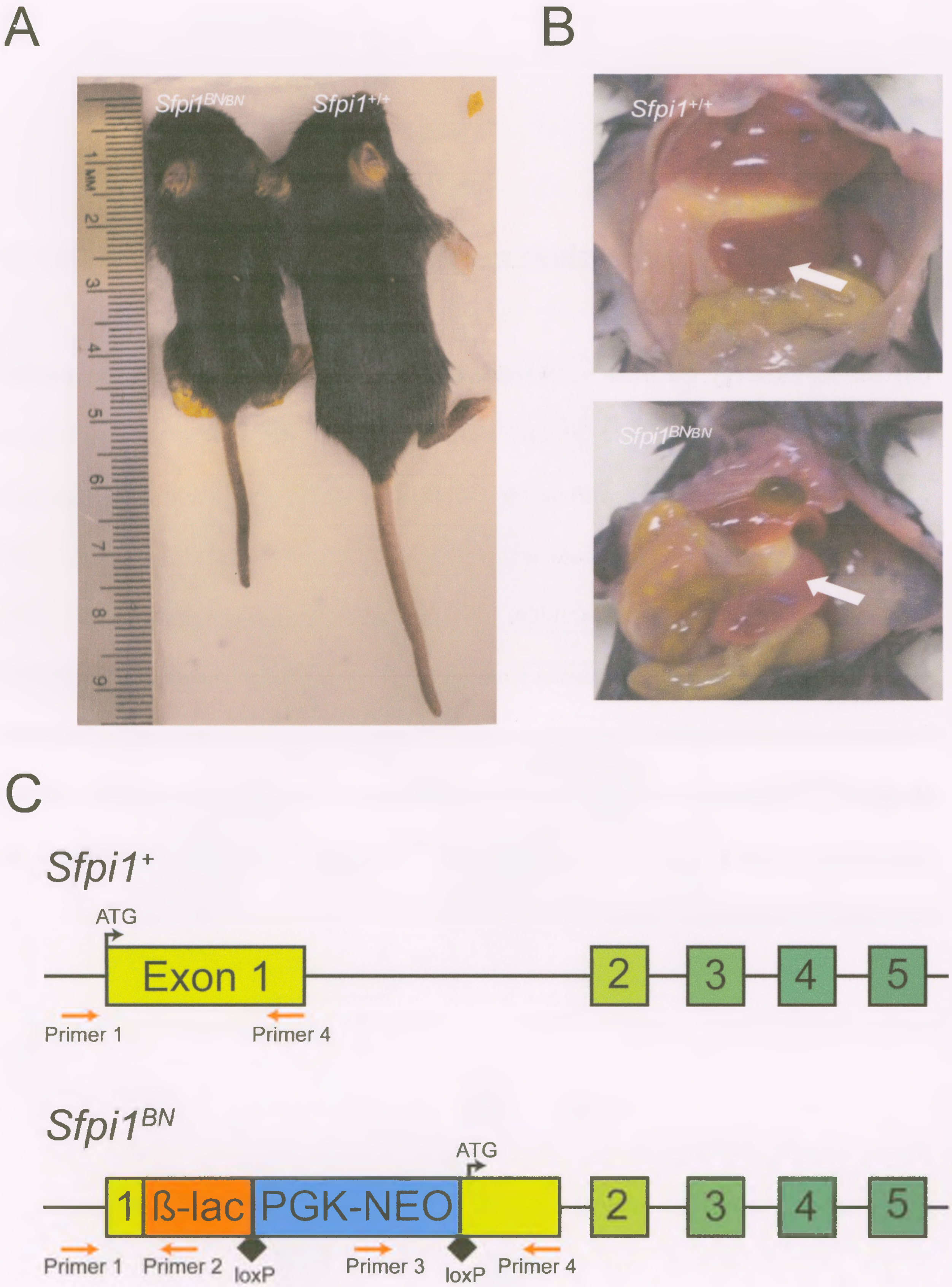
A
Sfpi1BN/BN
Sfpi1+/+
1 MM 2 3 4 5 6 7 8 9
B
Sfpi1+/+
Sfpi1BN/BN
C
Sfpi1+
ATG
Exon 1
2
3
4
5
Primer 1
Primer 4
Sfpi1BN
ATG
1
ß-lac
PGK-NEO
2
3
4
5
Primer 1
Primer 2
loxP
Primer 3
loxP
Primer 4

**Figure 3.2 *Sfpi1*$^{BN/BN}$ mouse spleens contain an increased population of immature myeloid cells.**

**(A) Gating Strategy for Flow cytometric analysis of spleen cells.** Cells were gated to exclude dead cells from analysis **(B) Flow cytometric analysis of the spleens of *Sfpi1*$^{BN/BN}$ mice shows a significantly increased population of immature myeloid lineage cells.** The upper panels show dot plots of CD11b vs. c-Kit whereas the lower panels show dot plots of Gr-1 vs. c-Kit. The left panels show results from *Sfpi1*$^{+/+}$ mice whereas the right panels show results from *Sfpi1*$^{BN/BN}$ mice. Representative dot plot from 3 separate experiments. **(B) Immature myeloid lineage cells are significantly increased in *Sfpi1*$^{BN/BN}$ spleens.** A bar graph shows the statistically significant difference between CD11b vs. c-Kit and Gr-1 vs. c-Kit in *Sfpi1*$^{+/+}$vs. *Sfpi1*$^{BN/BN}$ mice. Significance was determined by students T-test (n=3).

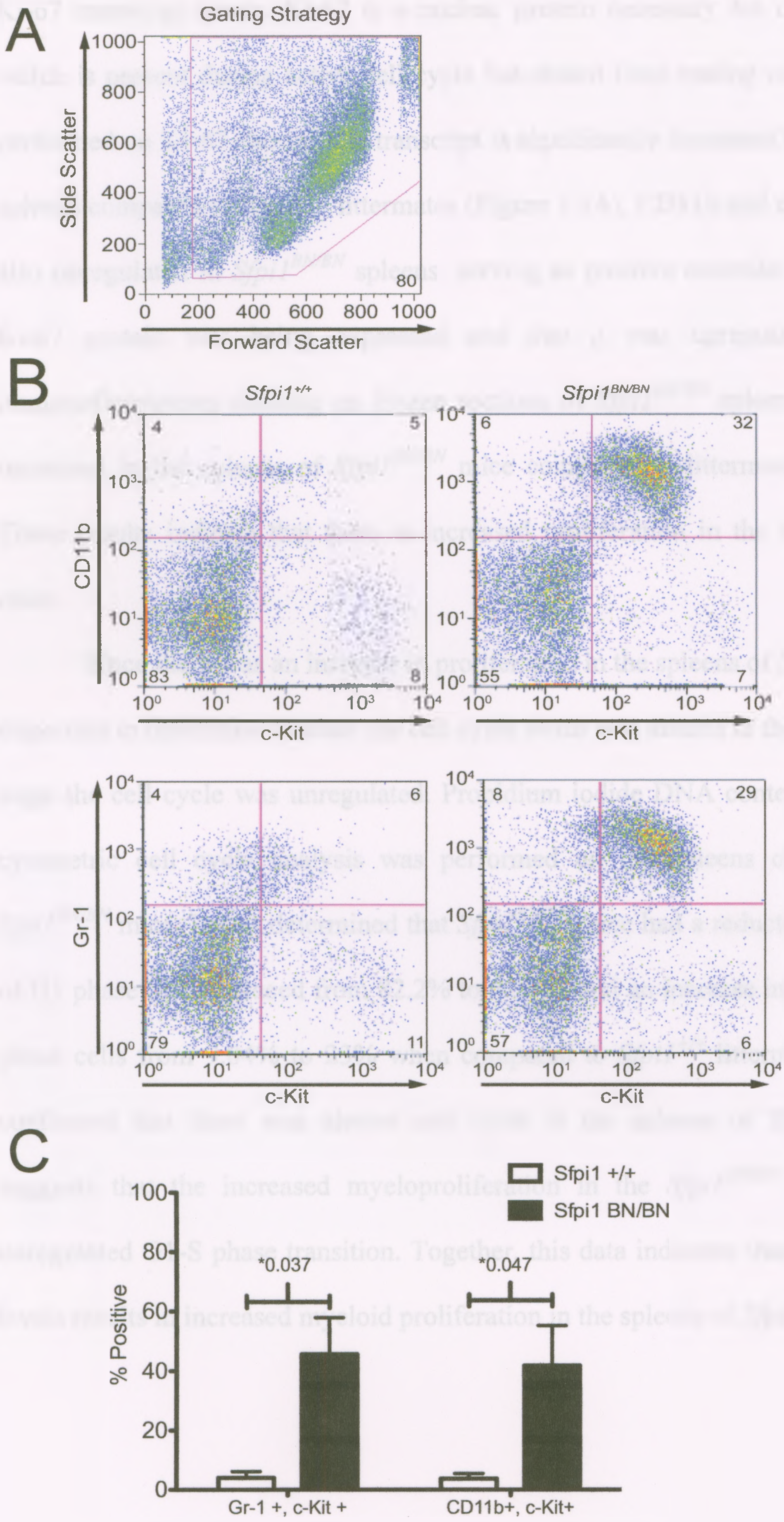
A
Gating Strategy
Side Scatter
1000
800
600
400
200
0
0 200 400 600 800 1000
Forward Scatter
80
B
Sfpi1+/+
Sfpi1BN/BN
CD11b
10⁴
10³
10²
10¹
10⁰
c-Kit
4
5
83
8
6
32
55
7
Gr-1
c-Kit
4
6
79
11
8
29
57
6
C
Sfpi1 +/+
Sfpi1 BN/BN
% Positive
100
80
60
40
20
0
*0.037
*0.047
Gr-1 +, c-Kit +
CD11b+, c-Kit+

Ki-67 transcript levels. Ki-67 is a nuclear protein necessary for cellular proliferation, which is present during active cell cycle but absent from resting cells (119). RT-qPCR performed on Ki-67 showed the transcript is significantly increased (3-fold) in *Sfpi1*$^{BN/BN}$ spleens compared to *Sfpi1*$^{+/+}$ littermates (Figure 3.3A). CD11b and c-Kit transcripts were also upregulated in *Sfpi1*$^{BN/BN}$ spleens, serving as positive controls. To confirm that the Ki-67 protein was being expressed and that it was upregulated, we performed immunofluorescent staining on frozen sections of *Sfpi1*$^{BN/BN}$ spleen. Ki-67 protein was increased in the spleens of *Sfpi1*$^{BN/BN}$ mice compared to littermate controls (Fig 3.3). These results indicate that there is increased proliferation in the spleens of *Sfpi1*$^{BN/BN}$ mice.

Since there was an increase in proliferation in the spleens of *Sfpi1*$^{BN/BN}$ mice it was important to determine whether the cell cycle status was altered in these cells, and at what stage the cell cycle was unregulated. Propidium iodide DNA content labeling and flow cytometric cell cycle analysis was performed on the spleens of both *Sfpi1*$^{+/+}$ and *Sfpi1*$^{BN/BN}$ mice. It was determined that *Sfpi1*$^{BN/BN}$ mice had a reduction in the percentage of G1 phase cells, reduced from 82.2% to 67.8%, and an increase in the percentage of S-phase cells from 9.04% to 23% when compared to *Sfpi1*$^{+/+}$ littermates (Fig. 1C). This confirmed that there was altered cell cycle in the spleens of *Sfpi1*$^{BN/BN}$ mice. This suggests that the increased myeloproliferation in the *Sfpi1*$^{BN/BN}$ mice is due to an unregulated G1-S phase transition. Together, this data indicates that a reduction in PU.1 levels results in increased myeloid proliferation in the spleens of *Sfpi1*$^{BN/BN}$ mice.

**Figure 3.3 *Sfpi1*$^{BN/BN}$ mice display increased proliferation in their spleens.**

**(A) RT-qPCR shows increased transcript levels of Ki-67 in *Sfpi1*$^{BN/BN}$ mice.** RT-qPCR was performed on sorted *Sfpi1*$^{BN/BN}$ and *Sfpi1*$^{+/+}$ mice spleens (Gating strategy shown in figure 3.11). *Sfpi1*$^{BN/BN}$ mice displayed increased levels of ki-67 expression compared to *Sfpi1*$^{+/+}$ littermate controls. Each result was performed in triplicate and significance was determined based using the students T-test. **(B) Immunofluorescent microscopy showing Ki-67 expression in splenic section.** Ki-67 RT-qPCR results were verified by immunofluorescent microscopy where frozen sections of spleen were stained with anti-Ki-67 antibodies. Green represents Ki67 staining, blue represents DAPI staining. *Sfpi1*$^{BN/BN}$ mice displayed increased Ki-67 staining compared to *Sfpi1*$^{+/+}$littermate controls. Representative images of results from 2 separate experiments. Scale bar represents 97 γm

A

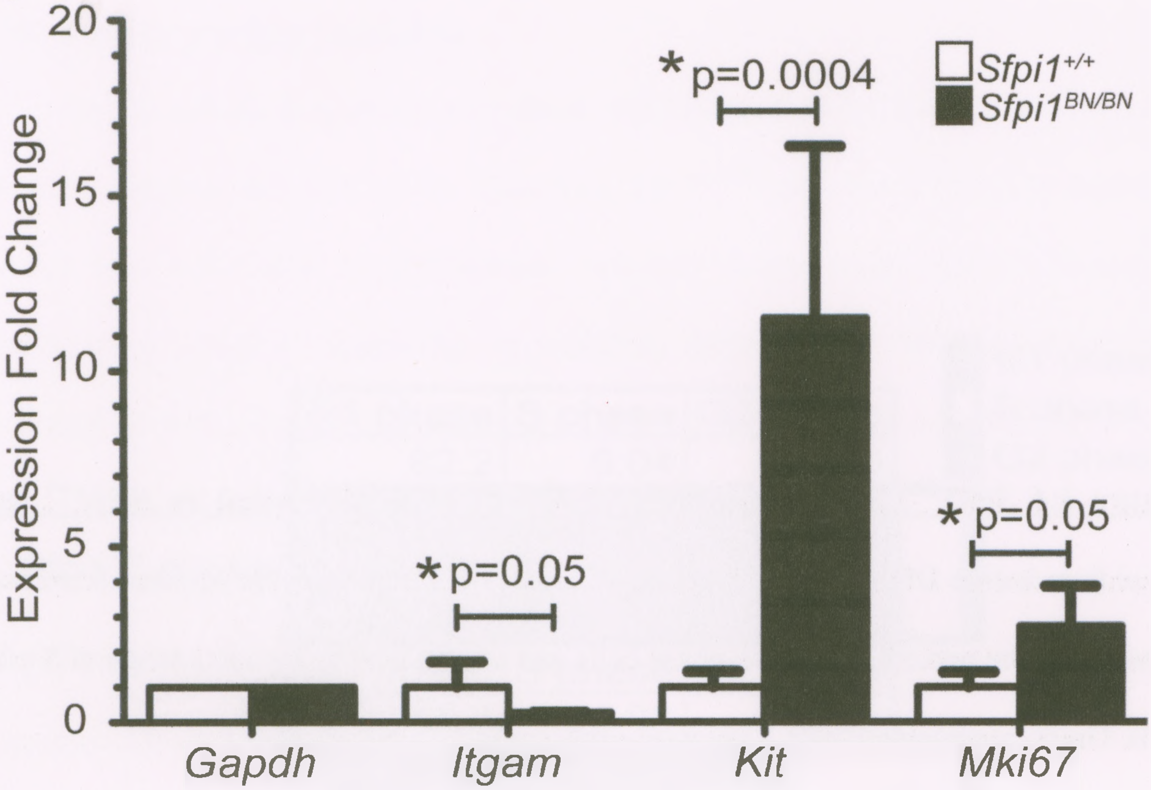

B

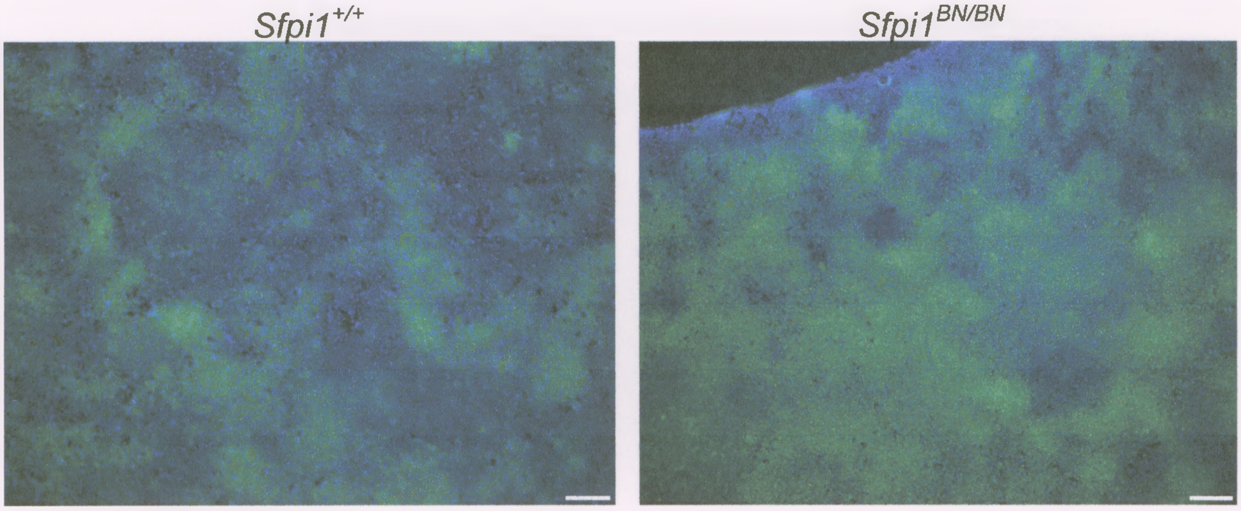
*Sfpi1*$^{+/+}$

*Sfpi1*$^{BN/BN}$

**Figure 3.4 *Sfpi1*$^{BN/BN}$ mice display altered cell cycle compared to *Sfpi1*$^{+/+}$ mice.** Propidium iodide DNA content labeling of *Sfpi1*$^{BN/BN}$ mouse spleens showed there was a decrease in the percentage of G1-phase cells and an increase in the percentage of S-phase cells. Graph representative of 3 separate experiments.

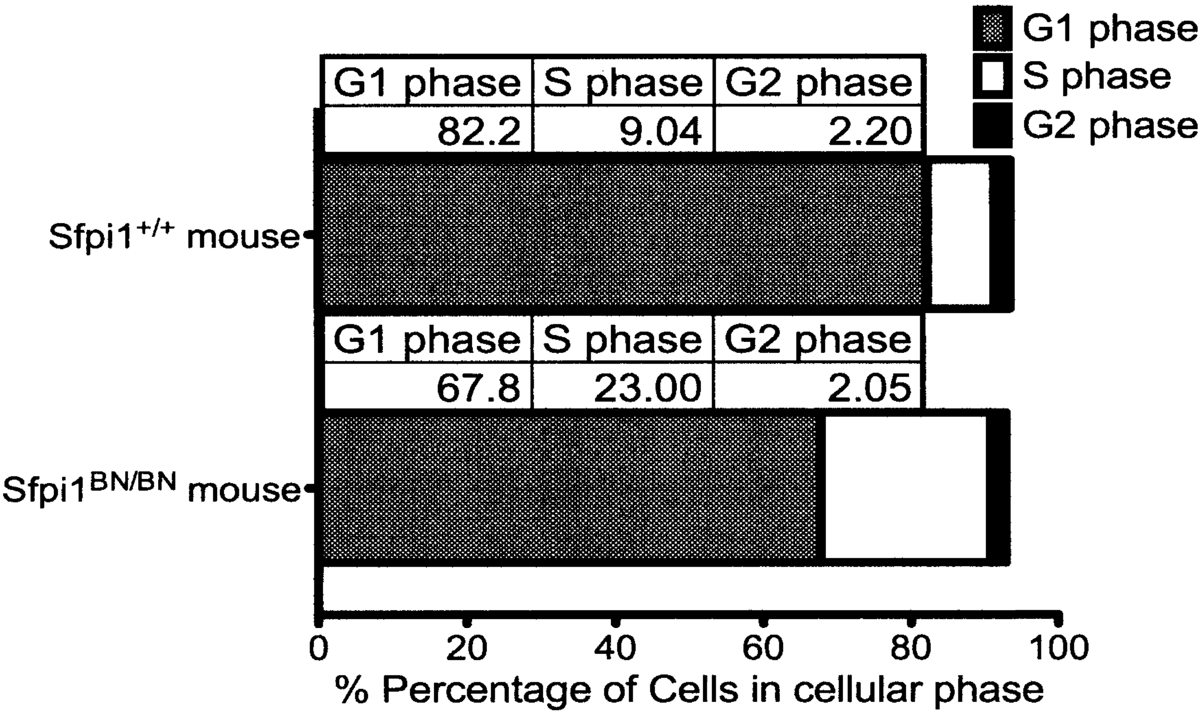

| G1 phase | S phase | G2 phase |
|---|---|---|
| 82.2 | 9.04 | 2.20 |

| G1 phase | S phase | G2 phase |
|---|---|---|
| 67.8 | 23.00 | 2.05 |

## 3.2 Reduced PU.1 levels results in increased serial colony formation ability in differentiating cytokine conditions

Hematopoietic progenitors stimulated with GM-CSF promote differentiation, such towards a myeloid cell type (120). Therefore, *Sfpi1*$^{BN/BN}$ cells were tested to determine whether they were able to differentiate normally towards the myeloid lineage in differentiating cytokine conditions. In addition, serial colony forming assays were performed to determine whether these cells have lost the ability to self-renewal *in-vitro*. If colony-forming capacity is arrested, then differentiated cells have lost the ability to self-renew. To test this, timed matings were performed to obtain embryonic day 14.5 (E14.5) fetal livers. This time point was chosen since it is the time point where maximal hematopoiesis is occurring in the livers of mice (12). After the fetal livers were phenotyped and homogenized to single cell suspensions, they were placed in methylcellulose media containing either GM-CSF or IL-3/ IL-6/ SCF (Figure 2.1). After 1 week total colony numbers were counted, cells were harvested, resuspended and replated in fresh methylcellulose media containing either cytokine cocktail.

When *Sfpi1*$^{+/+}$ or *Sfpi1*$^{+/BN}$ fetal liver cells were plated in GM-CSF, colony formation occurred for approximately 2 to 3 replatings after which no colonies formed. When *Sfpi1*$^{BN/BN}$ fetal liver cells were plated in GM-CSF, colony formation was significantly higher and occurred for up to 10 replatings compared to *Sfpi1*$^{+/+}$ or *Sfpi1*$^{+/BN}$ fetal liver cell controls (Figure 3.5). The experiment was terminated at the end of 10 weeks. At the end of the 10-week period, cells could be maintained in liquid culture as a cell line. Similar results were seen when

**Figure 3.5 *Sfpi1*$^{BN/BN}$ fetal liver cells expressing reduced levels of PU.1 can be cultured indefinitely in GMCSF or IL3/IL6/SCF.**

Colony formation assays were performed on fetal liver cells expressing wild-type allele of PU.1 (*Sfpi1*$^{+/+}$), heterozygous for BN allele (*Sfpi1*$^{+/BN}$) and homozygous for BN allele (*Sfpi1*$^{BN/BN}$) in various differentiating cytokine combinations. **(A) Serial colony forming assay in GM-CSF.** Fetal liver cells were grown in the differentiating cytokine GM-CSF after stimulation with IL3/IL6/SCF. Bar graph shows number of colonies per 50,000 cells plated. Significance was determined used a repeated measures ANOVA followed by a Tukey's post test. Bar graph represents average cell count +/- standard deviation of 3 experiments. **(B) Serial colony forming assay in IL-3/ IL-6/ SCF.** Fetal liver cells were grown in a differentiating cytokine combination of IL3/IL6/SCF. Bar graph shows the number of colonies per 50000 cells plated. Significance was determined used a paired T-test. Bar graph represents average cell count +/- standard deviation of 3 experiments. **(C) Cellular viability after transfer media supplemented with different cytokines.** Cell lines of *Sfpi1*$^{BN/BN}$ cultured in IL3 were washed 3 times with PBS, then cultured in media for 72 hours containing GM-CSF, IL3 or IMDM. Bar graph shows total number of viable cells measured by trypan blue exclusion. Graph represents average cell count +/- standard deviation of 3 experiments.

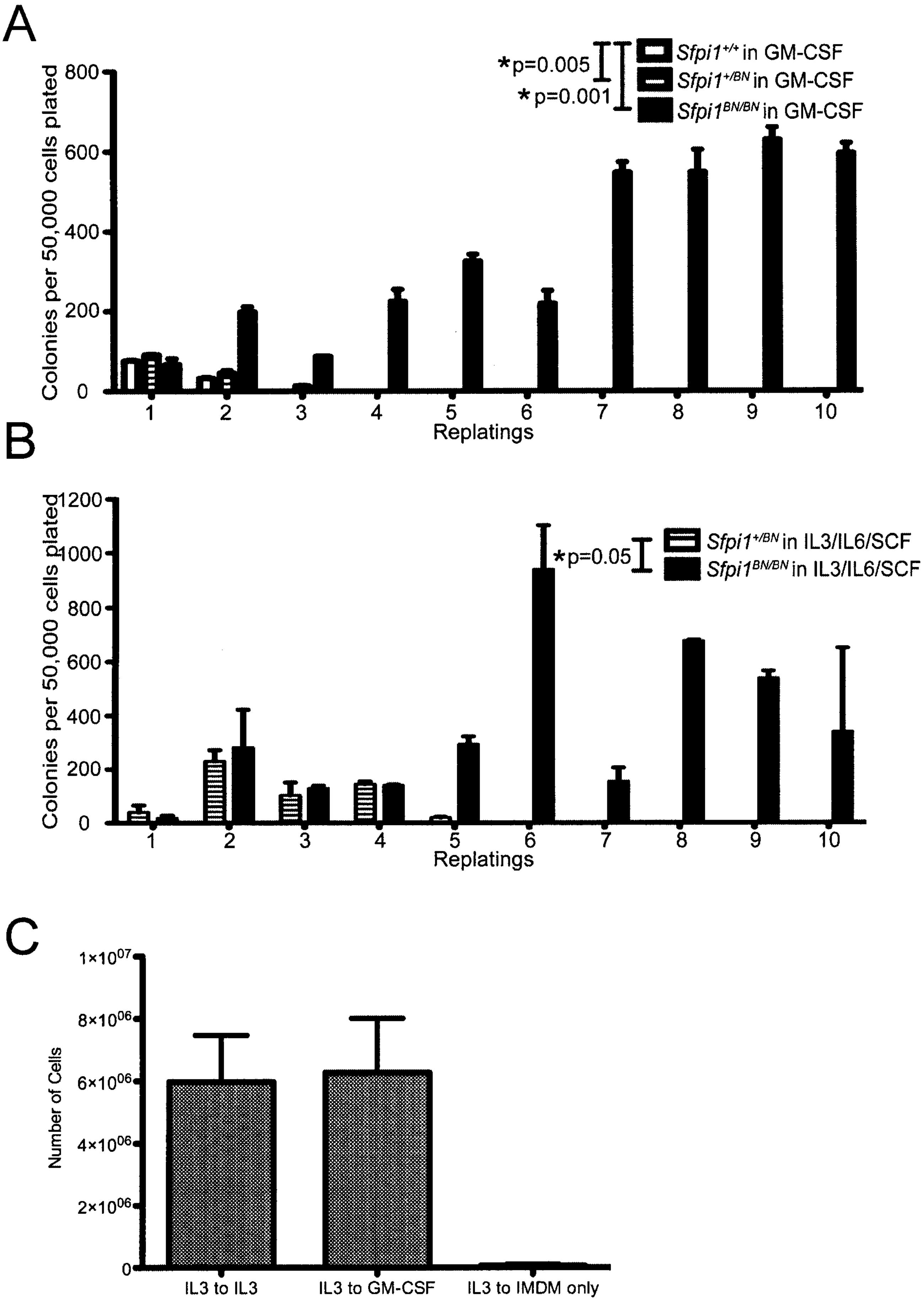
A
*p=0.005
*p=0.001
Sfpi1+/+ in GM-CSF
Sfpi1+/BN in GM-CSF
Sfpi1BN/BN in GM-CSF
Colonies per 50,000 cells plated
0
200
400
600
800
1
2
3
4
5
6
7
8
9
10
Replatings
B
*p=0.05
Sfpi1+/BN in IL3/IL6/SCF
Sfpi1BN/BN in IL3/IL6/SCF
Colonies per 50,000 cells plated
0
200
400
600
800
1000
1200
1
2
3
4
5
6
7
8
9
10
Replatings
C
Number of Cells
0
2×10^06
4×10^06
6×10^06
8×10^06
1×10^07
IL3 to IL3
IL3 to GM-CSF
IL3 to IMDM only

*Sfpi1*$^{BN/BN}$ cells were plated in a cytokine combination of IL-3/IL-6/SCF. These cells were able to proliferate indefinitely, whereas the *Sfpi1*$^{+/BN}$ controls stopped replating after approximately 4-5 weeks (Figure 3.5B). These cells also had the ability to be maintained as a cell line grown in liquid media containing IL-3. Furthermore, *Sfpi1*$^{BN/BN}$ cells, which were grown in liquid media, could be washed and transferred into liquid culture containing either IL-3 or GM-CSF demonstrating that they expressed the receptor for either cytokine (Figure 3.5C). This data confirmed that hematopoietic cells with reduced expression of PU.1 were able to serially replate indefinitely in the presence of differentiating cytokines. This shows that *Sfpi1*$^{BN/BN}$ myeloid progenitors are unable to terminally differentiate to myeloid cells.

## 3.3 Knockdown of PU.1 by miRNA results in increased colony formation in differentiating cytokine conditions

To determine whether knocking down PU.1 in *Sfpi1*$^{+/+}$ or *Sfpi1*$^{+/BN}$ fetal liver would result in increased proliferation, several miRNAs were designed to target the *Sfpi1* transcript. In order to assess the ability of each retroviral vector to "knock down" PU.1 protein expression, retroviral infection of the WEHI3B myeloid cell line was performed. Lysates were prepared from uninfected WEHI3B cells and from cells infected with each retroviral vector, LMP-PU1.1 and LMP-PU1.3. Western blot against PU.1 demonstrated that LMP-PU.1-1 was more effective at knocking down compared to LMP-PU.1-3 (Fig. 3.6A). Densitometry suggested that LMP-PU.1-1 was able to reduce PU.1 expression by approximately 90% (Figure 3.6A).

Before performing retroviral infection on fetal liver cells, hematopoetic

**Figure 3.6 Fetal liver cells expressing normal levels of PU.1 retrovirally infected with the PU.1 silencing shRNA LMP-PU.1-1 display increased self renewal compared to uninfected controls.**

**(A) PU.1 knockdown Western Blot and densitometric analysis** Densitometric analysis of a Western blot comparing uninfected, LMP-PU.1-1 and LMP-PU.1-3 WEHI-3B cells. LMP-PU.1-1 showed an approximate 90% knockdown of PU.1 levels whereas LMP-PU.1-3 showed an approximate 50% knockdown of PU.1 levels. **(B) Serial colony forming assay following PU.1 knockdown** Colony formation assays were performed on fetal liver cells expressing wild-type allele of PU.1 (*Sfpi1*$^{+/+}$), heterozygous for BN allele (*Sfpi1*$^{+/BN}$) after infection with PU.1 silencing shRNA LMP-PU.1-1. Bar graph displays total amount of colonies per 50,000 cells plated. Significance was determined used a repeated measures ANOVA followed by a Tukey's posttest. Graph represents average cell count +/- standard deviation of 3 experiments.

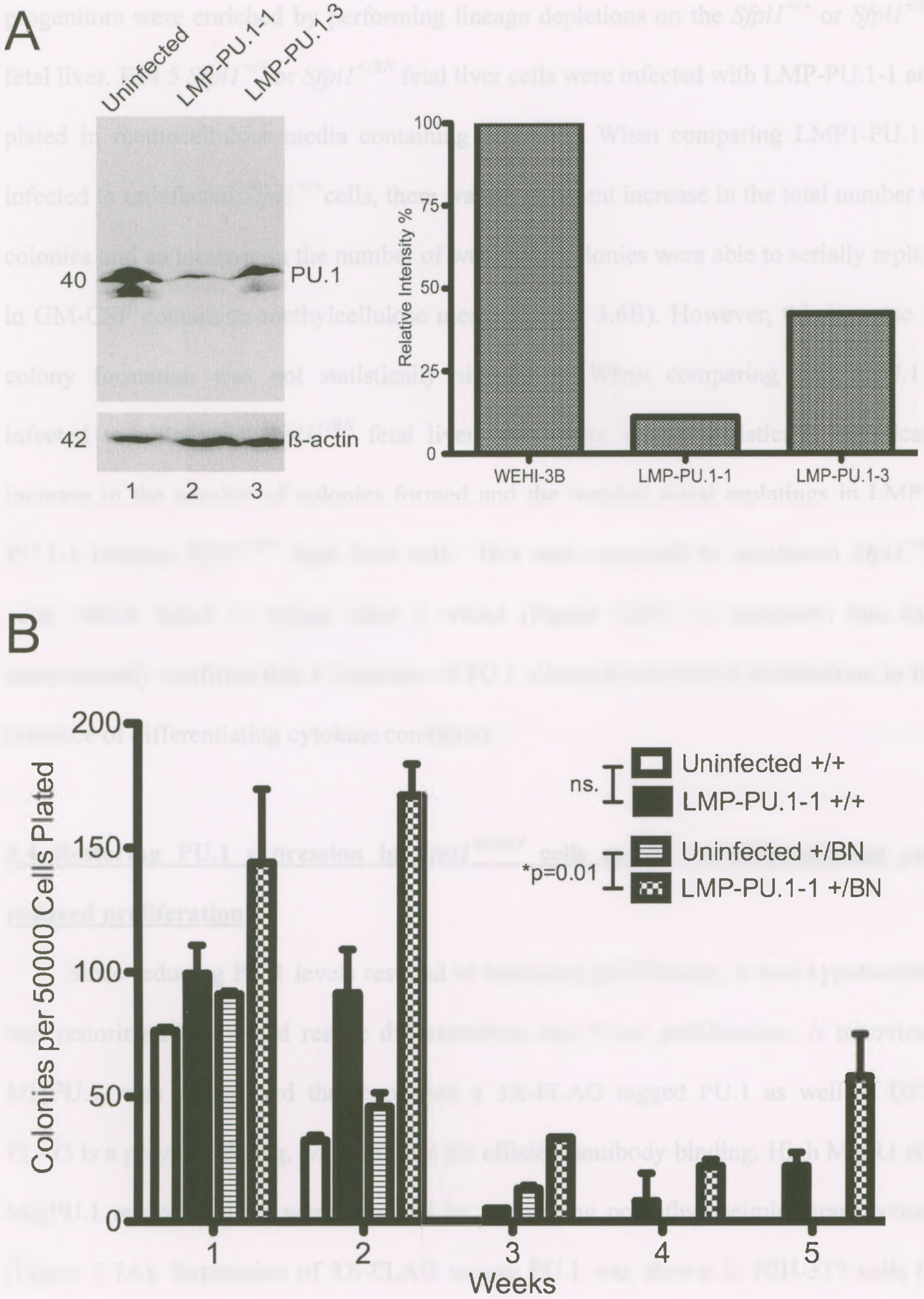
A
Uninfected
LMP-PU.1-1
LMP-PU.1-3
40
PU.1
42
ß-actin
1
2
3
Relative Intensity %
100
75
50
25
0
WEHI-3B
LMP-PU.1-1
LMP-PU.1-3
B
Colonies per 50000 Cells Plated
200
150
100
50
0
1
2
3
4
5
Weeks
ns.
*p=0.01
Uninfected +/+
LMP-PU.1-1 +/+
Uninfected +/BN
LMP-PU.1-1 +/BN

progenitors were enriched by performing lineage depletions on the *Sfpi1*$^{+/+}$ or *Sfpi1*$^{+/BN}$ fetal liver. E14.5 *Sfpi1*$^{+/+}$ or *Sfpi1*$^{+/BN}$ fetal liver cells were infected with LMP-PU.1-1 and plated in methocellulose media containing GM-CSF. When comparing LMP1-PU.1-1 infected to uninfected *Sfpi1*$^{+/+}$cells, there was a consistent increase in the total number of colonies and an increase in the number of weeks the colonies were able to serially replate in GM-CSF containing methylcellulose media (Figure 3.6B). However, this increase in colony formation was not statistically significant. When comparing LMP1-PU.1-1 infected to uninfected *Sfpi1*$^{+/BN}$ fetal liver cells, there was a statistically significant increase in the number of colonies formed and the number serial replatings in LMP1-PU.1-1 infected *Sfpi1*$^{+/BN}$ fetal liver cells. This was compared to uninfected *Sfpi1*$^{+/BN}$ cells, which failed to replate after 3 weeks (Figure 3.6B). In summary, this data independently confirms that a reduction of PU.1 allows for increased proliferation in the presence of differentiating cytokine conditions.

### 3.4 Restoring PU.1 expression in *Sfpi1*$^{BN/BN}$ cells results in differentiation and reduced proliferation

Since reducing PU.1 levels resulted in increased proliferation, it was hypothesized that restoring PU.1 would rescue differentiation and arrest proliferation. A retrovirus, MigPU.1, was constructed that expresses a 3X-FLAG tagged PU.1 as well as GFP. FLAG is a polypeptide tag, which allows for efficient antibody binding. High MigR1 and MigPU.1 retroviral titers were obtained by performing polyethyleneimine transfections (Figure 3.7A). Expression of 3X-FLAG tagged PU.1 was shown in NIH-3T3 cells by Western Blot (Figure 3.7B).

**Figure 3.7 Production of MigR1 and MigPU.1 retroviruses.**

**(A) MigR1 and MigPU.1 transfected cells** Images taken with an inverted fluorescent microscope (Zeiss Axio-Observer) showing GFP expression in MigR1 and MigPU.1 transfected PlatE cells at a 10x magnification. Scale bar represents 49.5 γm. **(B) Western blot for PU.1 and FLAG from MigR1 and MigPU.1 infected NIH-3T3 cell lysates.** Upper panel shows Western blot using anti-PU.1 antibodies of MigR1 and MigPU.1 infected NIH-3T3 cells. Middle panel shows Western blot using anti-FLAG antibodies of MigR1 and MigPU.1 infected NIH-3T3 cells. Lower panel shows Western blot using anti-ß-actin antibodies of MigR1 and MigPU.1 infected NIH-3T3 cells.

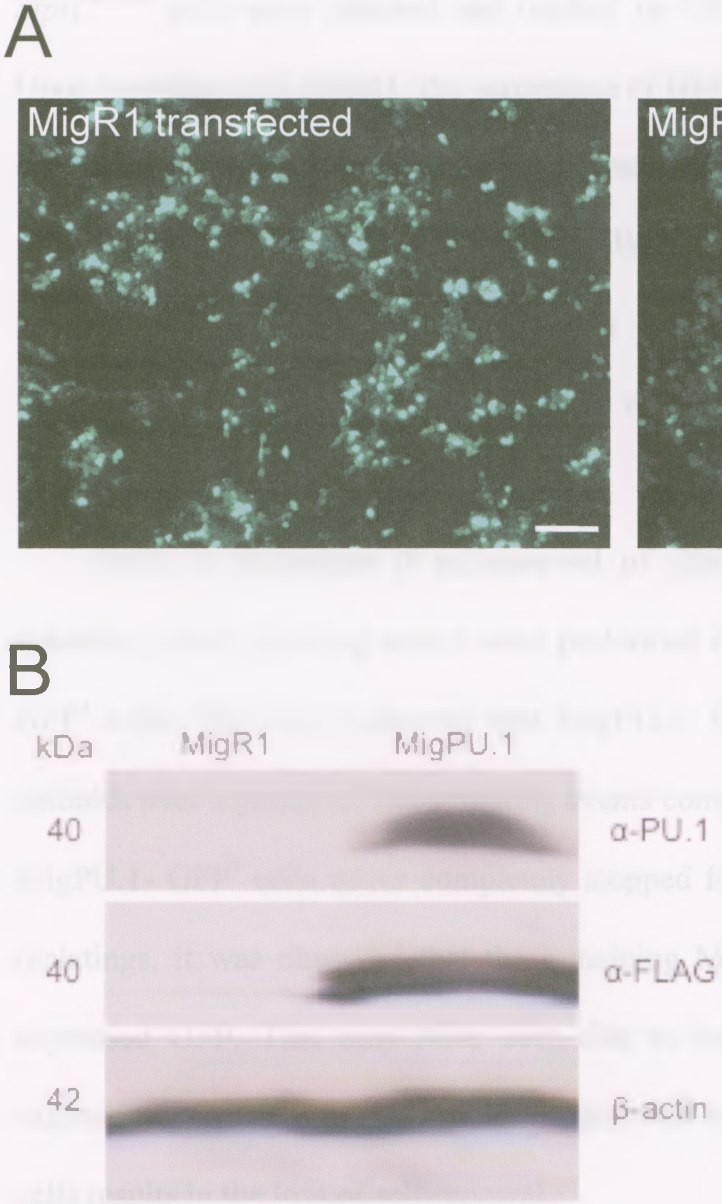
A
MigR1 transfected
MigPU.1 transfected
B
kDa
MigR1
MigPU.1
40
α-PU.1
40
α-FLAG
42
β-actin

*Sfpi1*$^{BN/BN}$ cells were infected and tracked by GFP expression levels in liquid culture. Upon infection with MigR1, the percentage of GFP$^{+}$ cells remained relatively constant over the period of the experiment. This suggested that proliferation was occurring at the same rate in infected cells as uninfected cells. Upon infection with MigPU.1, the percentage of GFP$^{+}$ cells decreased over time (Figure 3.8A). This suggested that MigPU.1 infected cells had reduced proliferation compared to uninfected cells.

Next, to determine if self-renewal of *Sfpi1*$^{BN/BN}$ cells was lost upon MigPU.1 infection, serial replating assays were performed on sorted MigR1- GFP$^{+}$ and MigPU.1- GFP$^{+}$ cells. The results showed that MigPU.1- GFP$^{+}$ cells formed significantly fewer colonies over a period of five replating events compared to MigR1- GFP$^{+}$ cells. While the MigPU.1- GFP$^{+}$ cells never completely stopped forming colonies at the end of the five replatings, it was observed that the remaining MigPU.1 infected cells were no longer expressed GFP. This may have been due to inefficient sorting or loss of MigPU.1 expression over time. These results suggest that restoring PU.1 expression in *Sfpi1*$^{BN/BN}$ cells results in the loss of self-renewal.

MigPU.1 infected cells became much larger and complex intracellularly compared to MigR1 and uninfected controls (Figure 3.9). This suggested that these cells were terminally differentiating towards the myeloid lineage. To test this idea, flow cytometry was performed on MigR1 and MigPU.1 infected cells. Analysis of forward scatter patterns, which demonstrate the relative size of the cells, revealed that MigPU.1 infected *Sfpi1*$^{BN/BN}$ cells were larger than MigR1 infected *Sfpi1*$^{BN/BN}$ cells. Analysis of side scatter patterns, which demonstrate the intracellular complexity of cells, revealed that MigPU.1

**Figure 3.8 Self-renewal is reduced in Sfpi1$^{BN/BN}$ cells retrovirally infected with PU.1.**

**(A) GFP expression in MigR1 and MigPU.1 infected Sfpi1$^{BN/BN}$ cells** *Sfpi1*$^{BN/BN}$ cells cultured in GM-CSF were retrovirally infected with PU.1 (MigPU.1) or an empty retroviral backbone as a control (MigR1). After infection, cells were cultured in media containing GM-CSF, and GFP levels of the cells were measured at multiple time points post-infection by flow cytometry. Graph shows relative GFP expression levels standardized to maximal GFP expression at 48-post infection. Significance was determined used a paired T-test. Graphs represents average cell count +/- standard deviation of 3 experiments. **(B) Serial colony forming assay of sorted MigR1-GFP$^+$ and MigPU.1-GFP$^+$ *Sfpi1*$^{BN/BN}$ cells.** *Sfpi1*$^{BN/BN}$ cells cultured in GM-CSF were retrovirally infected with endogenous PU.1 or an empty retroviral backbone as a control (MigR1) and flow cytometrically sorted to obtain a pure population of GFP+ cells, after which cells were placed in colony forming assays with GM-CSF. Significance was determined used a paired T-test. Graphs represents average cell count +/- standard deviation of 3 experiments.

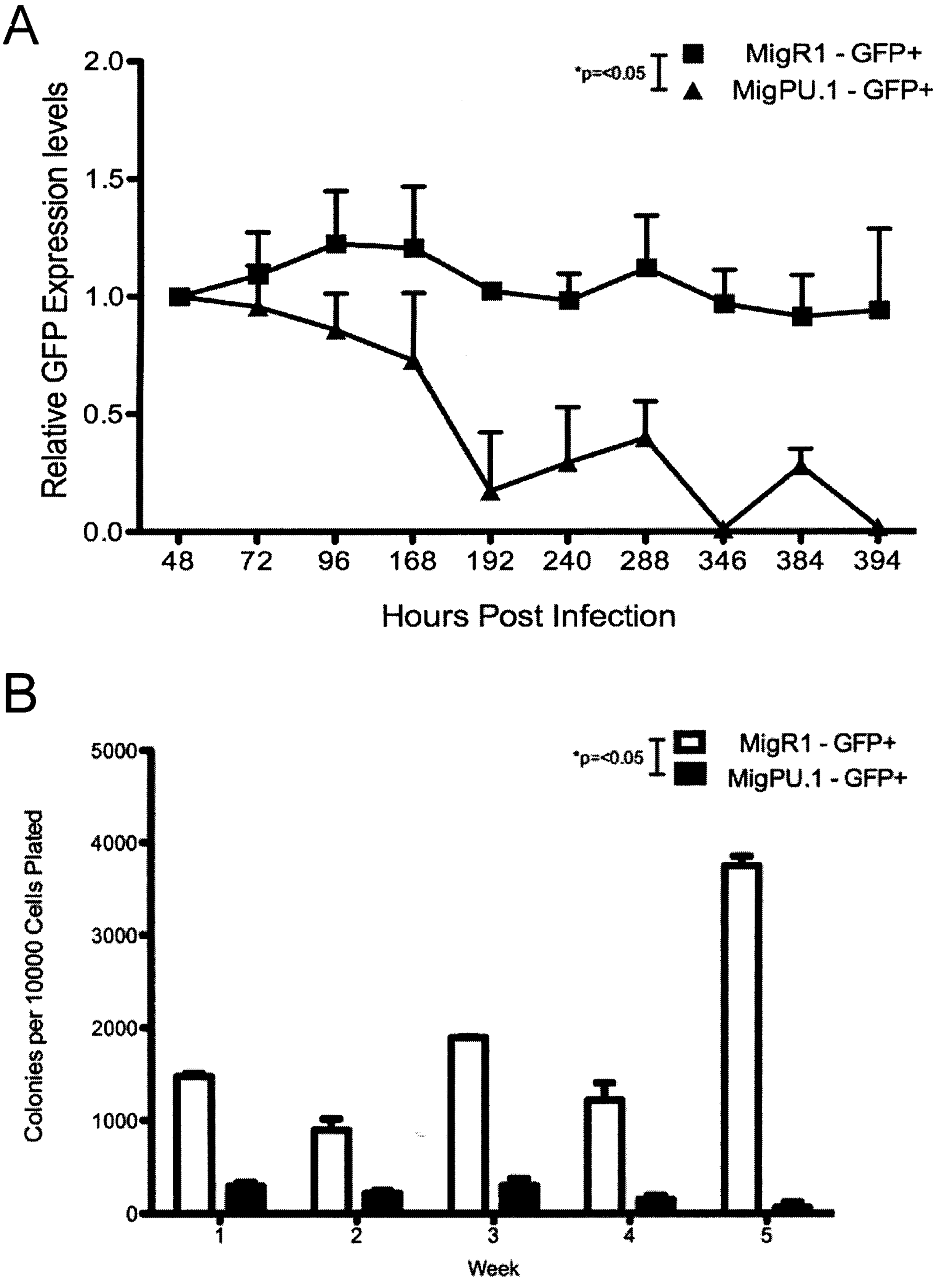
A
Relative GFP Expression levels
2.0
1.5
1.0
0.5
0.0
48
72
96
168
192
240
288
346
384
394
Hours Post Infection
*p=<0.05
■ MigR1 - GFP+
▲ MigPU.1 - GFP+
B
Colonies per 10000 Cells Plated
5000
4000
3000
2000
1000
0
1
2
3
4
5
Week
*p=<0.05
☐ MigR1 - GFP+
■ MigPU.1 - GFP+

**Figure 3.9 MigPU.1 infected *Sfpi1*$^{BN/BN}$ cells appear to change in morpholgy.**

Upon infection with MigPU.1, cells appear to be much larger and more complex intracellularly compared to MigR1 infected cells when looking under an inverted fluorescent microscope (Zeiss Axio-observer) at a magnification of 32x. Scale bar represents 15.5 γm.

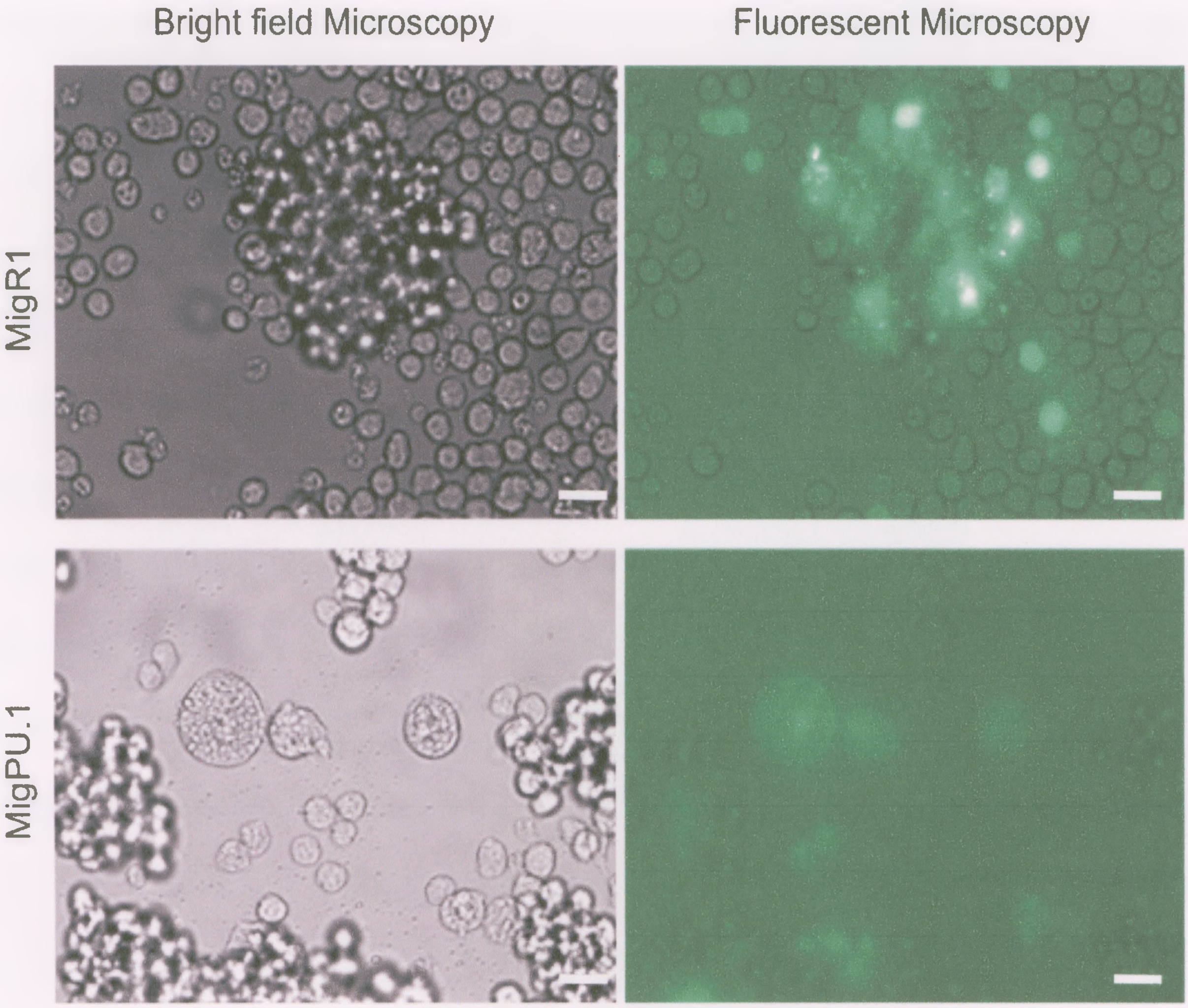
Bright field Microscopy
Fluorescent Microscopy
MigR1
MigPU.1

**Figure 3.10 *Sfpi1*$^{BN/BN}$ cells infected with MigPU.1 increase in size, intracellular complexity and upregulate CD11b expression**

The upper panel displays a histogram of MigR1 infected (open histogram) and MigPU.1 infected (filled histogram) *Sfpi1*$^{BN/BN}$ cells forward scatter pattern displayed as % of max (the % of Max is the normalize amount of cells, the % of Max is the number of cells in each bin divided by the number of cells in the bin that contains the largest number of cells). The middle panel displays a histogram of MigR1 infected (open histogram) and MigPU.1 infected (filled histogram) *Sfpi1*$^{BN/BN}$ cells side scatter pattern displayed as % of max. The lower panel displays a histogram of MigR1 infected (open histogram) and MigPU.1 infected (filled histogram) *Sfpi1*$^{BN/BN}$ cells CD11b staining pattern displayed as % of maximum. Significance was determined used a paired T-test. Representative graph of 3 experiments.

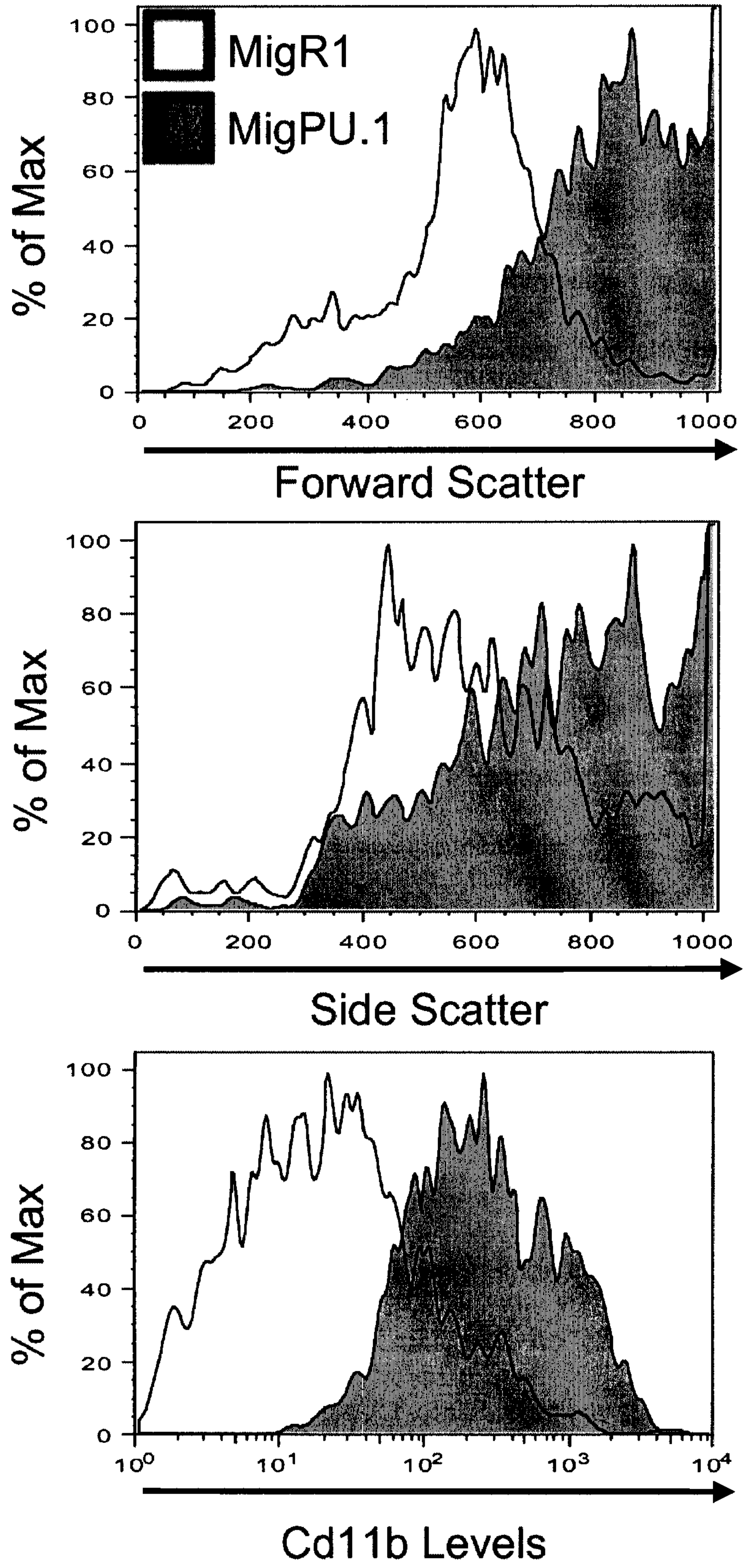
MigR1
MigPU.1
% of Max
100
80
60
40
20
0
0
200
400
600
800
1000
Forward Scatter
% of Max
100
80
60
40
20
0
0
200
400
600
800
1000
Side Scatter
% of Max
100
80
60
40
20
0
$10^0$
$10^1$
$10^2$
$10^3$
$10^4$
Cd11b Levels

infected *Sfpi1*$^{BN/BN}$ cells were more complex intracellularly compared to MigR1 infected *Sfpi1*$^{BN/BN}$ cells. Finally, analysis of CD11b, a myeloid lineage marker, showed that the mean fluorescence intensity (MFI) was increased in MigPU.1 infected *Sfpi1*$^{BN/BN}$ cells compared to MigR1 infected *Sfpi1*$^{BN/BN}$ cells, which suggest that these cells were terminally differentiating to the myeloid lineage. In summary, these results suggest that when PU.1 is restored in *Sfpi1*$^{BN/BN}$ cells, these cells lose their ability to proliferate and begin to terminally differentiate.

## **3.5 PU.1 controls the cell cycle by reducing E2F1 expression levels**

The experiments described above show that reduced expression of PU.1 results in increased proliferation. However, the mechanism by which PU.1 might control proliferation and the cell cycle is unknown. To determine the mechanism, transcript levels of various cell cycle regulators were compared in *Sfpi1*$^{+/+}$ and *Sfpi1*$^{BN/BN}$ cells. Spleens from *Sfpi1*$^{+/+}$ and *Sfpi1*$^{BN/BN}$ mice were collected and myeloid lineage cells were sorted based on the gating strategy described in Figure 3.11A. CD11b$^{+}$, c-Kit$^{-}$ cells were selected from *Sfpi1*$^{+/+}$ mice to represent the phenotypically normal macrophage population. The CD11b$^{low}$, c-Kit$^{+}$ population was selected in the *Sfpi1*$^{BN/BN}$ mice since this is the population which represents immature myeloid progenitors and would most likely show the largest difference in transcript levels in PU.1 target genes. Cell cycle regulators were analyzed by RT-qPCR including: p16, p21, p27, Rb, e2f1, e2f2, and e2f7. CD11b and c-Kit acted as internal controls for the RT-qPCR reactions since the cells were sorted based on CD11b and c-Kit levels. The only regulator for which transcript levels were significantly changed was E2F1, which promotes G1 to S phase progression.

**Figure 3.11 Determining cell cycle regulators under the control of PU.1 using *Sfpi1*$^{BN/BN}$ and *Sfpi1*$^{+/+}$ mice.**

**(A) Gating strategy for cell sorting.** The gating strategy used to obtain myeloid cells used to compare transcript levels between *Sfpi1*$^{BN/BN}$ and *Sfpi1*$^{+/+}$ mice. Cells used for RT-qPCR include CD11b$^{+}$c-Kit$^{-}$ from *Sfpi1*$^{+/+}$ mice as well CD11b$^{lo}$c-Kit$^{+}$ from *Sfpi1*$^{BN/BN}$ mice **(B) Changes in transcript levels of various cell cycle regulators between *Sfpi1*$^{BN/BN}$ and *Sfpi1*$^{+/+}$ mice.** RT-qPCR was performed on multiple cell cycle regulators. The y-axis shows the fold change between control *Sfpi1*$^{+/+}$ mice and *Sfpi1*$^{BN/BN}$ mice using the comparative threshold cycle method. Each result was performed in triplicate and significance was determined using the students T-test.

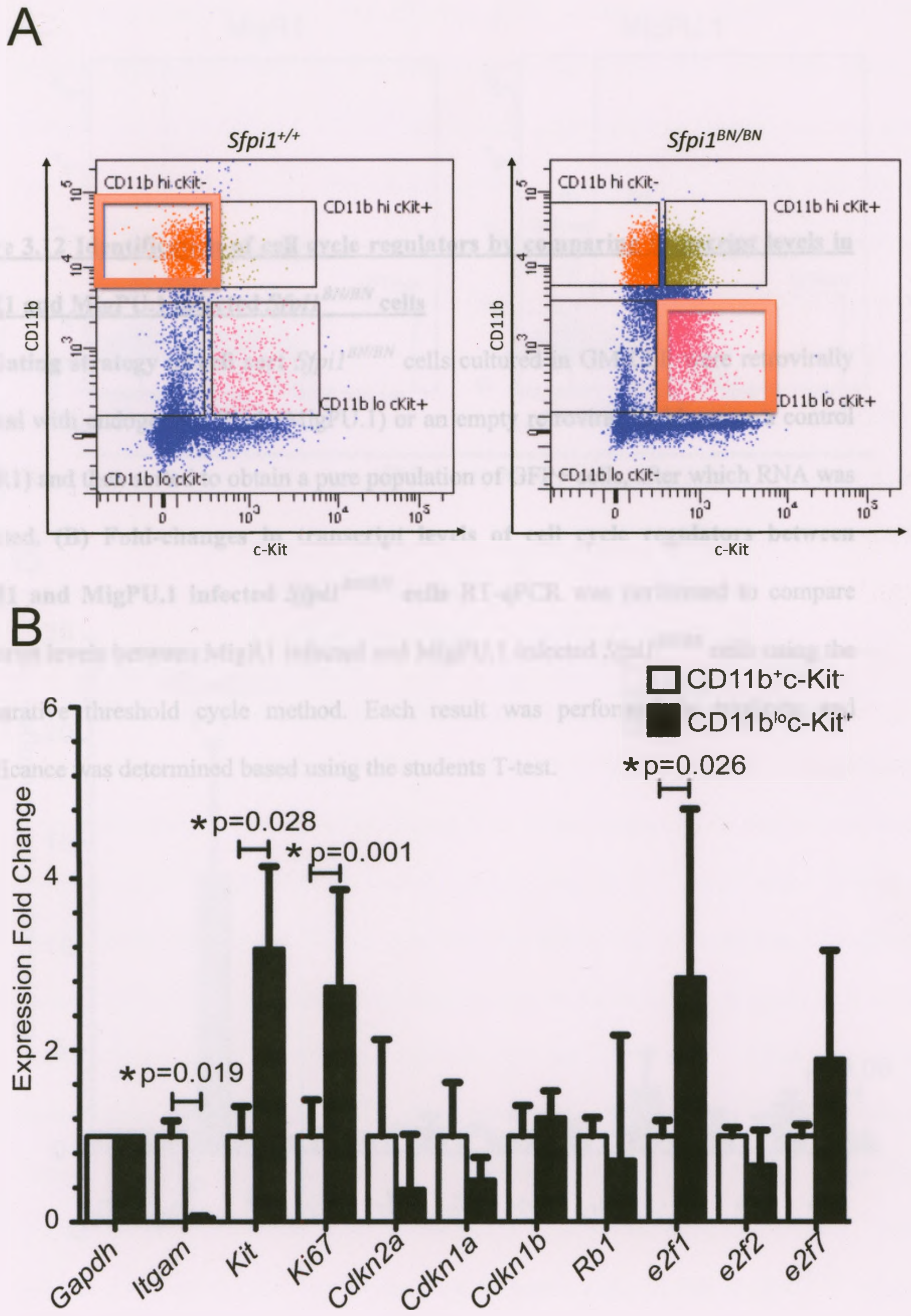
A
Sfpi1+/+
Sfpi1BN/BN
CD11b
c-Kit
CD11b hi cKit-
CD11b hi cKit+
CD11b lo cKit+
CD11b lo cKit-
0
10^3
10^4
10^5
B
CD11b+c-Kit-
CD11bloc-Kit+
Expression Fold Change
0
2
4
6
*p=0.019
*p=0.028
*p=0.001
*p=0.026
Gapdh
Itgam
Kit
Ki67
Cdkn2a
Cdkn1a
Cdkn1b
Rb1
e2f1
e2f2
e2f7

**Figure 3.12 Identification of cell cycle regulators by comparing transcript levels in MigR1 and MigPU.1 infected *Sfpi1*$^{BN/BN}$ cells**

**(A) Gating strategy of cell sort** *Sfpi1*$^{BN/BN}$ cells cultured in GM-CSF were retrovirally infected with endogenous PU.1 (MigPU.1) or an empty retroviral backbone as a control (MigR1) and then sorted to obtain a pure population of GFP+ cells, after which RNA was collected. **(B) Fold-changes in transcript levels of cell cycle regulators between MigR1 and MigPU.1 infected *Sfpi1*$^{BN/BN}$ cells** RT-qPCR was performed to compare transcript levels between MigR1 infected and MigPU.1 infected *Sfpi1*$^{BN/BN}$ cells using the comparative threshold cycle method. Each result was performed in triplicate and significance was determined based using the students T-test.

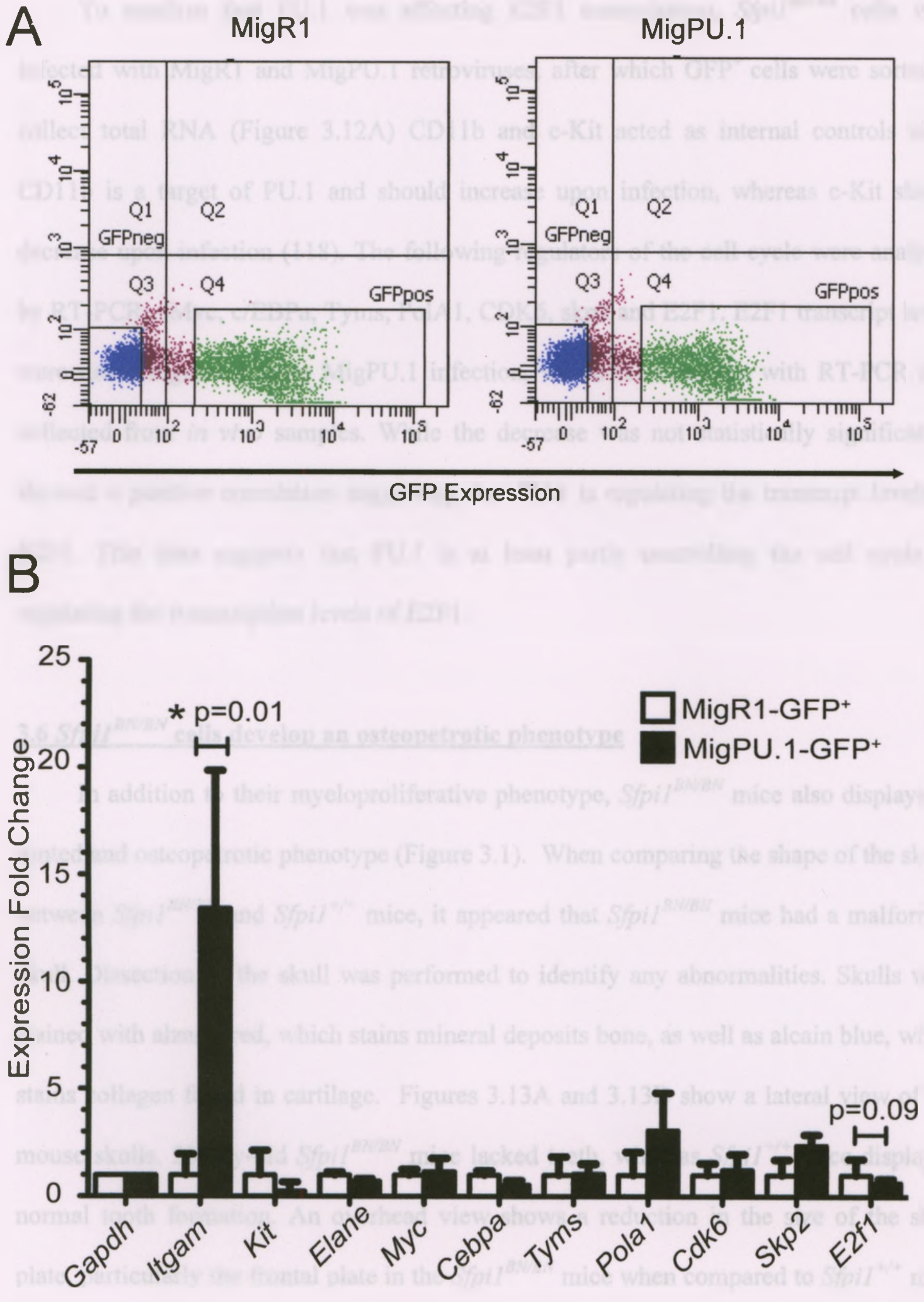
A
MigR1
MigPU.1
Q1
Q2
Q3
Q4
GFPneg
GFPpos
-62
0
$10^2$
$10^3$
$10^4$
$10^5$
-57
GFP Expression
B
25
20
15
10
5
0
Expression Fold Change
* p=0.01
p=0.09
MigR1-GFP+
MigPU.1-GFP+
Gapdh
Itgam
Kit
Elane
Myc
Cebpa
Tyms
Pola1
Cdk6
Skp2
E2f1

To confirm that PU.1 was affecting E2F1 transcription, *Sfpi1*$^{BN/BN}$ cells were infected with MigR1 and MigPU.1 retroviruses, after which GFP$^{+}$ cells were sorted to collect total RNA (Figure 3.12A) CD11b and c-Kit acted as internal controls since CD11b is a target of PU.1 and should increase upon infection, whereas c-Kit should decrease upon infection (118). The following regulators of the cell cycle were analyzed by RT-PCR: cMyc, c/EBPa, Tyms, PolA1, CDK6, skp2 and E2F1. E2F1 transcript levels were down regulated upon MigPU.1 infection, which is consistent with RT-PCR data collected from *in vivo* samples. While the decrease was not statistically significant it showed a positive correlation suggesting that PU.1 is regulating the transcript levels of E2F1. This data suggests that PU.1 is at least partly controlling the cell cycle by regulating the transcription levels of E2F1.

### 3.6 *Sfpi1*$^{BN/BN}$ cells develop an osteopetrotic phenotype

In addition to their myeloproliferative phenotype, *Sfpi1*$^{BN/BN}$ mice also displayed a runted and osteopetrotic phenotype (Figure 3.1). When comparing the shape of the skulls between *Sfpi1*$^{BN/BN}$ and *Sfpi1*$^{+/+}$ mice, it appeared that *Sfpi1*$^{BN/BN}$ mice had a malformed skull. Dissection of the skull was performed to identify any abnormalities. Skulls were stained with alzarin red, which stains mineral deposits bone, as well as alcain blue, which stains collagen found in cartilage. Figures 3.13A and 3.13B show a lateral view of the mouse skulls. 20-day-old *Sfpi1*$^{BN/BN}$ mice lacked teeth, whereas *Sfpi1*$^{+/+}$ mice displayed normal tooth formation. An overhead view shows a reduction in the size of the skull plate, particularly the frontal plate in the *Sfpi1*$^{BN/BN}$ mice when compared to *Sfpi1*$^{+/+}$ mice (Figure 3.13C and 3.13D). Furthermore, the fontenelle failed to fuse in *Sfpi1*$^{BN/BN}$ mice as

**Figure 3.13 Alzarin red and alcain blue staining of *Sfpi1*$^{BN/BN}$ and *Sfpi1*$^{+/+}$ mouse skulls.**

Red staining indicated mineral deposits in bone, blue staining indicates collagen staining in cartilage. **(A, B) Lateral view of the mouse skulls;** *Sfpi1*$^{BN/BN}$ mice lack tooth eruption. **(C, D) Overhead view of mouse skulls.** *Sfpi1*$^{BN/BN}$ mice have a reduction in the size of the skull plate, specifically the frontal plate. **(E, F) Overhead view of mouse skulls.** *Sfpi1*$^{BN/BN}$ mice lack of fontenelle fusion and a have general reduction in the thickness of bone in the skull. (A)(C)(E) *Sfpi1*$^{+/+}$ mice (B)(D)(F) *Sfpi1*$^{BN/BN}$ mice. Scale bar is representative of 1 mm. Image representative of 1 experiment.

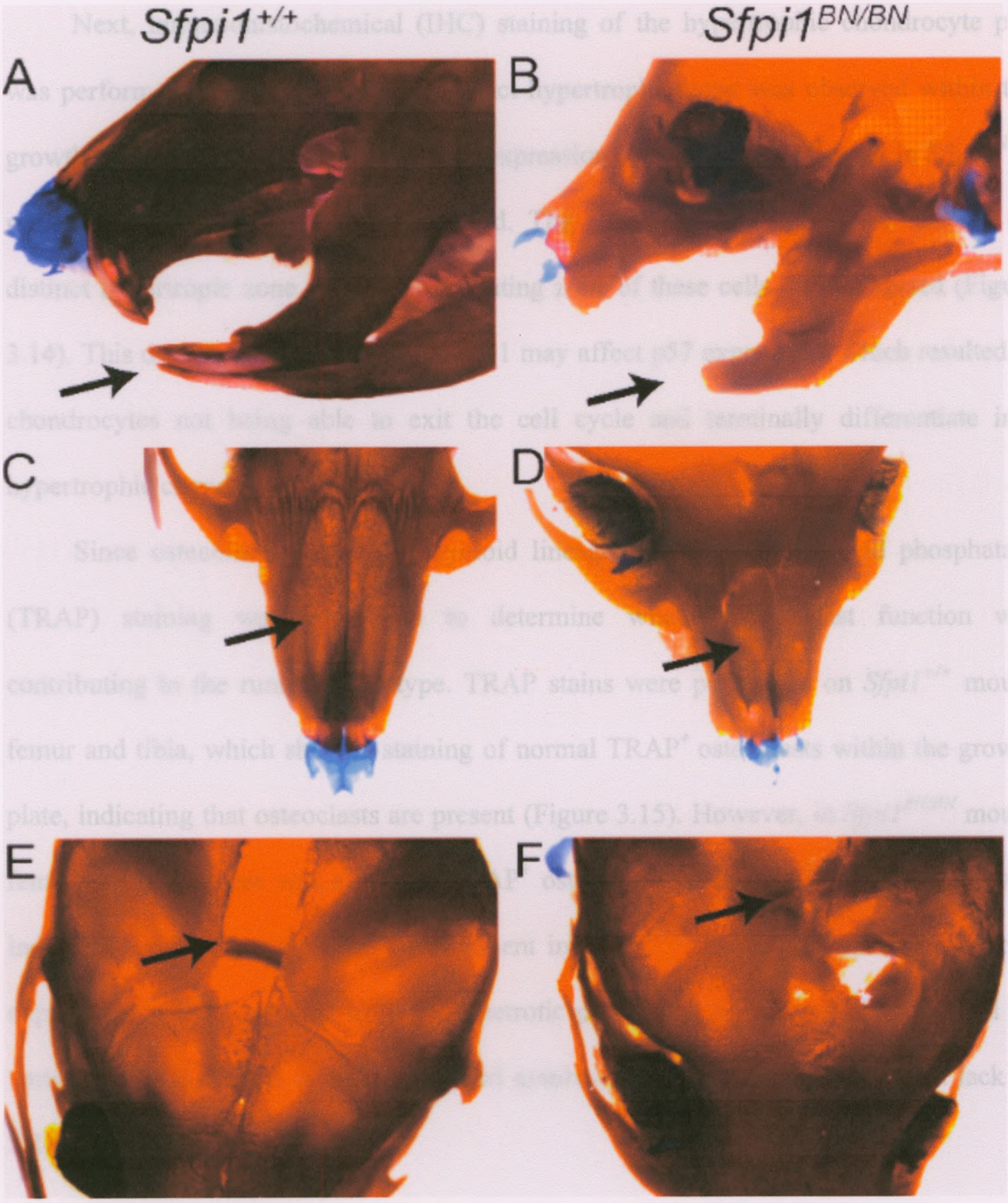
Sfpi1+/+
Sfpi1BN/BN
A
B
C
D
E
F

well an apparent reduction in bone thickness and density (Figure 3.13E, 3.13F).

Next, immunohistochemical (IHC) staining of the hypertrophic chondrocyte p57 was performed. In *Sfpi1*$^{+/+}$ mice, a distinct hypertrophic zone was observed within the growth plate based on high levels of p57 expression (Figure 3.14). However in *Sfpi1*$^{BN/BN}$ mice, p57 expression was downregulated. The remaining p57 expression showed no distinct hypertropic zone and the proliferating zone of these cells was elongated (Figure 3.14). This data suggests that reduced PU.1 may affect p57 expression, which resulted in chondrocytes not being able to exit the cell cycle and terminally differentiate into hypertrophic chondrocytes.

Since osteoclasts are of the myeloid lineage, tartrate resistant acid phosphatase (TRAP) staining was performed to determine whether osteoclast function was contributing to the runted phenotype. TRAP stains were performed on *Sfpi1*$^{+/+}$ mouse femur and tibia, which showed staining of normal TRAP$^{+}$ osteoclasts within the growth plate, indicating that osteoclasts are present (Figure 3.15). However, in *Sfpi1*$^{BN/BN}$ mouse femur and tibia, there was a lack of TRAP$^{+}$ osteoclasts within the samples. This result indicated a defect in osteoclast development in *Sfpi1*$^{BN/BN}$ mice. In summary, reduced expression of PU.1 resulted in an osteopetrotic phenotype, which was characterized by various skeletal defects including reduced numbers of p57$^{+}$ chondrocytes and a lack of TRAP$^{+}$ osteoclasts.

**Figure 3.14 p57 immunohistochemical (IHC) staining of the growth plate.**

IHC was performed on p57 on the growth plate of control *Sfpi1*$^{+/+}$ and *Sfpi1*$^{BN/BN}$ mice. Images shown were taken using a Retiga EC camera connected to a Leica DMRA2 fluorescence microscope at 10x and 40x magnification. Primary analyses were performed using OpenLab 4.0.4. software. 10x scalebar is representative of 97 γm. 40x scalebar is representative of 15 γm. Image representative of 2 experiments.

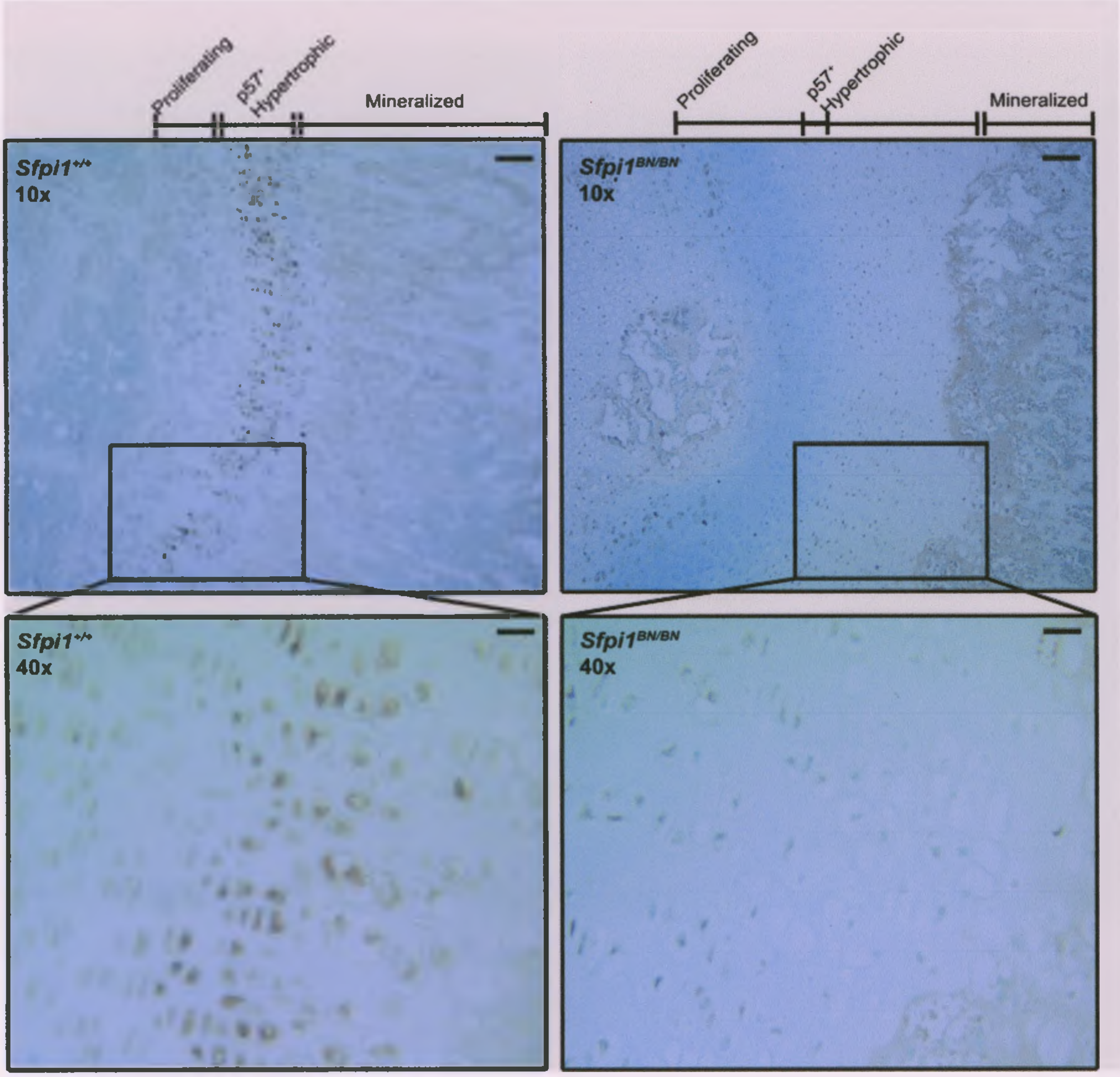
Proliferating
p57+
Hypertrophic
Mineralized
Sfpi1+/+
10x
Sfpi1BN/BN
10x
Sfpi1+/+
40x
Sfpi1BN/BN
40x

**Figure 3.15 Tartrate Resistant Acid Phosphatase (TRAP) staining of the growth plate in tibia and femur.**

TRAP staining was performed on the femur and tibia of control *Sfpi1*$^{+/+}$ and *Sfpi1*$^{BN/BN}$ mice. TRAP$^{+}$ cells are seen in purple. Images shown were taken using a Retiga EC camera connected to a Leica DMRA2 fluorescence microscope at 5x magnification. Primary analyses were performed using OpenLab 4.0.4. software. Scale bar is representative of 192 γm. Image representative of 2 experiments.

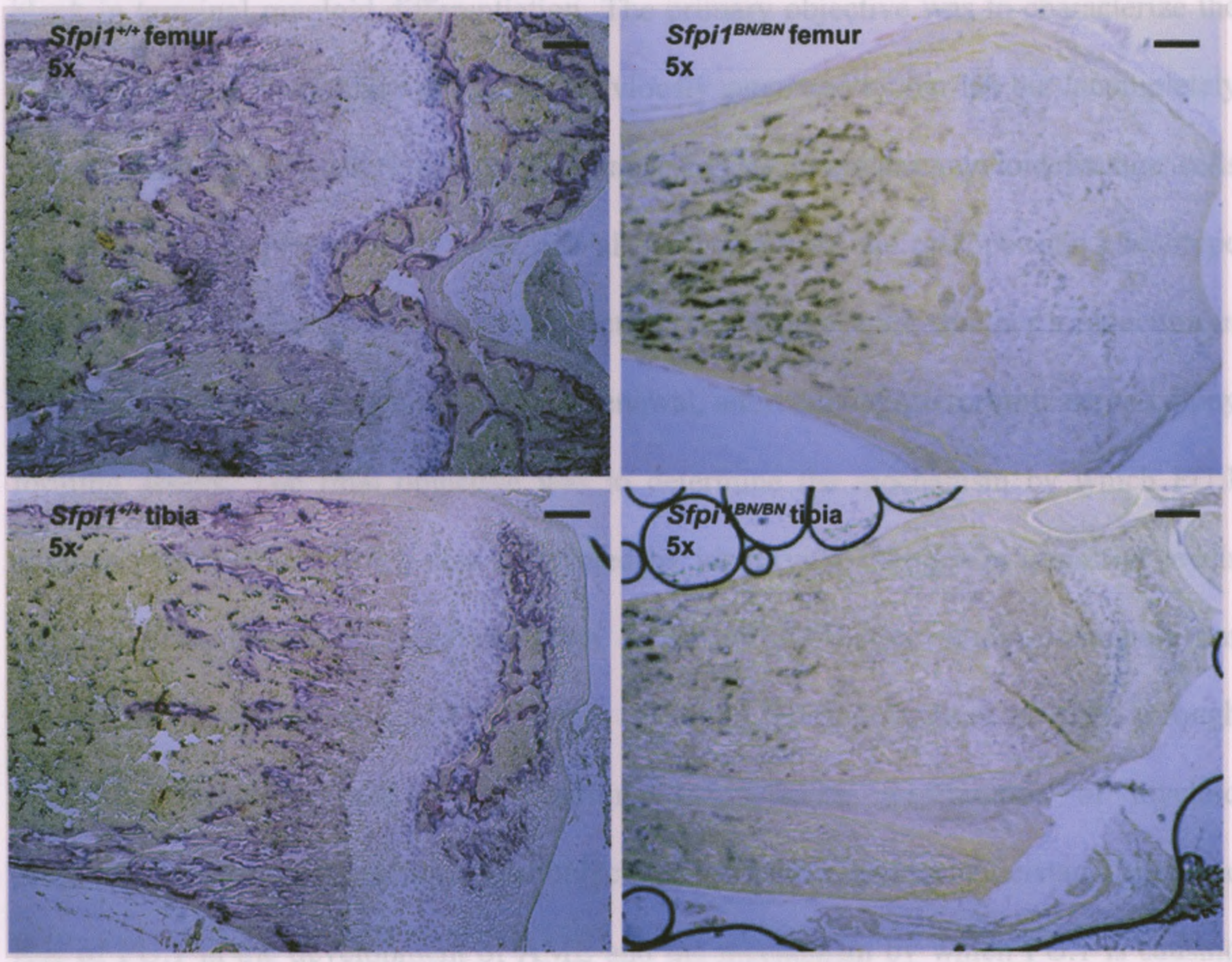
$Sfpi1^{+/+}$ femur
5x
$Sfpi1^{BN/BN}$ femur
5x
$Sfpi1^{+/+}$ tibia
5x
$Sfpi1^{BN/BN}$ tibia
5x

# CHAPTER 4: DISCUSSION

## 4.1 Overview

In this project we hypothesized that a reduction of PU.1 levels would result in the development of AML through dysregulation of the cell cycle, resulting in increased proliferation of myeloid progenitors. Furthermore, reduced PU.1 would also result in a block in terminal myeloid differentiation. The primary objective was to characterize the *Sfpi1*$^{BN/BN}$ mouse phenotype, which was previously generated by our lab but incompletely characterized. This work identified an exapansion of immature myeloid lineage cells occurring in the spleens of the mice and also characterized the osteopetrotic phenotype displayed by these mice. The second objective was to determine whether a reduction in PU.1 leads to increased myeloid cell self-renewal, addressed by performing serial colony forming assays. The final objective was to determine the mechanism by which PU.1 controls proliferation, which was completed by identifying changes in transcript levels between cells expressing low and high levels of PU.1. Our findings support our hypothesis that a reduction of PU.1 levels results in the development of AML through dysregulation of the cell cycle, resulting in increased proliferation of myeloid progenitors. By accomplishing these objectives we have a greater understanding of the role of PU.1 in the development of AML and the mechanism by which PU.1 is causing AML.

## 4.2 Cells with reduced PU.1 expression have increased self-renewal and acquire hallmarks of cancer.

This aim of this project was to characterize the *Sfpi1*$^{BN/BN}$ mouse phenotype and to show that a reduction in PU.1 expression resulted in abnormalities in myeloid differentiation. Analysis of the phenotype was performed by examining the spleen of the *Sfpi1*$^{BN/BN}$ mice and determining whether there was increased proliferation. It was determined that *Sfpi1*$^{BN/BN}$ mice had a significant expansion of CD11b$^{+}$, c-Kit$^{+}$ immature myeloid lineage cells within their spleens and Ki-67 protein levels were increased indicating increased proliferation. Furthermore, the spleens of *Sfpi1*$^{BN/BN}$ mice displayed altered cell cycle signified by the decrease in the percentage of G1 phase cells and an increase in S phase cells. This suggests increased proliferation is occurring in the spleens of *Sfpi1*$^{BN/BN}$ mice due to unregulated transition between the G1 and S-phase of the cell cycle.

As mentioned previously, the cell cycle is a tightly regulated process that has checkpoints to ensure proper progress. Breakdowns in cell cycle regulation may result in uncontrolled proliferation and cancer. This demonstrates that PU.1 levels affect one of the six hallmarks of cancer that were originally proposed in 2000 (121). The original six hallmarks include: 1) insensitivity to anti-growth signals 2) self-sufficiency in growth signals 3) evading apoptosis 4) tissue invasion and metastasis 5) sustained angiogenesis 6) limitless replicative potential (121). These hallmarks have been updated recently with the following hallmarks being added: 7) deregulating cellular energetics 8) avoiding immune destruction 9) tumor-promoting inflammation 10) genome instability & mutation (122). Increased proliferation within the spleen demonstrates the first hallmark of insensitivity to anti-growth signals within the spleen. In a normal situation, myeloid progenitors receive signals to enter a differentiated state and the cell cycle is arrested, however cancerous cells evade these signals and continue to proliferate. The G1 to S phase transition is particularly important since many oncogenes and tumor suppressors are associated with this checkpoint such as p53, retinoblastoma protein (Rb) and the E2F family of genes (123). These results imply that PU.1 may be directly regulating the expression of G1 to S phase regulators due to the altered cell cycle status of these cells.

Another hallmark of cancer and stem cells is limitless replicative potential otherwise known as self-renewal. Self-renewal is defined as the ability to undergo many cellular divisions while remaining undifferentiated. This ability is characteristic of hematopoietic stem cells and is lost during the process of differentiation. However, leukemic cells either retain this ability since they exhibit a differentiation block where they have not yet lost self-renewal ability or gain this ability by acquiring a mutation that allows self-renewal. Self-renewal ability was tested by performing serial colony-forming assays in methylcellulose media. This was confirmed by two separate tests. The first test was completed by collecting embryonic day 14.5 (E14.5) fetal liver cells from *Sfpi1*$^{+/+}$, *Sfpi1*$^{+/BN,}$ and *Sfpi1*$^{BN/BN}$ mice and placing them in methylcellulose media in the presence of the differentiating cytokines GM-CSF or in IL-3/IL-6/SCF. The second test was performed by retroviral infection containing a miRNA against PU.1, and knocking down PU.1 expression in *Sfpi1*$^{+/+}$ and *Sfpi1*$^{+/BN}$ hematopoietic progenitor cells. Both of these tests demonstrated that reduced levels of PU.1 resulted in colony formation that occurred for significantly more replatings, which suggested that these cells have increased self-renewal.

Serial colony forming assays provide useful information about the proliferative ability of cells *in vitro*, however the limitations of this assay must be acknowledged. Ideally, *in vitro* assays should be: quantitative, specific (measuring only the cells of interest), sensitive (many of the target cells are present at low frequency), and rapid (when compared to *in vivo* assays). These assays were performed in methylcellulose media that is well-defined media for demonstrating the proliferative ability of cells in differentiating cytokine conditions, with colony formation as a readout (124). Unfortunately these assays are not able to differentiate between the types of cells that are forming the colonies, either stem cells or progenitors that retained self-renewal capacity. These assays are not able to maintain stem cells efficiently since they are not the proper niche and do not provide the signals required to maintain self-renewal which are normally provided by the microenvironment. The cobblestone area-forming assay (CFAC) is one method to provide necessary signals since this assay utilizes a pre-established stromal layer, however it is labour-intensive (124). The gold standard for determining self-renewal capacity is performing *in vivo* serial transplantation assays (13, 125, 126). In these assays cells are first transplanted into a recipient mouse and evaluated for leukemia at various time points. If leukemia is detected, these cells are then engrafted to a second recipient mouse and tested for leukemia as before. While *in vivo* transplantation assays require much time as well as expenses, they remain the conclusive assay to demonstrate self-renewal.

Since reduced levels of PU.1 resulted in increased proliferation and self-renewal, the next objective was to determine whether restoring PU.1 expression forces differentiation of *Sfpi1*$^{BN/BN}$ cells and causes the cells to reverse their self-renewal capacity. This was completed by infecting *Sfpi1*$^{BN/BN}$ cell lines with MigPU.1, a retrovirus that constitutively expressed PU.1 as well as a GFP marker. Upon retroviral infection with MigPU.1, cells displayed reduced ability to proliferate and a loss in self-renewal capacity as demonstrated in serial colony forming assays as well as liquid assays. Furthermore, upon infection with MigPU.1, *Sfpi1*$^{BN/BN}$ cells showed signs of differentiation by changing their morphology and expressing terminally differentiation markers (CD11b). Together, this data demonstrates that PU.1 expression levels regulate self-renewal in cells of the myeloid lineage *in vitro*. Low levels of PU.1 expression result in increased self-renewal as well as proliferation whereas high levels of expression of PU.1 result in decreased self-renewal and promoted the ability to differentiate in the myeloid lineage.

All of these results were performed in *Sfpi1*$^{BN/BN}$ mice, however an alternative mouse model exists for graded reduction of PU.1. This mouse model was created by Dr. Tenen's group where an upstream regulatory region (URE) which decreased PU.1 expression by 80%. There are both similarities and differences when comparing the *Sfpi1*$^{BN/BN}$ mice and the URE knockout mice. Both models display a reduction in PU.1 expression levels within the myeloid lineage, however unlike *Sfpi1*$^{BN/BN}$ mice which display a global knockdown of PU.1 levels, the URE knockout mice display a PU.1 knockdown in particular lineages, whereas other lymphoid lineages display an increase in PU.1 expression. Another similarity is both models with a reduction in PU.1 die due to their reduction in PU.1, however, the *Sfpi1*$^{BN/BN}$ mice die at around 21 days of age whereas the *Sfpi1*$^{BN/BN}$ mice die anywhere from 3-9 months. Both of these mouse models experience an increase in immature myeloid cells, which are c-Kit$^{+}$, CD11b$^{+}$ and Gr-1$^{+}$.

Once significant difference between the two mice is that URE knockout mouse does not exhibit the same osteopetrotic phenotype as the *Sfpi1*$^{BN/BN}$ mice. This is an unusual observation since osteoclasts, which remodel bone, are part of the myeloid lineage and many factors required to differentiate into myeloid cells are under the control of PU.1. While the reason for the lack the osteopetrotic phenotype is unknown, it demonstrates the need for multiple models since each model may reveal different information.

### 4.3 The mechanism by which PU.1 alters the cell cycle

While PU.1 has been implicated in the development of AML, the role by which PU.1 is affecting the cell cycle is poorly understood. PU.1 has been shown to act as both a transcriptional activator and a repressor of various genes (127, 128). PU.1 was shown to affect proliferation in part through deregulated cell cycle progression at the G1 to S phase transition. Therefore, we hypothesized that PU.1 expression may be controlling G1 to S phase transition either by activating a gene involved in cell cycle repression, or repressing a gene involved in cell cycle progression.

To determine potential target genes of PU.1, quantitative real-time PCR was used to determine transcript level changes based on PU.1 expression levels. Two separate strategies were utilized to collect RNA samples. The first strategy utilized *Sfpi1*$^{BN/BN}$ cells that were infected with MigR1 and MigPU.1 and then sorted the MigR1-GFP$^{+}$ infected *Sfpi1*$^{BN/BN}$ cells and MigPU.1-GFP$^{+}$ infected *Sfpi1*$^{BN/BN}$ cells to obtain pure populations, which were used to measure differences in transcript levels. The second strategy utilized *Sfpi1*$^{+/+}$ and *Sfpi1*$^{BN/BN}$ mice and compared the transcript levels of sorted populations in the spleens. *Sfpi1*$^{+/+}$ CD11b$^{+}$, c-Kit$^{lo}$ and *Sfpi1*$^{BN/BN}$ CD11b$^{low}$, c-Kit$^{+}$ cells were sorted and used to compare gene transcript levels. This gating strategy was used because it was hypothesized that the greatest differences in transcript levels would be seen in these populations. *Sfpi1*$^{+/+}$ CD11b$^{+}$, c-Kit$^{lo}$ cells were representative of differentiated macrophages and were expected to have displayed normal cell cycle regulatory transcript levels, whereas *Sfpi1*$^{BN/BN}$ c-Kit $^{hi}$ CD11b$^{low}$ cells were immature myeloid lineage cells still regulated by PU.1. However they should have had altered levels of gene expression due to the low levels of PU.1 expression.

Since PU.1 was shown to influence the G1 to S phase cell cycle checkpoint, many cell cycle regulators were analyzed to determine whether they were controlling the cell cycle. The first hypothesis tested was whether *Tyms, Pola* and *Skp2* transcript levels were altered by PU.1. The rationale behind this hypothesis was that these genes are under the transcriptional control of *Gabpa,* which is a member of the ETS transcription factor family (129). Since all ETS family transcription factors have ETS DNA binding domains which bind to the same GGAA core motif (130), it is reasonable to believe that PU.1 may target the same genes but have a different effect. *Tyms, Pola* and *Skp2* are all required for cell cycle progression, particularly into S-phase for several reasons. The role of *Tyms* is to generate the deoxynucleotide dTTP (131), *Pola* is the DNA polymerase $\alpha$ p180 catalytic subunit that initiates DNA replication in S phase (132), *Skp2* is an E3 ligase that regulates the cell cycle-dependent ubiquitination and degradation of cell cycle inhibitors p21 and p27 (133). Therefore, our hypothesis was that one or more of *Tyms, Pola* or *Skp2* would be transcriptionally repressed by high levels of PU.1 expression. RT-qPCR analysis found that these transcript levels remained relatively unchanged upon MigPU.1 infection, suggesting that PU.1 does not control the cell cycle through these genes.

*cMyc, cEBPα* and *CDK6* were also tested by RT-qPCR to determine whether their transcript levels changed upon MigPU.1 infection. *cMyc* was chosen as a target since it is a gene commonly affected in many cancers, and was shown to be upregulated in other models where PU.1 is downregulated (76). *cEBPα* was chosen since it is also a transcription factor mutated in many forms of AML and finally CDK6 since it is important for G1 to S phase progression in the cell cycle (107, 134). RT-qPCR once again revealed no significant changes in transcript levels upon MigPU.1 infection.

Due to the technical difficulty of infecting *Sfpi1*$^{BN/BN}$ cells with retrovirus, the following sets of genes were tested by comparing transcript levels in *Sfpi1*$^{+/+}$ and *Sfpi1*$^{BN/BN}$ mouse spleens. The first set of proteins that were tested were: *p15, p16, p21* and *p27. P15* and *p16* were chosen since they are members of the INK4 family of cell cycle progression inhibitors and levels of these proteins have been shown to be altered in cases of AML, as well as interact with PU.1 (135, 136). *P21* and *p27* were chosen since they are members of the Cip/Kip family of cell cycle progression inhibitors (137). No transcripts of p15 were detected by RT-qPCR (Data not shown). Furthermore, RT-qPCR was performed on *p16, p21* and *p27* and it was shown that transcript levels for these genes were not significantly changed for any of these cell cycle regulators.

Next, retinoblastoma protein *(Rb), e2f1, e2f2* and *e2f7* transcript levels were compared by RT-PCR. Rb was chosen since it is a regulator of the E2F family of transcription factors, which controls the transcription of S-phase genes. Furthermore, it has been implicated in multiple cancers. The E2F family of genes is essential in the regulation of cellular proliferation and function in both an activating and repressive manner. *E2f1* and *e2f2* are transcriptional activators that allow for G1 to S phase progression. Overexpression of these transcription factors is sufficient to cause quiescent cells to reenter the cell cycle (111). Furthermore, in certain situations, overexpression of these transcription factors may override growth arrest signals (138-140). *E2f7* was also tested since it is a transcriptional repressor and blocks cellular proliferation (141, 142).

When RT-qPCR was performed on *Rb, e2F2* and *e2f7*, there were no significant changes found in the transcript levels. Conversely, when *E2f1*was tested it was found that transcript levels of *e2f1* were significantly increased in *Sfpi1*$^{BN/BN}$ mice where PU.1 is reduced. This supports the hypothesis that PU.1 would function by inhibiting a cell cycle regulator that promotes cell cycle progression. To confirm the results seen in *Sfpi1*$^{+/+}$ and *Sfpi1*$^{BN/BN}$ sorted cells, *e2f1* transcript levels were tested in *Sfpi1*$^{BN/BN}$ cells infected with MigR1 and MigPU.1. Upon MigPU.1 infection, e2f1 transcript was decreased, although it did not meet statistical significance. Overall these results suggest that PU.1 expression levels may be regulating *e2f1* levels, where low levels of PU.1 resulted in increased *e2f1* transcript levels which in turn result in increased proliferation.

While we have shown that PU.1 correlates with *e2f1* expression, the mechanism by which PU.1 is regulating the expression remains unclear. We hypothesize that PU.1 may be regulating *e2f1* by activating another regulator which in turn blocks *e2f1* transcription, or by directly regulating the promoter region and repressing its expression, or a combination of the two. We have generated a working hypothesis that PU.1 regulates *e2f1* transcript levels by regulation of a microRNA, miR-223. Previous data supporting the notion that PU.1 activates the expression of miR-223 in the myeloid lineage (143). MicroRNAs are tiny noncoding RNAs, which regulates the expression of target genes by binding to complementary sequences in the target gene resulting in transcript degradation or translational repression (144). MiR-223 knockout mice display defects in granulopoiesis (145). Furthermore, miR-223 is inactivated by the AML1/ ETO fusion oncoprotein, which is present in many forms of AML (146). It has also been shown that miR-223 targets *e2f1* and forms a negative feedback loop repressing *e2f1* (147). Therefore we hypothesize that PU.1 is regulating the expression microRNA, miR-223, which in turn regulates *e2f1*. Under normal conditions when PU.1 is expressed at high levels in differentiated myeloid progenitors, this would result in high levels of expression of miR-223 and in suppression of *e2f1* and cell cycle progression beyond the G1-S phase boundary. However, when PU.1 expression is repressed, miR-223 is not expressed resulting in increased E2F1 expression and continual cell cycle progression (Figure 4.1). Another mechanism by which PU.1 may be regulating *e2f1* is by directly regulating the promoter of *e2f1*. Chromatin immunoprecipitation studies of PU.1 have shown the ability of PU.1 to bind directly to the E2F1 promoter (148).

In summary, we have shown that PU.1 expression correlates with transcript levels of *e2f1*. However, it remains to be determined whether *e2f1* is directly regulated by PU.1 or if this is performed through *e2f1* is regulated by PU.1 indirectly through miR-223.

### 4.4 The osteopetrotic phenotype of *Sfpi1*$^{BN/BN}$ mice

In addition to their myeloproliferative phenotype, *Sfpi1*$^{BN/BN}$ mice also appear runted. This phenotype was investigated in greater detail to establish the role of PU.1 in skeletal development. First, *Sfpi1*$^{BN/BN}$ and *Sfpi1*$^{+/+}$ mouse skulls were stained with alzarin red to stain mineralized tissue and alcain blue which stains cartilage. It was observed that 20-day-old mice *Sfpi1*$^{BN/BN}$ mice had no tooth eruption, reduced skull plate, lack fontelle

**Figure 4.1 Proposed Mechanism of PU.1 regulation of E2F1**

**(A) Mechanism during normal PU.1 expression levels.** In situations where PU.1 is expressed at normal levels, PU.1 activates miR-223 transcription. Upon transcription, miR-223 blocks e2f1 translation, which results in G1 to S phase arrest. **(B) Mechanism during reduced PU.1 expression levels.** In situations where PU.1 is expressed at low levels, PU.1 is unable to activate miR-223 transcription. This results e2f1 transcription and translation allowing cell cycle progression. Furthermore, e2f1 further represses miR-223 transcription through a negative feedback loop.

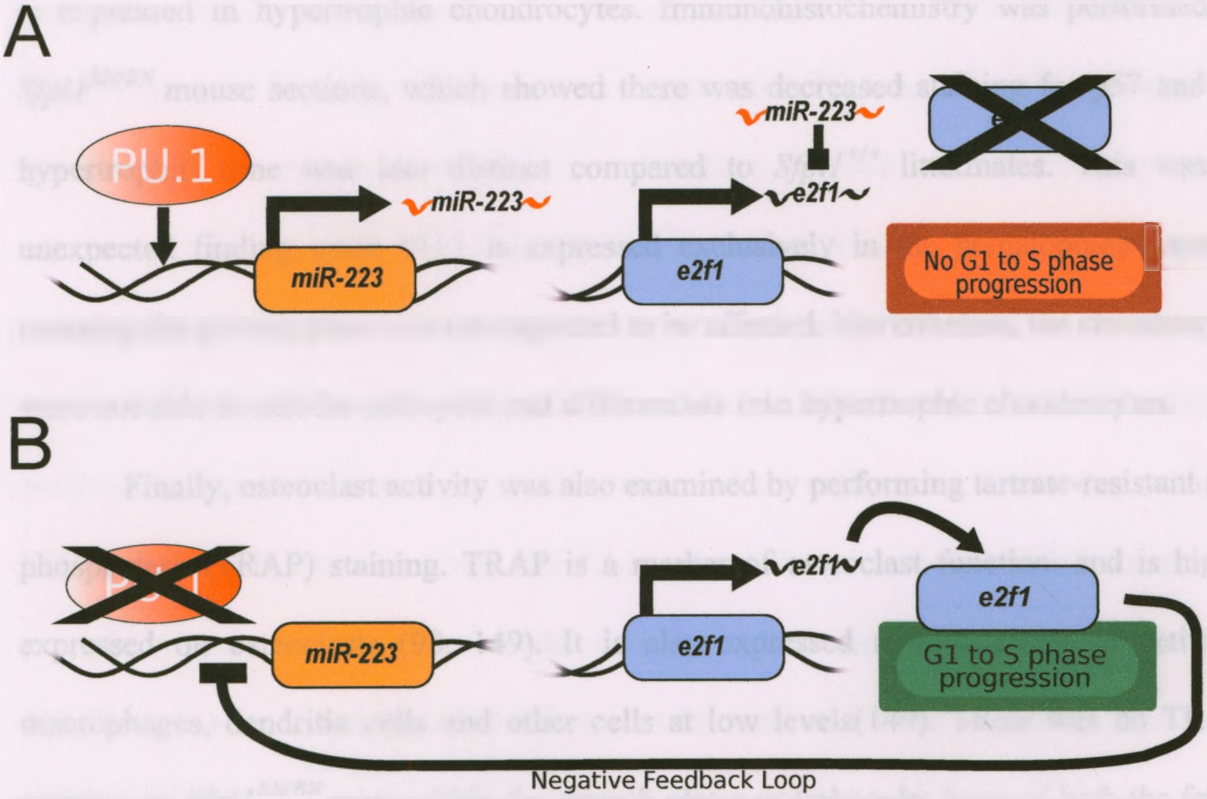
A
PU.1
miR-223
miR-223
e2f1
miR-223
e2f1
e2f1
No G1 to S phase progression
B
PU.1
miR-223
e2f1
e2f1
e2f1
G1 to S phase progression
Negative Feedback Loop

fusion, and had a general reduction in density and thickness when compared to *Sfpi1*$^{+/+}$ mouse littermates. This suggests that the mice develop some form of osteopetrosis since they are unable to remodel their bone, demonstrated with the lack of tooth eruption.

Next, the growth plates of the long bones were analyzed for p57 expression. P57 is a cell cycle regulator that arrests cells in the G1 phase. Furthermore, it is a marker that is expressed in hypertrophic chondrocytes. Immunohistochemistry was performed on *Sfpi1*$^{BN/BN}$ mouse sections, which showed there was decreased staining for p57 and the hypertrophic zone was less distinct compared to *Sfpi1*$^{+/+}$ littermates. This was an unexpected finding since PU.1 is expressed exclusively in the hematopoietic system meaning the growth plate was not expected to be affected. Nevertheless, the chondrocytes were not able to exit the cell cycle and differentiate into hypertrophic chondrocytes.

Finally, osteoclast activity was also examined by performing tartrate-resistant acid phosphatase (TRAP) staining. TRAP is a marker of osteoclast function, and is highly expressed on osteoclasts (98, 149). It is also expressed at low levels on activated macrophages, dendritic cells and other cells at low levels(149). There was no TRAP$^{+}$ staining on *Sfpi1*$^{BN/BN}$ mice within the growth plates or trabecular bone of both the femur and the tibia. This result was to a certain extent expected since macrophage colony stimulating factor receptor (M-CSFR) is regulated by PU.1 and M-CSF is required for the differentiation of macrophages (150). Similar results are seen in the osteopetrotic op/op mice, which have a mutation in m-csf. Together, these results demonstrate that PU.1 plays a significant role in skeletal development and disease.

### 4.5 Future directions

This project provided insight into the role that PU.1 plays in the development and regulation of AML. However, there are still many questions that need to be addressed. The first question is whether PU.1 is regulating *e2f1* expression directly or indirectly. In this project, it was shown that PU.1 expression regulates the amount of E2F1 transcript levels. However, it was not determined conclusively what is the mechanism which PU.1 is performing the function. Some evidence suggests that PU.1 may directly regulate E2F1 expression (148). Therefore it would be interesting to prove whether PU.1 is directly regulating *e2f1* in *Sfpi1*$^{+/+}$ and *Sfpi1*$^{BN/BN}$ mice. By performing a chromatin immunoprecipitation for PU.1 we can determine whether PU.1 is found on the promoter region of E2F1. If this is the case, many avenues of research may be available such as performing biochemical analysis to determine which regions are interacting with the E2F1 promoter. If it is determined that PU.1 is not directly interacting with the promoter, it would be necessary to determine what pathway leads to these effects. It was mentioned that PU.1 is able to regulate E2F1 functions through miR-223 (147). This would also need to be verified experimentally. It would also need to be determined if this was the only form of regulation, or whether miR-223 acts to fine-tune the actual mechanism since it has been shown that many microRNAs act by fine tuning transcript levels of genes.

Once the mechanism is elucidated, the next step will be to conclusively determine whether the proliferation occurring in the spleens of these mice is AML. The gold standard to determine whether this is leukemia would be to perform transplantation experiments *in vivo*. While it is known that primary engraftment does occur (unpublished data), it must still be determined whether the recipient mice develop any form of AML.

Limiting dilution transplantation experiments would be necessary to determine the frequency of cells that are leukemic stem cells. Additionally, hematopathology and histology should be completed on these mice to determine whether their white blood cell count and differential is altered. These experiments are critical in establishing the AML diagnosis in this model and would strengthen the conclusions from this project.

Finally, an interesting avenue of research would be to determine whether the transcription factor SpiB is acting redundantly to PU.1. Our lab has observed that CD19$^{+/cre}$, *Sfpi1*$^{lox/lox}$, *SpiB*$^{-/-}$, develop a pre-B cell acute lymphoblastic leukemia before 30 weeks of age (151). SpiB is an ETS family transcription factor that has high homology to PU.1 and has been shown to act redundantly in other cell types. Therefore, it would be interesting to determine whether the mice which pass away earlier develop AML. Furthermore, it would be interesting to cross the *Sfpi1*$^{BN/BN}$ mice to *SpiB*$^{-/-}$ in the hopes of breeding *Sfpi1*$^{BN/BN}$, *SpiB*$^{-/-}$ mice to investigate whether these mice first survive, and also whether they develop AML more frequently or a more aggressive form of AML than *Sfpi1*$^{BN/BN}$ alone. This will help us determine whether the same redundancy in the myeloid cell lineage as is seen in the B cell lineage.

## 4.6 Summary and Conclusions

The goal of this project was to determine the role of PU.1 in the regulation of self-renewal in AML. I hypothesized that reduced levels of PU.1 cause AML by promoting self-renewal of myeloid progenitors through deregulation of the cell cycle, which results in increased proliferation and a block in terminal differentiation; where I define self-renewal as an increase in cell division in the absence of differentiation. This work has shown to be in support of the central hypothesis. This work demonstrated that a reduction of PU.1 expression resulted in unregulated proliferation of immature myeloid lineage cells in the spleen by an increased G1 to S phase transition. Furthermore, reduced expression of PU.1 in $\mathit{Sfpi1}^{BN/BN}$ fetal liver cells resulted in increased self-renewal and proliferation; whereas restoring PU.1 expression in $\mathit{Sfpi1}^{BN/BN}$ cells resulted in diminished proliferation and differentiation. We determined that PU.1 controls the cell cycle through regulation of *e2f1* transcription, however it remains to be determined whether this is direct or indirect effect. Finally, this project characterized the osteopetrotic phenotype in $\mathit{Sfpi1}^{BN/BN}$ mice. These mice lack TRAP$^+$ osteoclasts within the growth plate and trabecular bone as well as reduced expression of p57 which marks differentiated hypertrophic chondrocytes. Together, these results suggest that reduced PU.1 expression results in increased myeloid cell self-renewal, which then promotes an AML-like phenotype.

# BIBLIOGRAPHY

1. Howlader N NA, Krapcho M, Neyman N, Aminou R, Waldron W, Altekruse SF, Kosary CL, Ruhl J, Tatalovich Z, Cho H, Mariotto A, Eisner MP, Lewis DR, Chen HS, Feuer EJ, Cronin KA, Edwards BK. 2011. EER Cancer Statistics Review, 1975-2008. *National Cancer Institute*
2. Estey E, Dohner H. 2006. Acute myeloid leukaemia. *Lancet* 368: 1894-907
3. Appelbaum FR, Gundacker H, Head DR, Slovak ML, Willman CL, Godwin JE, Anderson JE, Petersdorf SH. 2006. Age and acute myeloid leukemia. *Blood* 107: 3481-5
4. Lowenberg B, Downing JR, Burnett A. 1999. Acute myeloid leukemia. *N Engl J Med* 341: 1051-62
5. Appelbaum FR, Rowe JM, Radich J, Dick JE. 2001. Acute myeloid leukemia. *Hematology Am Soc Hematol Educ Program*: 62-86
6. de Lima M, Strom SS, Keating M, Kantarjian H, Pierce S, O'Brien S, Freireich E, Estey E. 1997. Implications of potential cure in acute myelogenous leukemia: development of subsequent cancer and return to work. *Blood* 90: 4719-24
7. Rosenbauer F, Tenen DG. 2007. Transcription factors in myeloid development: balancing differentiation with transformation. *Nat Rev Immunol* 7: 105-17
8. Speck NA, Gilliland DG. 2002. Core-binding factors in haematopoiesis and leukaemia. *Nat Rev Cancer* 2: 502-13
9. Mizuki M, Schwable J, Steur C, Choudhary C, Agrawal S, Sargin B, Steffen B, Matsumura I, Kanakura Y, Bohmer FD, Muller-Tidow C, Berdel WE, Serve H. 2003. Suppression of myeloid transcription factors and induction of STAT response genes by AML-specific Flt3 mutations. *Blood* 101: 3164-73
10. Mueller BU, Pabst T, Fos J, Petkovic V, Fey MF, Asou N, Buergi U, Tenen DG. 2006. ATRA resolves the differentiation block in t(15;17) acute myeloid leukemia by restoring PU.1 expression. *Blood* 107: 3330-8
11. Spangrude GJ, Heimfeld S, Weissman IL. 1988. Purification and characterization of mouse hematopoietic stem cells. *Science* 241: 58-62
12. Morrison SJ, Hemmati HD, Wandycz AM, Weissman IL. 1995. The purification and characterization of fetal liver hematopoietic stem cells. *Proc Natl Acad Sci U S A* 92: 10302-6
13. Osawa M, Hanada K, Hamada H, Nakauchi H. 1996. Long-term lymphohematopoietic reconstitution by a single CD34-low/negative hematopoietic stem cell. *Science* 273: 242-5
14. Orkin SH. 2000. Diversification of haematopoietic stem cells to specific lineages. *Nat Rev Genet* 1: 57-64
15. Murry CE, Keller G. 2008. Differentiation of embryonic stem cells to clinically relevant populations: lessons from embryonic development. *Cell* 132: 661-80
16. Mestas J, Hughes CC. 2004. Of mice and not men: differences between mouse and human immunology. *J Immunol* 172: 2731-8
17. Haley PJ. 2003. Species differences in the structure and function of the immune system. *Toxicology* 188: 49-71

18. Orkin SH, Zon LI. 2008. Hematopoiesis: an evolving paradigm for stem cell biology. *Cell* 132: 631-44
19. Moore MA, Metcalf D. 1970. Ontogeny of the haemopoietic system: yolk sac origin of in vivo and in vitro colony forming cells in the developing mouse embryo. *Br J Haematol* 18: 279-96
20. Cumano A, Godin I. 2007. Ontogeny of the hematopoietic system. *Annu Rev Immunol* 25: 745-85
21. Medvinsky AL, Samoylina NL, Muller AM, Dzierzak EA. 1993. An early pre-liver intraembryonic source of CFU-S in the developing mouse. *Nature* 364: 64-7
22. Christensen JL, Wright DE, Wagers AJ, Weissman IL. 2004. Circulation and chemotaxis of fetal hematopoietic stem cells. *PLoS Biol* 2: E75
23. Doulatov S, Notta F, Eppert K, Nguyen LT, Ohashi PS, Dick JE. 2010. Revised map of the human progenitor hierarchy shows the origin of macrophages and dendritic cells in early lymphoid development. *Nat Immunol* 11: 585-93
24. Akashi K, Traver D, Miyamoto T, Weissman IL. 2000. A clonogenic common myeloid progenitor that gives rise to all myeloid lineages. *Nature* 404: 193-7
25. Kawamoto H, Ikawa T, Masuda K, Wada H, Katsura Y. 2010. A map for lineage restriction of progenitors during hematopoiesis: the essence of the myeloid-based model. *Immunol Rev* 238: 23-36
26. Adolfsson J, Mansson R, Buza-Vidas N, Hultquist A, Liuba K, Jensen CT, Bryder D, Yang L, Borge OJ, Thoren LA, Anderson K, Sitnicka E, Sasaki Y, Sigvardsson M, Jacobsen SE. 2005. Identification of Flt3+ lympho-myeloid stem cells lacking erythro-megakaryocytic potential a revised road map for adult blood lineage commitment. *Cell* 121: 295-306
27. DeKoter RP, Kamath MB, Houston IB. 2007. Analysis of concentration-dependent functions of PU.1 in hematopoiesis using mouse models. *Blood Cells Mol Dis* 39: 316-20
28. Simon MC. 1998. PU.1 and hematopoiesis: lessons learned from gene targeting experiments. *Semin Immunol* 10: 111-8
29. Tjian R, Maniatis T. 1994. Transcriptional activation: a complex puzzle with few easy pieces. *Cell* 77: 5-8
30. Friedman AD. 2002. Transcriptional regulation of myelopoiesis. *Int J Hematol* 75: 466-72
31. Friedman AD. 2007. Transcriptional control of granulocyte and monocyte development. *Oncogene* 26: 6816-28
32. Rosmarin AG, Yang Z, Resendes KK. 2005. Transcriptional regulation in myelopoiesis: Hematopoietic fate choice, myeloid differentiation, and leukemogenesis. *Exp Hematol* 33: 131-43
33. Tenen DG, Hromas R, Licht JD, Zhang DE. 1997. Transcription factors, normal myeloid development, and leukemia. *Blood* 90: 489-519
34. McKercher SR, Torbett BE, Anderson KL, Henkel GW, Vestal DJ, Baribault H, Klemsz M, Feeney AJ, Wu GE, Paige CJ, Maki RA. 1996. Targeted disruption of the PU.1 gene results in multiple hematopoietic abnormalities. *EMBO J* 15: 5647-58

35. Scott EW, Simon MC, Anastasi J, Singh H. 1994. Requirement of transcription factor PU.1 in the development of multiple hematopoietic lineages. *Science (New York, N.Y.)* 265: 1573-7
36. Su GH, Chen HM, Muthusamy N, Garrett-Sinha LA, Baunoch D, Tenen DG, Simon MC. 1997. Defective B cell receptor-mediated responses in mice lacking the Ets protein, Spi-B. *EMBO J* 16: 7118-29
37. Maroulakou IG, Bowe DB. 2000. Expression and function of Ets transcription factors in mammalian development: a regulatory network. *Oncogene* 19: 6432-42
38. Dahl R, Ramirez-Bergeron DL, Rao S, Simon MC. 2002. Spi-B can functionally replace PU.1 in myeloid but not lymphoid development. *The EMBO journal* 21: 2220-30
39. Kohyama M, Ise W, Edelson BT, Wilker PR, Hildner K, Mejia C, Frazier WA, Murphy TL, Murphy KM. 2009. Role for Spi-C in the development of red pulp macrophages and splenic iron homeostasis. *Nature* 457: 318-21
40. Zhang DE, Zhang P, Wang ND, Hetherington CJ, Darlington GJ, Tenen DG. 1997. Absence of granulocyte colony-stimulating factor signaling and neutrophil development in CCAAT enhancer binding protein alpha-deficient mice. *Proc Natl Acad Sci U S A* 94: 569-74
41. Hirai H, Zhang P, Dayaram T, Hetherington CJ, Mizuno S, Imanishi J, Akashi K, Tenen DG. 2006. C/EBPbeta is required for 'emergency' granulopoiesis. *Nat Immunol* 7: 732-9
42. Yamanaka R, Barlow C, Lekstrom-Himes J, Castilla LH, Liu PP, Eckhaus M, Decker T, Wynshaw-Boris A, Xanthopoulos KG. 1997. Impaired granulopoiesis, myelodysplasia, and early lethality in CCAAT/enhancer binding protein epsilon-deficient mice. *Proceedings of the National Academy of Sciences of the United States of America* 94: 13187-92
43. Hock H, Hamblen MJ, Rooke HM, Traver D, Bronson RT, Cameron S, Orkin SH. 2003. Intrinsic requirement for zinc finger transcription factor Gfi-1 in neutrophil differentiation. *Immunity* 18: 109-20
44. van der Meer LT, Jansen JH, van der Reijden BA. 2010. Gfi1 and Gfi1b: key regulators of hematopoiesis. *Leukemia : official journal of the Leukemia Society of America, Leukemia Research Fund, U.K* 24: 1834-43
45. Eferl R, Sibilia M, Hilberg F, Fuchsbichler A, Kufferath I, Guertl B, Zenz R, Wagner EF, Zatloukal K. 1999. Functions of c-Jun in liver and heart development. *The Journal of cell biology* 145: 1049-61
46. Laslo P, Spooner CJ, Warmflash A, Lancki DW, Lee HJ, Sciammas R, Gantner BN, Dinner AR, Singh H. 2006. Multilineage transcriptional priming and determination of alternate hematopoietic cell fates. *Cell* 126: 755-66
47. Min IM, Pietramaggiori G, Kim FS, Passegue E, Stevenson KE, Wagers AJ. 2008. The transcription factor EGR1 controls both the proliferation and localization of hematopoietic stem cells. *Cell stem cell* 2: 380-91
48. Feinberg MW, Wara AK, Cao Z, Lebedeva MA, Rosenbauer F, Iwasaki H, Hirai H, Katz JP, Haspel RL, Gray S, Akashi K, Segre J, Kaestner KH, Tenen DG, Jain MK. 2007. The Kruppel-like factor KLF4 is a critical regulator of monocyte differentiation. *EMBO J* 26: 4138-48

49. Laricchia-Robbio L, Premanand K, Rinaldi CR, Nucifora G. 2009. EVI1 Impairs myelopoiesis by deregulation of PU.1 function. *Cancer research* 69: 1633-42
50. Stehling-Sun S, Dade J, Nutt SL, DeKoter RP, Camargo FD. 2009. Regulation of lymphoid versus myeloid fate 'choice' by the transcription factor Mef2c. *Nature immunology* 10: 289-96
51. Tsai S, Bartelmez S, Heyman R, Damm K, Evans R, Collins SJ. 1992. A mutated retinoic acid receptor-alpha exhibiting dominant-negative activity alters the lineage development of a multipotent hematopoietic cell line. *Genes & development* 6: 2258-69
52. Okuda T, van Deursen J, Hiebert SW, Grosveld G, Downing JR. 1996. AML1, the target of multiple chromosomal translocations in human leukemia, is essential for normal fetal liver hematopoiesis. *Cell* 84: 321-30
53. Wilson A, Murphy MJ, Oskarsson T, Kaloulis K, Bettess MD, Oser GM, Pasche AC, Knabenhans C, Macdonald HR, Trumpp A. 2004. c-Myc controls the balance between hematopoietic stem cell self-renewal and differentiation. *Genes & development* 18: 2747-63
54. Mucenski ML, McLain K, Kier AB, Swerdlow SH, Schreiner CM, Miller TA, Pietryga DW, Scott WJ, Jr., Potter SS. 1991. A functional c-myb gene is required for normal murine fetal hepatic hematopoiesis. *Cell* 65: 677-89
55. Moore KJ. 1995. Insight into the microphthalmia gene. *Trends in genetics : TIG* 11: 442-8
56. Moreau-Gachelin F, Tavitian A, Tambourin P. 1988. Spi-1 is a putative oncogene in virally induced murine erythroleukaemias. *Nature* 331: 277-80
57. Moreau-Gachelin F. 1994. Spi-1/PU.1: an oncogene of the Ets family. *Biochim Biophys Acta* 1198: 149-63
58. Ray D, Bosselut R, Ghysdael J, Mattei MG, Tavitian A, Moreau-Gachelin F. 1992. Characterization of Spi-B, a transcription factor related to the putative oncoprotein Spi-1/PU.1. *Mol Cell Biol* 12: 4297-304
59. Nguyen VC, Ray D, Gross MS, de Tand MF, Frezal J, Moreau-Gachelin F. 1990. Localization of the human oncogene SPI1 on chromosome 11, region p11.22. *Hum Genet* 84: 542-6
60. Nishiyama C, Nishiyama M, Ito T, Masaki S, Masuoka N, Yamane H, Kitamura T, Ogawa H, Okumura K. 2004. Functional analysis of PU.1 domains in monocyte-specific gene regulation. *FEBS Lett* 561: 63-8
61. Klemsz MJ, McKercher SR, Celada A, Van Beveren C, Maki RA. 1990. The macrophage and B cell-specific transcription factor PU.1 is related to the ets oncogene. *Cell* 61: 113-24
62. Behre G, Whitmarsh AJ, Coghlan MP, Hoang T, Carpenter CL, Zhang DE, Davis RJ, Tenen DG. 1999. c-Jun is a JNK-independent coactivator of the PU.1 transcription factor. *J Biol Chem* 274: 4939-46
63. Rekhtman N, Radparvar F, Evans T, Skoultchi AI. 1999. Direct interaction of hematopoietic transcription factors PU.1 and GATA-1: functional antagonism in erythroid cells. *Genes Dev* 13: 1398-411
64. Nagulapalli S, Pongubala JM, Atchison ML. 1995. Multiple proteins physically interact with PU.1. Transcriptional synergy with NF-IL6 beta (C/EBP delta, CRP3). *J Immunol* 155: 4330-8

65. Rechsteiner M, Rogers SW. 1996. PEST sequences and regulation by proteolysis. *Trends Biochem Sci* 21: 267-71
66. Fisher RC, Olson MC, Pongubala JM, Perkel JM, Atchison ML, Scott EW, Simon MC. 1998. Normal myeloid development requires both the glutamine-rich transactivation domain and the PEST region of transcription factor PU.1 but not the potent acidic transactivation domain. *Mol Cell Biol* 18: 4347-57
67. Eisenbeis CF, Singh H, Storb U. 1995. Pip, a novel IRF family member, is a lymphoid-specific, PU.1-dependent transcriptional activator. *Genes Dev* 9: 1377-87
68. Back J, Allman D, Chan S, Kastner P. 2005. Visualizing PU.1 activity during hematopoiesis. *Exp Hematol* 33: 395-402
69. Nutt SL, Metcalf D, D'Amico A, Polli M, Wu L. 2005. Dynamic regulation of PU.1 expression in multipotent hematopoietic progenitors. *J Exp Med* 201: 221-31
70. Nerlov C, Graf T. 1998. PU.1 induces myeloid lineage commitment in multipotent hematopoietic progenitors. *Genes Dev* 12: 2403-12
71. Chang HC, Sehra S, Goswami R, Yao W, Yu Q, Stritesky GL, Jabeen R, McKinley C, Ahyi AN, Han L, Nguyen ET, Robertson MJ, Perumal NB, Tepper RS, Nutt SL, Kaplan MH. 2010. The transcription factor PU.1 is required for the development of IL-9-producing T cells and allergic inflammation. *Nat Immunol* 11: 527-34
72. Kastner P, Chan S. 2008. PU.1: a crucial and versatile player in hematopoiesis and leukemia. *Int J Biochem Cell Biol* 40: 22-7
73. Chen H, Ray-Gallet D, Zhang P, Hetherington CJ, Gonzalez DA, Zhang DE, Moreau-Gachelin F, Tenen DG. 1995. PU.1 (Spi-1) autoregulates its expression in myeloid cells. *Oncogene* 11: 1549-60
74. Chen H, Zhang P, Radomska HS, Hetherington CJ, Zhang DE, Tenen DG. 1996. Octamer binding factors and their coactivator can activate the murine PU.1 (spi-1) promoter. *J Biol Chem* 271: 15743-52
75. Okuno Y, Huang G, Rosenbauer F, Evans EK, Radomska HS, Iwasaki H, Akashi K, Moreau-Gachelin F, Li Y, Zhang P, Gottgens B, Tenen DG. 2005. Potential autoregulation of transcription factor PU.1 by an upstream regulatory element. *Mol Cell Biol* 25: 2832-45
76. Rosenbauer F, Wagner K, Kutok JL, Iwasaki H, Le Beau MM, Okuno Y, Akashi K, Fiering S, Tenen DG. 2004. Acute myeloid leukemia induced by graded reduction of a lineage-specific transcription factor, PU.1. *Nat Genet* 36: 624-30
77. Huang G, Zhang P, Hirai H, Elf S, Yan X, Chen Z, Koschmieder S, Okuno Y, Dayaram T, Growney JD, Shivdasani RA, Gilliland DG, Speck NA, Nimer SD, Tenen DG. 2008. PU.1 is a major downstream target of AML1 (RUNX1) in adult mouse hematopoiesis. *Nat Genet* 40: 51-60
78. Schroeder T, Kohlhof H, Rieber N, Just U. 2003. Notch signaling induces multilineage myeloid differentiation and up-regulates PU.1 expression. *J Immunol* 170: 5538-48

79. Scott EW, Simon MC, Anastasi J, Singh H. 1994. Requirement of transcription factor PU.1 in the development of multiple hematopoietic lineages. *Science* 265: 1573-7
80. Rosenbauer F, Owens BM, Yu L, Tumang JR, Steidl U, Kutok JL, Clayton LK, Wagner K, Scheller M, Iwasaki H, Liu C, Hackanson B, Akashi K, Leutz A, Rothstein TL, Plass C, Tenen DG. 2006. Lymphoid cell growth and transformation are suppressed by a key regulatory element of the gene encoding PU.1. *Nat Genet* 38: 27-37
81. Houston IB, Kamath MB, Schweitzer BL, Chlon TM, DeKoter RP. 2007. Reduction in PU.1 activity results in a block to B-cell development, abnormal myeloid proliferation, and neonatal lethality. *Exp Hematol* 35: 1056-68
82. Smith LT, Hohaus S, Gonzalez DA, Dziennis SE, Tenen DG. 1996. PU.1 (Spi-1) and C/EBP alpha regulate the granulocyte colony-stimulating factor receptor promoter in myeloid cells. *Blood* 88: 1234-47
83. Zhang DE, Hetherington CJ, Chen HM, Tenen DG. 1994. The macrophage transcription factor PU.1 directs tissue-specific expression of the macrophage colony-stimulating factor receptor. *Mol Cell Biol* 14: 373-81
84. Hohaus S, Petrovick MS, Voso MT, Sun Z, Zhang DE, Tenen DG. 1995. PU.1 (Spi-1) and C/EBP alpha regulate expression of the granulocyte-macrophage colony-stimulating factor receptor alpha gene. *Mol Cell Biol* 15: 5830-45
85. Pahl HL, Rosmarin AG, Tenen DG. 1992. Characterization of the myeloid-specific CD11b promoter. *Blood* 79: 865-70
86. Rosmarin AG, Levy R, Tenen DG. 1992. Cloning and analysis of the CD18 promoter. *Blood* 79: 2598-604
87. Perez C, Coeffier E, Moreau-Gachelin F, Wietzerbin J, Benech PD. 1994. Involvement of the transcription factor PU.1/Spi-1 in myeloid cell-restricted expression of an interferon-inducible gene encoding the human high-affinity Fc gamma receptor. *Mol Cell Biol* 14: 5023-31
88. Feinman R, Qiu WQ, Pearse RN, Nikolajczyk BS, Sen R, Sheffery M, Ravetch JV. 1994. PU.1 and an HLH family member contribute to the myeloid-specific transcription of the Fc gamma RIIIA promoter. *EMBO J* 13: 3852-60
89. Moulton KS, Semple K, Wu H, Glass CK. 1994. Cell-specific expression of the macrophage scavenger receptor gene is dependent on PU.1 and a composite AP-1/ets motif. *Mol Cell Biol* 14: 4408-18
90. Ghisletti S, Barozzi I, Mietton F, Polletti S, De Santa F, Venturini E, Gregory L, Lonie L, Chew A, Wei CL, Ragoussis J, Natoli G. 2010. Identification and characterization of enhancers controlling the inflammatory gene expression program in macrophages. *Immunity* 32: 317-28
91. Chung UI, Kawaguchi H, Takato T, Nakamura K. 2004. Distinct osteogenic mechanisms of bones of distinct origins. *J Orthop Sci* 9: 410-4
92. Hall BK, Miyake T. 2000. All for one and one for all: condensations and the initiation of skeletal development. *Bioessays* 22: 138-47
93. Noonan KJ, Hunziker EB, Nessler J, Buckwalter JA. 1998. Changes in cell, matrix compartment, and fibrillar collagen volumes between growth-plate zones. *J Orthop Res* 16: 500-8

94. Zhang P, Liegeois NJ, Wong C, Finegold M, Hou H, Thompson JC, Silverman A, Harper JW, DePinho RA, Elledge SJ. 1997. Altered cell differentiation and proliferation in mice lacking p57KIP2 indicates a role in Beckwith-Wiedemann syndrome. *Nature* 387: 151-8
95. Burger EH, Van der Meer JW, van de Gevel JS, Gribnau JC, Thesingh GW, van Furth R. 1982. In vitro formation of osteoclasts from long-term cultures of bone marrow mononuclear phagocytes. *J Exp Med* 156: 1604-14
96. Kurihara N, Chenu C, Miller M, Civin C, Roodman GD. 1990. Identification of committed mononuclear precursors for osteoclast-like cells formed in long term human marrow cultures. *Endocrinology* 126: 2733-41
97. Suda T, Takahashi N, Martin TJ. 1992. Modulation of osteoclast differentiation. *Endocr Rev* 13: 66-80
98. Burstone MS. 1959. Histochemical demonstration of acid phosphatase activity in osteoclasts. *J Histochem Cytochem* 7: 39-41
99. Minkin C. 1982. Bone acid phosphatase: tartrate-resistant acid phosphatase as a marker of osteoclast function. *Calcif Tissue Int* 34: 285-90
100. Gowen M, Meikle MC, Reynolds JJ. 1983. Stimulation of bone resorption in vitro by a non-prostanoid factor released by human monocytes in culture. *Biochim Biophys Acta* 762: 471-4
101. Yates AJ, Boyce BF, Favarato G, Aufdemorte TB, Marcelli C, Kester MB, Walker R, Langton BC, Bonewald LF, Mundy GR. 1992. Expression of human transforming growth factor alpha by Chinese hamster ovarian tumors in nude mice causes hypercalcemia and increased osteoclastic bone resorption. *J Bone Miner Res* 7: 847-53
102. Yoshida H, Hayashi S, Kunisada T, Ogawa M, Nishikawa S, Okamura H, Sudo T, Shultz LD. 1990. The murine mutation osteopetrosis is in the coding region of the macrophage colony stimulating factor gene. *Nature* 345: 442-4
103. Pfeilschifter J, Chenu C, Bird A, Mundy GR, Roodman GD. 1989. Interleukin-1 and tumor necrosis factor stimulate the formation of human osteoclastlike cells in vitro. *J Bone Miner Res* 4: 113-8
104. Kurihara N, Bertolini D, Suda T, Akiyama Y, Roodman GD. 1990. IL-6 stimulates osteoclast-like multinucleated cell formation in long term human marrow cultures by inducing IL-1 release. *J Immunol* 144: 4226-30
105. Girasole G, Passeri G, Jilka RL, Manolagas SC. 1994. Interleukin-11: a new cytokine critical for osteoclast development. *J Clin Invest* 93: 1516-24
106. Vermeulen K, Van Bockstaele DR, Berneman ZN. 2003. The cell cycle: a review of regulation, deregulation and therapeutic targets in cancer. *Cell Prolif* 36: 131-49
107. Malumbres M, Barbacid M. 2009. Cell cycle, CDKs and cancer: a changing paradigm. *Nat Rev Cancer* 9: 153-66
108. Sherr CJ, Roberts JM. 1995. Inhibitors of mammalian G1 cyclin-dependent kinases. *Genes Dev* 9: 1149-63
109. Trimarchi JM, Lees JA. 2002. Sibling rivalry in the E2F family. *Nat Rev Mol Cell Biol* 3: 11-20
110. Johnson DG, Cress WD, Jakoi L, Nevins JR. 1994. Oncogenic capacity of the E2F1 gene. *Proc Natl Acad Sci U S A* 91: 12823-7

111. Johnson DG, Schwarz JK, Cress WD, Nevins JR. 1993. Expression of transcription factor E2F1 induces quiescent cells to enter S phase. *Nature* 365: 349-52
112. Singh P, Wong SH, Hong W. 1994. Overexpression of E2F-1 in rat embryo fibroblasts leads to neoplastic transformation. *EMBO J* 13: 3329-38
113. Wu L, Timmers C, Maiti B, Saavedra HI, Sang L, Chong GT, Nuckolls F, Giangrande P, Wright FA, Field SJ, Greenberg ME, Orkin S, Nevins JR, Robinson ML, Leone G. 2001. The E2F1-3 transcription factors are essential for cellular proliferation. *Nature* 414: 457-62
114. Mueller BU, Pabst T, Osato M, Asou N, Johansen LM, Minden MD, Behre G, Hiddemann W, Ito Y, Tenen DG. 2002. Heterozygous PU.1 mutations are associated with acute myeloid leukemia. *Blood* 100: 998-1007
115. Morita S, Kojima T, Kitamura T. 2000. Plat-E: an efficient and stable system for transient packaging of retroviruses. *Gene Ther* 7: 1063-6
116. Chu YW, Wang R, Schmid I, Sakamoto KM. 1999. Analysis with flow cytometry of green fluorescent protein expression in leukemic cells. *Cytometry* 36: 333-9
117. Livak KJ, Schmittgen TD. 2001. Analysis of relative gene expression data using real-time quantitative PCR and the 2(-Delta Delta C(T)) Method. *Methods* 25: 402-8
118. Ashman LK. 1999. The biology of stem cell factor and its receptor C-kit. *Int J Biochem Cell Biol* 31: 1037-51
119. Scholzen T, Gerdes J. 2000. The Ki-67 protein: from the known and the unknown. *J Cell Physiol* 182: 311-22
120. Burgess AW, Metcalf D. 1980. The nature and action of granulocyte-macrophage colony stimulating factors. *Blood* 56: 947-58
121. Hanahan D, Weinberg RA. 2000. The hallmarks of cancer. *Cell* 100: 57-70
122. Hanahan D, Weinberg RA. 2011. Hallmarks of cancer: the next generation. *Cell* 144: 646-74
123. Polager S, Ginsberg D. 2009. p53 and E2f: partners in life and death. *Nat Rev Cancer* 9: 738-48
124. van Os R, Kamminga LM, de Haan G. 2004. Stem cell assays: something old, something new, something borrowed. *Stem Cells* 22: 1181-90
125. Szilvassy SJ, Lansdorp PM, Humphries RK, Eaves AC, Eaves CJ. 1989. Isolation in a single step of a highly enriched murine hematopoietic stem cell population with competitive long-term repopulating ability. *Blood* 74: 930-9
126. Benveniste P, Cantin C, Hyam D, Iscove NN. 2003. Hematopoietic stem cells engraft in mice with absolute efficiency. *Nat Immunol* 4: 708-13
127. Kihara-Negishi F, Yamamoto H, Suzuki M, Yamada T, Sakurai T, Tamura T, Oikawa T. 2001. In vivo complex formation of PU.1 with HDAC1 associated with PU.1-mediated transcriptional repression. *Oncogene* 20: 6039-47
128. Klemsz MJ, Maki RA. 1996. Activation of transcription by PU.1 requires both acidic and glutamine domains. *Mol Cell Biol* 16: 390-7
129. Yang ZF, Mott S, Rosmarin AG. 2007. The Ets transcription factor GABP is required for cell-cycle progression. *Nat Cell Biol* 9: 339-46

130. Sharrocks AD. 2001. The ETS-domain transcription factor family. *Nat Rev Mol Cell Biol* 2: 827-37

131. Rudge TL, Johnson LF. 2002. Synergistic activation of the TATA-less mouse thymidylate synthase promoter by the Ets transcription factor GABP and Sp1. *Exp Cell Res* 274: 45-55

132. Izumi M, Yokoi M, Nishikawa NS, Miyazawa H, Sugino A, Yamagishi M, Yamaguchi M, Matsukage A, Yatagai F, Hanaoka F. 2000. Transcription of the catalytic 180-kDa subunit gene of mouse DNA polymerase alpha is controlled by E2F, an Ets-related transcription factor, and Sp1. *Biochim Biophys Acta* 1492: 341-52

133. Imaki H, Nakayama K, Delehouzee S, Handa H, Kitagawa M, Kamura T, Nakayama KI. 2003. Cell cycle-dependent regulation of the Skp2 promoter by GA-binding protein. *Cancer Res* 63: 4607-13

134. Choe KS, Ujhelly O, Wontakal SN, Skoultchi AI. 2010. PU.1 directly regulates cdk6 gene expression, linking the cell proliferation and differentiation programs in erythroid cells. *J Biol Chem* 285: 3044-52

135. Bies J, Sramko M, Fares J, Rosu-Myles M, Zhang S, Koller R, Wolff L. 2010. Myeloid-specific inactivation of p15Ink4b results in monocytosis and predisposition to myeloid leukemia. *Blood* 116: 979-87

136. Suzuki M, Yamada T, Kihara-Negishi F, Sakurai T, Hara E, Tenen DG, Hozumi N, Oikawa T. 2006. Site-specific DNA methylation by a complex of PU.1 and Dnmt3a/b. *Oncogene* 25: 2477-88

137. Tschan MP, Reddy VA, Ress A, Arvidsson G, Fey MF, Torbett BE. 2008. PU.1 binding to the p53 family of tumor suppressors impairs their transcriptional activity. *Oncogene* 27: 3489-93

138. DeGregori J, Leone G, Ohtani K, Miron A, Nevins JR. 1995. E2F-1 accumulation bypasses a G1 arrest resulting from the inhibition of G1 cyclin-dependent kinase activity. *Genes Dev* 9: 2873-87

139. Schwarz JK, Bassing CH, Kovesdi I, Datto MB, Blazing M, George S, Wang XF, Nevins JR. 1995. Expression of the E2F1 transcription factor overcomes type beta transforming growth factor-mediated growth suppression. *Proc Natl Acad Sci U S A* 92: 483-7

140. Mann DJ, Jones NC. 1996. E2F-1 but not E2F-4 can overcome p16-induced G1 cell-cycle arrest. *Curr Biol* 6: 474-83

141. Lammens T, Li J, Leone G, De Veylder L. 2009. Atypical E2Fs: new players in the E2F transcription factor family. *Trends Cell Biol* 19: 111-8

142. Li J, Ran C, Li E, Gordon F, Comstock G, Siddiqui H, Cleghorn W, Chen HZ, Kornacker K, Liu CG, Pandit SK, Khanizadeh M, Weinstein M, Leone G, de Bruin A. 2008. Synergistic function of E2F7 and E2F8 is essential for cell survival and embryonic development. *Dev Cell* 14: 62-75

143. Fukao T, Fukuda Y, Kiga K, Sharif J, Hino K, Enomoto Y, Kawamura A, Nakamura K, Takeuchi T, Tanabe M. 2007. An evolutionarily conserved mechanism for microRNA-223 expression revealed by microRNA gene profiling. *Cell* 129: 617-31

144. Lagos-Quintana M, Rauhut R, Lendeckel W, Tuschl T. 2001. Identification of novel genes coding for small expressed RNAs. *Science* 294: 853-8

145. Johnnidis JB, Harris MH, Wheeler RT, Stehling-Sun S, Lam MH, Kirak O, Brummelkamp TR, Fleming MD, Camargo FD. 2008. Regulation of progenitor cell proliferation and granulocyte function by microRNA-223. *Nature* 451: 1125-9
146. Fazi F, Racanicchi S, Zardo G, Starnes LM, Mancini M, Travaglini L, Diverio D, Ammatuna E, Cimino G, Lo-Coco F, Grignani F, Nervi C. 2007. Epigenetic silencing of the myelopoiesis regulator microRNA-223 by the AML1/ETO oncoprotein. *Cancer Cell* 12: 457-66
147. Pulikkan JA, Dengler V, Peramangalam PS, Peer Zada AA, Muller-Tidow C, Bohlander SK, Tenen DG, Behre G. 2010. Cell-cycle regulator E2F1 and microRNA-223 comprise an autoregulatory negative feedback loop in acute myeloid leukemia. *Blood* 115: 1768-78
148. Wontakal SN, Guo X, Will B, Shi M, Raha D, Mahajan MC, Weissman S, Snyder M, Steidl U, Zheng D, Skoultchi AI. 2011. A Large Gene Network in Immature Erythroid Cells Is Controlled by the Myeloid and B Cell Transcriptional Regulator PU.1. *PLoS Genet* 7: e1001392
149. Oddie GW, Schenk G, Angel NZ, Walsh N, Guddat LW, de Jersey J, Cassady AI, Hamilton SE, Hume DA. 2000. Structure, function, and regulation of tartrate-resistant acid phosphatase. *Bone* 27: 575-84
150. Douglass TG, Driggers L, Zhang JG, Hoa N, Delgado C, Williams CC, Dan Q, Sanchez R, Jeffes EW, Wepsic HT, Myers MP, Koths K, Jadus MR. 2008. Macrophage colony stimulating factor: not just for macrophages anymore! A gateway into complex biologies. *Int Immunopharmacol* 8: 1354-76
151. Sokalski KM, Li SK, Welch I, Cadieux-Pitre HA, Gruca MR, Dekoter RP. 2011. Deletion of genes encoding PU.1 and Spi-B in B cells impairs differentiation and induces pre-B cell acute lymphoblastic leukemia. *Blood*

# APPENDIX

## Animal Use Protocol

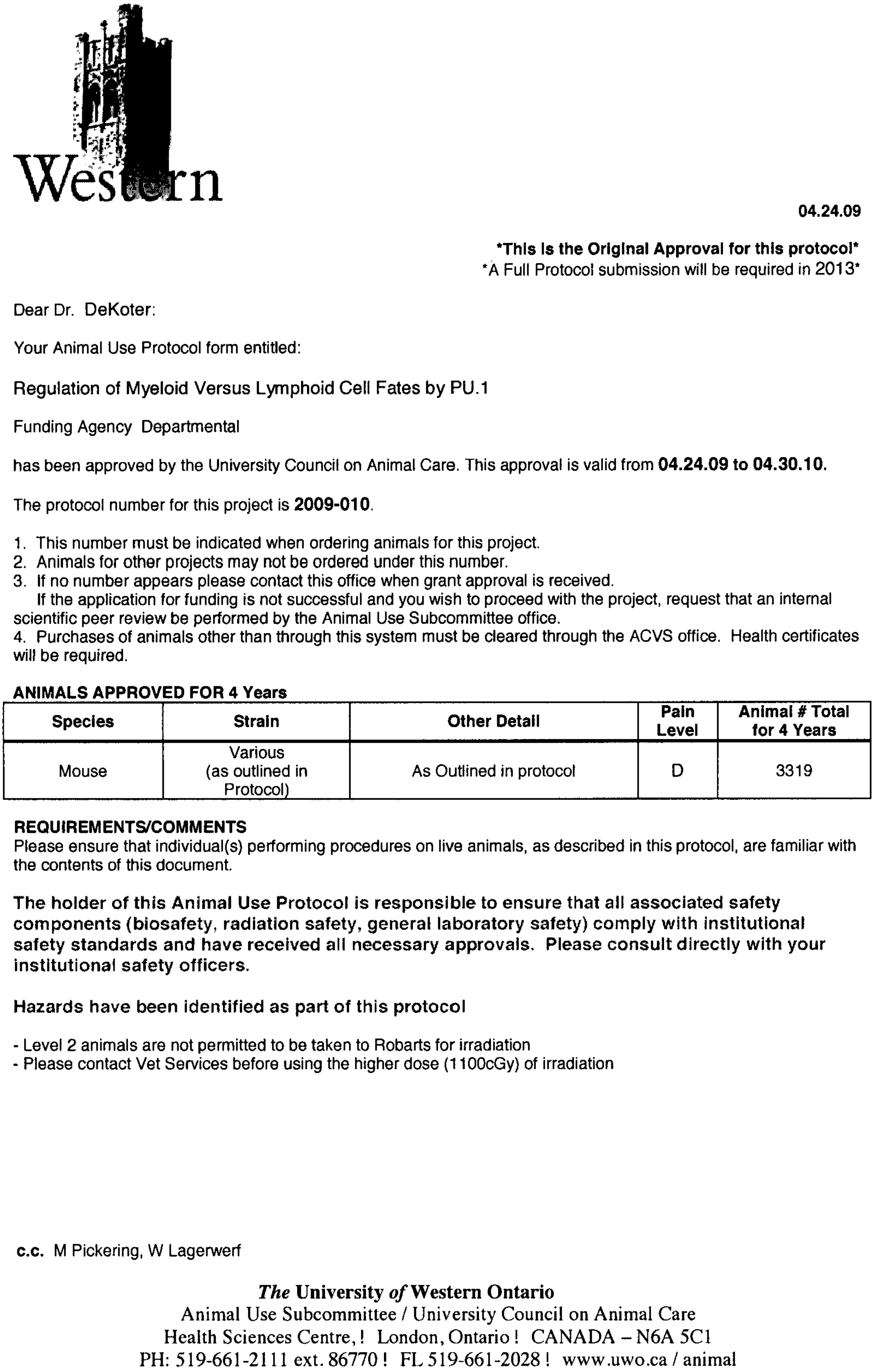

Western

**04.24.09**

***This is the Original Approval for this protocol***
*A Full Protocol submission will be required in 2013*

Dear Dr. DeKoter:

Your Animal Use Protocol form entitled:

Regulation of Myeloid Versus Lymphoid Cell Fates by PU.1

Funding Agency Departmental

has been approved by the University Council on Animal Care. This approval is valid from **04.24.09 to 04.30.10.**

The protocol number for this project is **2009-010**.

1. This number must be indicated when ordering animals for this project.
2. Animals for other projects may not be ordered under this number.
3. If no number appears please contact this office when grant approval is received.
   If the application for funding is not successful and you wish to proceed with the project, request that an internal scientific peer review be performed by the Animal Use Subcommittee office.
4. Purchases of animals other than through this system must be cleared through the ACVS office. Health certificates will be required.

**ANIMALS APPROVED FOR 4 Years**

| Species | Strain | Other Detail | Pain Level | Animal # Total for 4 Years |
|---|---|---|---|---|
| Mouse | Various (as outlined in Protocol) | As Outlined in protocol | D | 3319 |

**REQUIREMENTS/COMMENTS**
Please ensure that individual(s) performing procedures on live animals, as described in this protocol, are familiar with the contents of this document.

**The holder of this Animal Use Protocol is responsible to ensure that all associated safety components (biosafety, radiation safety, general laboratory safety) comply with institutional safety standards and have received all necessary approvals. Please consult directly with your institutional safety officers.**

**Hazards have been identified as part of this protocol**

- Level 2 animals are not permitted to be taken to Robarts for irradiation
- Please contact Vet Services before using the higher dose (1100cGy) of irradiation

**c.c.** M Pickering, W Lagerwerf

***The* University *of* Western Ontario**
Animal Use Subcommittee / University Council on Animal Care
Health Sciences Centre,! London, Ontario! CANADA – N6A 5C1
PH: 519-661-2111 ext. 86770 ! FL 519-661-2028 ! www.uwo.ca / animal